POLITECNICO DI MILANO

School of Industrial and Information Engineering

Department of Aerospace Science and Technology

Master of Science in Space Engineering

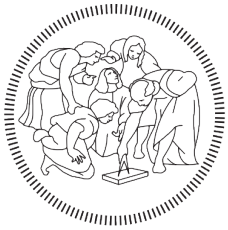

POLITECNICO
MILANO 1863

STORABLE GREEN OXIDIZERS FOR HYBRID ROCKET PROPULSION

Space Propulsion Laboratory

SPlab
POLIMI

Advisor:
Dr. Chistian PARAVAN

M.Sc. Dissertation of:
Quentin PAQUOT
Matr. 935841

Academic Year 2020-2021

Abstract

Liquid oxygen is the most used oxidizer in actual hybrid rocket engines thanks to its high specific impulse, availability and heritage. The cryogenic nature of liquid oxygen (LOX) complicates the plumbing and feed systems of the implemented HRE and makes it non suitable for long term in-space missions. Despite its high performances, LOX is not suitable for many military and space applications when storability or simplicity are required. Storable oxidizers as nitrogen tetroxide have raised concerns during last decades for their pollutant impact on the environment and their high toxicity. Due to these reasons, there are increasing motivations in studying and developing these storable green oxidizers for hybrid rocket applications. The most promising storable green oxidizers are hydrogen peroxide (H_2O_2), nitrous oxide (N_2O), and hydroxyl ammonium nitrate (HAN). As an additional advantage, the exothermic decomposition of these storable oxidizers makes them suitable for monopropellant applications and simplifies the engine ignition hardware.

Open literature studies and publications about the three storable green oxidizers H_2O_2, N_2O, and HAN are wide and have been reviewed in this work.

Oxidizers' physical properties, decomposition and catalysis, availability, storability, advantages and constraints in monopropellant devices are discussed. Then their applications and performances in hybrid rocket engines are studied. Finally, a thermochemical analysis of storable green oxidizers in combustion with paraffin fuel is conducted using NASA CEA code. Especially, their performances in terms of chamber flame temperature and vacuum specific impulse in a hybrid paraffin-fueled rocket engine are studied. In combustion with paraffin fuel and with a nozzle expansion ratio of 40, hydrogen peroxide provides a vacuum specific impulse up to 330 s. In the same conditions, nitrous oxide and HAN reach respectively a maximum performance of 315 s and 302 s.

Acknowledgments

I wish to show my gratitude to Professor Christian Paravan from the Space Propulsion Laboratory of Polimi for its guidance throughout this work.

I would also like to thank my friends with whom I shared my studies at Politecnico di Milano.

Contents

List of Tables

List of Figures

Nomenclature

$\dot{m}$	mass flow rate
$\dot{r}$	fuel regression rate
$\dot{V}$	volumetric flow rate
η	decomposition efficiency
$\eta_{\Delta T}$	decomposition temperature efficiency
η_{c*}	characteristic velocity efficiency
γ	heat capacity ratio
λ	decomposition parameter
ρ	density
ρ_f	solid fuel density
$\tilde{\epsilon}$	bed porosity
A	Arrhenius pre-exponential factor
a	regression rate coefficient
A_t	throat area
C	molar concentration
c^*	characteristic velocity
C_F	thrust coefficient
D_p	pellet diameter
D_{port}	solid fuel burning port diameter
E_a	activation energy
F	thrust
f	hydrogen peroxide mass fraction
G	bed load
g_0	acceleration of gravity of the Earth at sea level
G_{ox}	oxidizer mass flux
Isp	specific impulse
k	kinetic parameter
K_1	equilibrium adsorption constant
L_{DF}	length of diffusion flame
L_{SF}	solid fuel length
M	molecular weight
n	regression rate exponent
N_s	number of active adsorption sites per unit volume of the catalytic bed
O/F	oxidizer to fuel ratio
O/F_{st}	stoichiometric mixture ratio
p	pressure
q	heat
R	gas constant
Re_p	pellet Reynolds number
S_L	speed of the laminar deflagration wave
T	temperature
T_{50}	light-off temperature
u	flow velocity
Y	H_2O_2 mass concentration
ABS	acrylonitrile butadiene styrene

AN ammonium nitrate

BHA barium hexaaluminate

BIFA $BaIr_xFe_{1-x}Al_{11}O_{19-\alpha}$ hexaaluminate catalysts

CB carbon black

CSI contact surface index

EGA evolved gas analysis

ESA European space agency

GOX gaseous oxygen

GPRCS green propellant reaction control system

HAN hydroxyl-ammonium nitrate

HC hollow cone injector

HDPE high density polyethylene

HIPS high-impact-polystyrene

HP hydrogen peroxide

HRE hybrid rocket engine

HTP high test peroxide

HTPB hydroxyl-terminated polybutadiene

HYROPS hybrid rocket performance simulator

JAXA Japan aerospace exploration agency

LDPE low density polyethylene

LEO low Earth orbit

LOX liquid oxygen

PE polyethylene

PMMA polymethylmethacrylate

PSW pressure swirl injector

PTFE polytetrafluoroethylene

RAPIS rapid innovative payload demonstration satellite

SH showerhead injector

SRM solid rocket motor

TRL technology readiness level

UHMW ultra-high molecular weight fuels

VOR vortex injector

Chapter 1

Introduction

1.1 Motivations

Thermo-chemical propulsion systems are the leading technology for access to space and serve in several in-space missions.

Thermal hybrid rocket engines are characterized by the storage of fuel and oxidizer in different states of matter. Conventional hybrid employs a liquid (or gaseous) oxidizer reacting with a solid fuel. Combustion is ruled by a diffusion flame originated by the atomized gaseous oxidizer and the fuel vapors. The scheme of a conventional hybrid rocket engine is presented in Fig. 1.1.

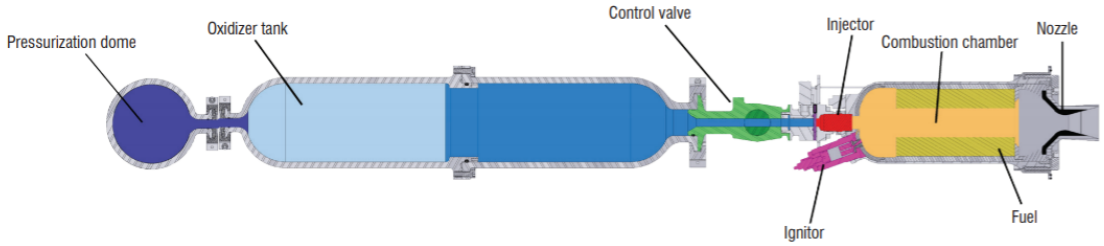

Figure 1.1: Scheme of a conventional hybrid rocket engine [1].

The development of hybrid rocket engines, considered as an intermediate between solid and liquid rocket engines, has been hampered by several inherent issues such as low regression rate and poor combustion efficiency, hindering their numerous advantages. Indeed, the hybrid rocket engine concept displays several advantages over classical and more mature solid and liquid rocket engines:

- Safety, as the reactants are separately stored in different phases;
- Re-ignition capability, an interesting feature distinguishing HRE from SRM;
- Thrust throttling, varying the oxidizer mass flow rate;
- Insensitivity to cracks in the grain fuel (due to the diffusive nature of the flame);
- High theoretical specific impulse also for non-metallized fuel formulations.

Being typically considered as a possible replacement for SRMs, large scale HREs have been implemented with liquid oxygen (LOX) as oxidizer. This is due to the fact that

LOX offers high specific impulse performance together with relatively high regression rates (in turn due to the high flame temperature originated during the combustion). Yet, cryogenic oxidizer implies a complicated design of the propulsion system, with increased costs over the storable counterpart and is not suitable in long term in-space missions. As a consequence, storable oxidizers are of interest in HREs, in particular for secondary propulsion. Storable oxidizers as N_2O_4 are dangerous for both humans and the environment. Storable green oxidizers as hydrogen peroxide, nitrous oxide, and HAN has long been limited in use because of their slightly lower performance than systems using LOX. However, the increasing concerns about the environmental impact of space industry, the necessity to provide storable propellants, and the theoretical high performances and advantages of hybrid rocket engines have raised the interest in these oxidizers for hybrid rocket engine applications.

The search for better oxidizers requires a clear description of the desirable attributes for the oxidizing component of the propellant system which can be listed as:

- High density for a better volumetric efficiency;
- Chemical stability for safety and long term storage;
- Low toxicity;
- Low freezing point for storability under normal conditions;
- Ease of handling;
- Low cost.

Furthermore, the exothermic decomposition of these oxidizers makes them suitable for monopropellant applications. Monopropellant rocket engines can be seen as hybrid rocket engines without the solid fuel. Instead of a combustion reaction in a combustion chamber, the propellant releases its energy in a decomposition reaction by passing through a catalytic bed. Monopropellant devices usually provide small thrust (1-20N) for applications such as satellite attitude control, station keeping, and de-orbiting. Hydrazine is a common propellant in those devices.

As the study of storable green oxidizers in hybrid rocket engine applications first faces the monopropellant scenario (i.e. the decomposition phenomena and the catalytic bed design), H_2O_2, N_2O, and HAN are also studied as promising propellants to substitute the highly pollutant hydrazine in monopropellant applications [2].

During last decade a lot effort in space industry have been put to overcome the limitations of hybrid rocket engines and to provide sufficient research publications on storable green oxidizers at such a point that the future technologies of hybrid rocket engines are potentially market disruptive in space propulsion field. [3][4][5][6]

1.2 Objectives

This thesis aims to provide a wide literature survey of storable green oxidizers. It focuses on hydrogen peroxide, nitrous oxide and hydroxyl-ammonium nitrate applied to monopropellant and hybrid rocket engines.

The work first faces the issues encounter during the design of a monopropellant rocket engine: properties and performances of the propellant, model of decomposition, architecture constraints induced by the propellant itself.

Then the objective is to study the application of those storable green oxidizers in hybrid rocket engines. From the open literature, this thesis described models and experimental data of paraffin-fuel regression rate vs oxidizer mass flow rate. At the end, the thesis provides some keys for the design of monopropellant and hybrid rocket engines that face the architecture constraints implied by the oxidizers properties.

Finally, a NASA CEA thermochemical analysis compares the performances of those three storable green oxidizers in term of chamber flame temperature and vacuum specific impulse in a hybrid rocket engine.

1.3 Outline

- **Chapter 2: Hydrogen Peroxide**. Physical properties and their consequences on devices are described. Discussion about the concentration of H_2O_2, its availability, and its storage. Presentation of the theoretical model of decomposition, application and performance in monopropellant thrusters. Regression rate vs oxidizer mass flux model and experimental data in HRE are presented. Applications and architecture constraints in HRE are detailed.

- **Chapter 3: Nitrous Oxide**. Physical properties and their consequences on devices are described. Discussion on Nytrox mixtures advantages and constraints. Presentation of the decomposition path, application and performance in monopropellant thrusters. Regression rate vs oxidizer mass flux data and applications in HRE from the open literature are presented.

- **Chapter 4: Hydroxyl-Ammonium Nitrate**. Physical properties and their consequences on devices are described. Discussion on HAN-based monopropellants advantages and constraints. Presentation of the particular decomposition path, catalytic decomposition, application and performance in monopropellant thrusters. Short discussion on the difficulties to develop a HAN hybrid rocket engine.

- **Chapter 5: Thermochemical Analysis NASA CEA**. Thermochemical analysis with the NASA CEA code using those three storable green oxidizers in HRE are presented. Performance with paraffin $C_{50}H_{102}$ in terms of chamber flame temperature and vacuum specific impulse are compared between hydrogen peroxide, nitrous oxide, and hydroxyl-ammonium nitrate.

- **Chapter 6: Conclusions**. A concise summary of the work is presented.

Chapter 2

Hydrogen Peroxide

This chapter summarizes all existing open literature data, experiments and relevant information about hydrogen peroxide application to monopropellant and hybrid rocket engines. Hydrogen peroxide (HP) is actually the most promising storable green oxidizer thanks to its storability, versatility, high density, low vapor pressure, and relatively weak O/F dependence of the specific impulse with typical solid fuels.

2.1 Characteristics

2.1.1 Physical properties

Hydrogen peroxide is a dense, low vapour pressure, totally transparent and low viscosity liquid that has the appearance of water. Hydrogen peroxide in pure form is of scientific interest only and is not produced on an industrial scale so HP is most commonly available as a solution in water. An hydrogen peroxide solution is typically characterized by its mass fraction of H_2O_2 in the aqueous solution. In space propulsion applications, HP shows different grades from 85% to 98% and this mass concentration has an impact on the properties and performances of the HP. The main physical properties of hydrogen peroxide at concentrations of 98% and 90% are detailed in the Table 2.1. Liquid oxygen and hydrazine are also added in this table as elements of comparison because they are very common propellants in monopropellant and hybrid rocket engines. [7]

	LOX	**Hydrazine**	**HP 98%**	**HP 90%**
Active O_2 content [%]	100	-	46	42
Boiling point at 1 atm $[K]$	90	386	422	414
Freezing point $[K]$	54	274	270	261
Density (293 K liquid) [g / cm^3]	1.141	1.01	1.431	1.395
Vapour pressure [Pa]	5200 ($89K$)	1400 ($293K$)	133 ($293K$)	200 ($293K$)
Molar mass [g / mol]	32	32.05	33.7	32.4

Table 2.1: Physical properties of hydrogen peroxide, liquid oxygen, and hydrazine.

The non-cryogenic nature and very high boiling point of HP make it easier and cheaper to handle than LOX. The vapour pressure of HP much lower than for the other propellants makes it even more easy to handle and store. This is suitable for small and medium devices where simplicity and low cost solutions are prioritized. HP is 23% denser than LOX and 40% denser than hydrazine. High density provides an higher tank volumetric efficiency. The more HP is concentrated the better the properties are and so the better the performances will be.

Hydrogen peroxide has good performances for a storable oxidizer because it stores an important proportion of O_2 (up to 46% in mass for HP 98%) in a high density storable liquid. This O_2 is produced in the exothermic decomposition of the H_2O_2 by the following chemical reaction :

$$H_2O_2 \longrightarrow H_2O \ + \ \frac{1}{2}\,O_2 \ + \ q\,; \quad q = -98.1\,\mathrm{kJ\,/\,mol} \tag{2.1}$$

The heat released during the reaction is equal to 2.887MJ/kg which is similar to the exothermic decomposition of hydrazine. Hydrogen peroxide is used as an oxidizer in hybrid rocket engines but due to the capability of exothermic decomposition it may also act as a monopropellant. Details of the decomposition process is discussed in section 2.2: Decomposition and catalysis.

2.1.2 Performance characteristics in space propulsion

This section provides performance data as a collection of all information that can be found in the open literature. The values come from different sources [6][8][9][10] and so arise from different theoretical models and different experimental measurement process. Therefore, the values reported here do not have to be taken as exact values for comparison or for a sizing calculation. The objective is to show the pertinence in term of performance in using hydrogen peroxide in monopropellant and hybrid rocket engines. An analysis of performance using NASA CEA is preformed in chapter 5 to provide comparison elements between the different concentrations of HP and other storable green oxidizers.

Table 2.2 shows the monopropellant performances of hydrogen peroxide at 90% and 98% grades. It is compared to hydrazine, one of the most performing monopropellant and the most used one.

	Hydrazine	**HP 98%**	**HP 90%**
Specific Impulse Isp [s]	240	190	160
Density Specific Impulse x10^3 [$\mathrm{kg\,.\,s\,/\,m^3}$]	242	272	265
Flame Temperature T_c [K]	1100	1250	1050

Table 2.2: Monopropellant performance characteristics of hydrogen peroxide and hydrazine.

Hydrogen peroxide has monopropellant performances comparable to hydrazine. The slightly lower specific impulse is compensated by its higher density which provides a better density specific impulse. The flame temperature indicated corresponds to the theoretical temperature of a perfect decomposition of the propellant. In reality this temperature will be lower depending on the efficiency of the decomposition. H_2O_2 decomposition products

low molecular mass H_2O, so HP benefits from a high specific impulse even at lower flame temperature as $Isp \propto \sqrt{T_c/M}$.

Table 2.3 shows the performances of hydrogen peroxide at 70% and 90% in a common hybrid rocket engine configuration using PE as fuel [11]. HP is compared to LOX which is the most powerful oxidizer and the most used one in hybrid rocket engines when the highest performance is the design driving parameter. This table gives an overview of advantages of HP over LOX in hybrid rocket engines. Performances of HP with specific fuels in hybrid rocket engines are detailed in section 2.4: Hybrid rocket engine applications.

	LOX	**HP 90%**	**HP 70%**
Optimum O/F ratio	2.53	7.2	10.4
Specific Impulse Isp [s]	300	274	243
Flame Temperature T_c $[K]$	3655	2800	2232
Characteristic velocity c^* [m/s]	1803	1613	1446

Table 2.3: Performance characteristics of hydrogen peroxide and liquid oxygen in a hybrid rocket engine configuration using PE as fuel.

The 7.2 optimum O/F ratio with HP 90% is much higher than with LOX and this is responsible for a lower combustion temperature T_c. Lower combustion temperature reduces the size of the high cost fuel section which must withstand full combustion pressures and temperatures.

In addition, the monopropellant characteristics of hydrogen peroxide provide substantial system-level advantages over LOX-based systems. The decomposition energy of HP provides ignition systems requiring no other fluid. Systems using HP can make use of the monopropellant nature of this fluid to simplify engine cycles, and enjoy a density impulse advantage over that of LOX.

As it is expected, the denser HP is (high concentration) the more effective the propulsion device is (Isp and temperature of decomposition or combustion). However, the higher the concentration grade of hydrogen peroxide the less it is available, the more difficult it is to store and the more expensive it is to produce.

Cost and logistic aside, the concentration of HP is a main parameter in the study of its decomposition and catalysis and it has a strong impact in the design of the catalytic bed. This is discussed in the next section 2.2: Decomposition and catalysis.

2.1.3 Production and storage

Hydrogen peroxide offers better propulsive performances at higher concentration but highest grades are difficult to produce and face stronger constraints and regulations for the storage. For transportation, hydrogen peroxide concentration is currently regulated below 60% for handing, storage and shipping safety. This induce high shipping cost and the need to produce the desired grade of HP at the delivery point. Industries are planning to increase the concentration up to 70% for transportation in near future for saving about 15% shipping cost [9].

Hydrogen peroxide for space propulsion applications becomes interesting in terms of performance at concentrations higher than 85% and it is usually used at concentrations greater than 90%. The highest grade of hydrogen peroxide is known as HTP (98%+), high test peroxide, an aqueous solution of hydrogen peroxide of over 98% concentration and high purity. The European Space Agency (ESA) is conducting extensive experimental research in HTP for its practical utilisation in space propulsion applications, as it may be successfully used in various rocket engines. Even if HTP is very expensive to produce compared to transportable grades, hydrogen peroxide remains a low cost propellant. Pure hydrazine is 20 more expensive than HP 99% and LOX cryogenic nature makes its storage and operability way more expensive than HP. In Europe, HTP is mainly produced by the Polish Institute of Aviation (IoA) laboratory but the production is limited to 300kg per year because of the cost and complexity. Rocket grade hydrogen peroxide (90%+) are highly purified and stabilized to be stored at ambient temperature. However, the stabilizer added (0.5% sodium pyrophosphate) which rise stability, partially suppress decomposition function of catalyst.

Hydrogen peroxide of any class is not considered as a flammable, explosive or toxic substance but factors may cause spontaneous decomposition of HTP, and, as a consequence, fire or even explosion may occur. HTP is a very stable material under normal conditions, when properly stored. Ready to use HTP is stored under controlled conditions (280 K) in special vessels [4].

2.1.4 Environmental and toxicity considerations

Monopropellant thrusters using hydrogen peroxide product almost only vapor water. The residual H_2O_2 that has not been decomposed is considered as a non toxic substance and has a low environmental impact. Comparatively, hydrazine itself and its decomposition products have an high environmental impact. Hydrazine is also highly toxic, its mutagen and carcinogen effects impose the most stringent quantity distance requirements. This is a strong disadvantage for manned missions.

Fig. 2.1 from the American Institute of Aeronautics and Astronautics shows the mole fraction of combustion products at nozzle exit of HP/PE (left) and LOX/PE (right) hybrid rocket. It gives a first insight of the potential of HP to reduce the environmental impact of actual hybrid rocket engines. In this example, CO and CO_2 fraction in the exhaust are reduced by two thirds by using hydrogen peroxide instead of liquid oxygen which is already considered as a low pollutant propellant.

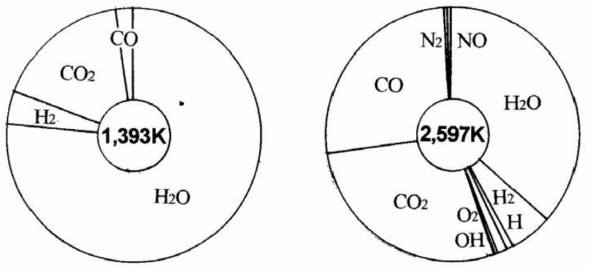

Figure 2.1: Mole fraction comparison of combustion products at nozzle exit of (left) HP/PE and (right) LOX/PE hybrid rocket engine [9].

2.2 Decomposition and catalysis

2.2.1 Decomposition path

Hydrogen peroxide decomposition reaction produces the gaseous O_2 required for the combustion and H_2O generally in liquid phase. The stoichiometric reaction (Eq. 2.2) releases 98.1 kJ/mol (2.887 MJ/kg) of heat which heats the products up to 1220 K and almost instantly vaporises the H_2O produced. The exothermic nature of HP decomposition offers substantial system-level advantages in hybrid rocket engines and makes it usable as a monopropellant.

$$H_2O_{2\ (aq)} \xrightarrow{k} H_2O_{\ (l)} + \frac{1}{2} O_{2\ (g)} + q\,; \quad q = -98.1\,\mathrm{kJ\,/\,mol} \tag{2.2}$$

The kinetics of this reaction, defined by the kinetic parameter k, is an important parameter for space propulsion. The mass flow rate of HP in the engine should be adapted to its decomposition rate (production rate of the oxidizer O_2) and to the residential time of HP in the decomposition chamber. A better and faster decomposition allows an increase of the mass flow rate of HP and so increases the thrust capability of the engine [12]. The kinetic parameter is linked to the activation energy E_a and to the temperature (expressed in Kelvin) of HP via the Arrhenius law (Eq. 2.3).

$$k = A\,\mathrm{e}^{-E_a/RT} \tag{2.3}$$

R is the gas constant (8.3145 J/K mol), and A the pre-exponential factor. The activation energy for uncatalysed hydrogen peroxide decomposition is 75 kJ/mol [13] and the decomposition energy of 98.1 kJ/mol of HP are shown in Fig. 2.2.

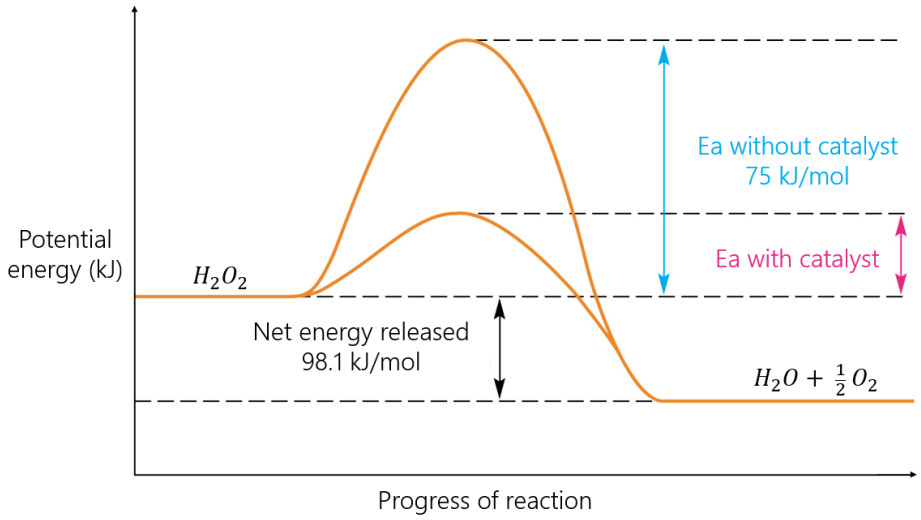

Figure 2.2: Hydrogen peroxide decomposition energy state with reaction progress. [13]

Activation energy barrier must be overcome to realise the decomposition. The energy of molecules in the HP solution is not uniform but distributed. Even with a low additional thermal energy compared to the activation barrier, at certain time, some molecules have high enough energy to decompose. So even at ambient temperature, HP decomposes but at a very low rate (<1% per year). When thermal energy increases, more molecules overcome the energy barrier and so the decomposition is faster. This phenomenon is described by the exponential nature of the Arrhenius Law.

In order to increase the kinetic parameter of the decomposition reaction two ways exist:

- increase the temperature of the hydrogen peroxide to overcome the activation energy barrier. This is called the thermal decomposition;
- use a catalyst in order to lower the activation energy of the reaction as it is shown in Fig. 2.2. In presence of a catalyst material, HP decomposes faster. This is the catalytic decomposition.

Thermal decomposition of hydrogen peroxide has only recently found some applications in propulsion systems due to the difficulty in exceeding the activation barrier of decomposition reaction. According to McLane [14], hydrogen peroxide decomposes thermally in the temperature 740 K-810 K so the propellant requires a pre-heating [15]. The low vapor pressure of HP prevent the risk of rapid vaporization yielding to explosion. Issues related to the thermal decomposition in space propulsive applications are not observed in the open literature because pure thermal decomposition is never used. Applying a heterogeneous catalyst is a more practical solution. Catalyst lowers the activation energy, making possible to initiate its decomposition at ambient temperature. According to Wernimont et al.[16] 82% HP may be catalytically decomposed at 255 K, which is close to its freezing point.

In the open literature, activation energy values for HP decomposition on different catalysts are usually not stated. As discussed later in sections 2.2.3 and 2.3.1, catalyst materials in monopropellant and hybrid rocket engines are rather characterized by their decomposition efficiency which depends on the activation energy. However, some values have been found and have been reported below but the context and materials do not always correspond to propulsive applications.

The uncatalysed reaction of HP decomposition generally has a value of activation energy of 75 kJ/mol [13][17], 71 kJ/mol is found in [18]. A value of 63.6 kJ/mol is reported in [19] at pH=10. Hiroki and LaVerne [18] report values for activation energy of HP decomposition in aqueous suspensions of nanometer-sized particles of different oxides: 36 kJ/mol with TiO_2, 38 kJ/mol with Al_2O_3, 40 kJ/mol with CeO_2, 42 kJ/mol with ZrO_2 (33$\pm$1.0 kJ/mol in [20]), 48 kJ/mol with SiO_2. The enzyme-catalysed reaction lowers the activation energy to 17.5 kJ/mol in [21], 11.2 kJ/mol in [17], 12.9$\pm$0.7 kJ/mol in [22], 19.8 kJ/mol in [23], 23.5 kJ/mol in [24], and in presence of inhibitor $K_2[B_3O_3F_4OH]$ it is 37.8 kJ/mol [17]. Finally, a value of 18.9 kJ/mol is reported in [25] with multi-walled carbon nanotubes.

2.2.2 Thermal decomposition

Hydrogen peroxide is continuously thermally decomposed but at a very low rate when properly stored at ambient temperature (<1% per year). The thermal decomposition is significant only at very high temperature. In order to avoid heating systems that are power and mass demanding, catalytic beds are used to decompose HP at its initial ambient temperature. The catalyst beds become quite bulky in higher mass flow applications and there is an interest in a separate injection of hydrogen peroxide downstream of a catalyst bed exhaust in order to minimize system mass and maximize the decomposition. In this concept, the after-injected HP is mixed to the hot exhausts of the catalytic bed and undergoes evaporation and thermal decomposition easily. A model of this thermal decomposition post catalytic bed is given by Corpening et al. in reference [26].

In monopropellant engines, catalyst beds are necessary and actually there is no other solution to efficiently decompose the hydrogen peroxide and ensure the re-ignitablity. However in hybrid rocket engines, an alternative non-catalytic ignition method to initiate combustion is in development by Utah State University [13]. The alternative method is based on controlled thermal decomposition and ensures the re-ignitablity. An external source provides sufficient heat to overcome the activation energy only at ignition. The large amount of energy released by the decomposition is not sufficient to maintain the continuous thermal decomposition of HP but it is sufficient to pyrolyze the fuel and start the combustion. The heat released by the combustion is sufficient to continuously decomposes the HP while it is injected in the combustion chamber. This configuration enables a important save in mass and volume because there is no catalyst bed but the external source of energy should not be heavy and ensure the re-ignitablity. The main drawback is the difficulty to provide a safe, controlled, and multiple ignition.

Previous methods tested have involved pyrotechnics and present a significant risk of an uncontrolled reaction and explosion. The alternative non catalytic ignition method is based on an electrical arc technology. The arc-ignition technology uses the electrical properties of certain 3-D printed thermoplastic fuels such as acrylonitrile butadiene styrene (ABS), low density polyethylene (LDPE) and high-impact-polystyrene (HIPS). The 3-D printed fuels are manufactured with the integrated electrode paths for the creation of the electric arc.

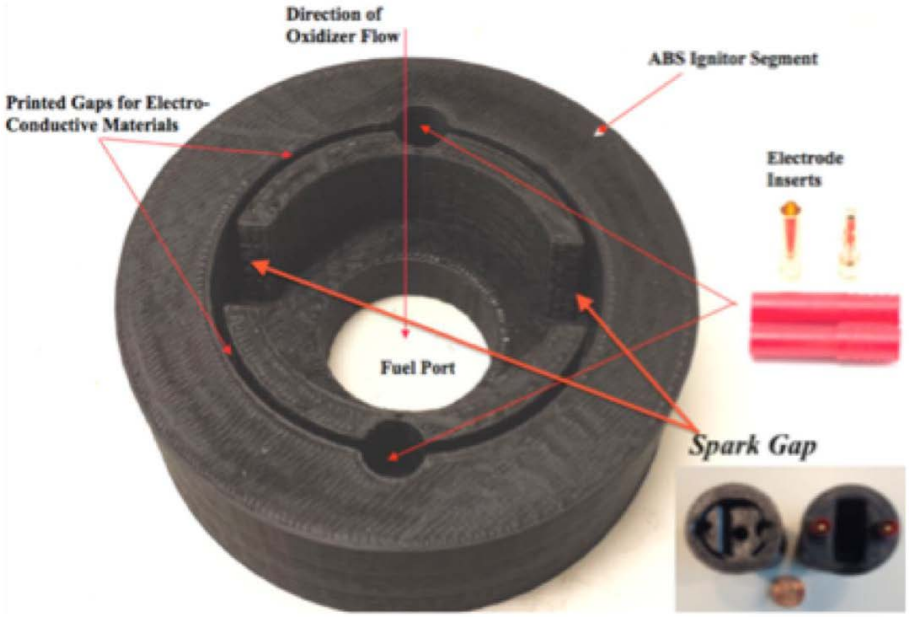

Figure 2.3: Additively-manufactured fuel grain with integrated electrode paths [13].

The performances of this system and its application in hybrid rocket engines are discussed in section 2.4 Hybrid rocket engine applications.

No other relevant thermal ignition system exists for HP decomposition in propulsive applications. Catalytic decomposition is widely used for its heritage, safety, multiple use and good performance.

2.2.3 Catalytic decomposition

The catalyst has to fulfill several requirements:

- high activity and stability in a wide range of operating conditions (varying from H_2O_2 in liquid phase to H_2O_2 in vapor phase at elevated temperature);
- high resistance to thermal and mechanical shocks associated to ignition/shut down cycles;
- high resistance to the stabilizing agents normally added to HTP solutions to improve the long-term storability;
- short response time.

The development of a catalytic chamber able to simultaneously satisfy the above requirements is not an easy task and different technological solutions have been proposed in literature [12]:

- **Packed catalysts:** Unstructured, they are usually obtained by properly stacking metallic gauzes or ceramic pellets;
- **Monolithic catalysts:** Structured, they rely on the utilization of honeycomb support similar to those used in automotive catalytic converters.

Temperature of the decomposed gaseous products is a key parameter in monopropellant and hybrid rocket engines because it drives the performances of the engine. This temperature highly depends on the grade of the HP and on the extent of the decomposition which is never perfect. This is why HP at high concentration level offers better performance. Catalytic beds are characterised by the efficiency of the decomposition they provide for a given mass flow rate of HP solution. Thus, choosing appropriate catalytic bed geometries and materials is critical in order to obtain an efficient enough decomposition, especially in hybrid rockets to avoid a wet start that may affect ignitability of the system.

From the catalytic bed efficiency, an effective mass ratio of hydrogen peroxide in the solution can be formulated. The general reaction for catalytic decomposition of hydrogen peroxide is written as:

$$f H_2O_2 \; + \; (1-f)\frac{M_{H_2O_2}}{M_{H_2O}} H_2O \rightarrow \eta f \left(H_2O + \frac{1}{2} O_2 \right) \; + \; (1-f)\frac{M_{H_2O_2}}{M_{H_2O}} H_2O + (1-\eta) f H_2O_2 \tag{2.4}$$

where, f is the hydrogen peroxide mass fraction in the solution and η is the decomposition efficiency. The effective solution mass ratio of active HP in the solution is defined as the mass of desired products over mass of hydrogen peroxide added to the mass of undesired products [13]. Inspection of Eq. 2.4 shows that the effective solution mass ratio for decomposition is:

$$\eta_{effective} = \frac{\eta \; f}{1 + (1-\eta) f} \tag{2.5}$$

The concentration identified by Eq. 2.5 leads directly to an estimation of HP decomposition temperature T_0 reported in Fig. 2.4. Temperature of decomposed products reaches 1220 K for HTP (+98%).

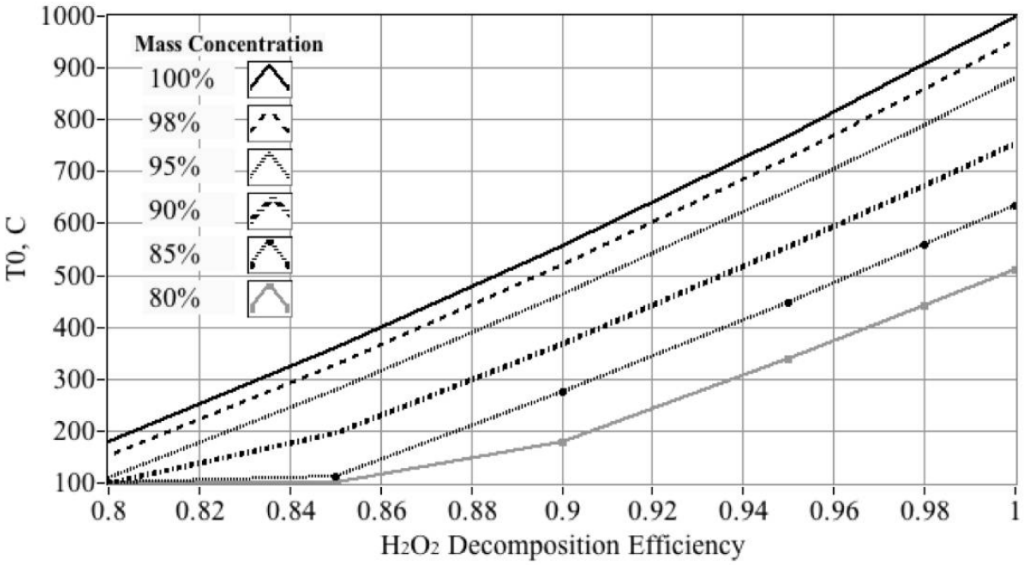

Figure 2.4: Estimated hydrogen peroxide decomposition temperature as a function of catalytic bed efficiency and mass concentration [13].

Materials used for the catalysis should resist to the decomposition temperature. Therefore, they differ with the grade of HP used. Geometry of active elements in the catalytic bed provides the sufficient surface area for a fast and efficient decomposition of HP and ensures an adapted loading factor to the mass flow rate of HP. Indeed, a pressure drop occurs across the catalytic bed and the bed loading has a strong effect on pressure losses. This pressure drop cools the decomposition products, potentially dropping the temperatures to levels that are below the pyrolysis temperature of the fuel in hybrid rocket engines. The compromise between decomposition efficiency and pressure drop leads to use materials highly active with the hydrogen peroxide while fulfilling the requirements mentioned before.

The catalyst performance depends on the combination of the active phase and of the support material and shape. Among numerous compounds catalyzing the hydrogen peroxide decomposition, manganese oxides, platinum, and silver are preferred and are the most represented in available literature.

A simple and efficient solution of packed catalytic bed is a properly stacking of metallic gauzes. Composed of silver and silver-plated nickel mesh sheets for the high reactivity of hydrogen peroxide in presence of silver, they run at efficiency over 95% [12]. The high surface area achieving this level of efficiency creates a large pressure drop involving the use of a larger and heavier feed pressure system. Made of silver and nickel those catalytic bed are also heavy and expensive. The limiting factors are the low melting temperature of silver at 1235 K and the fact that silver can poisonously react with stabilizers added in HP solution of high concentration. For those reasons, 90% is the highest concentration of HP that can be run on these beds. For HTP (+98%) decomposition, a very interesting alternative seems to be platinum supported on metal-ceramic wire mesh as shown in Fig. 2.5. Platinum has better thermal and mechanical resistance properties than silver but its slightly lower activity with HP at low temperatures increases the ignition time of the engine [27]. Platinum metal catalysts can lower the activation energy from 75 kJ/mol to about 49 kJ/mol [13].

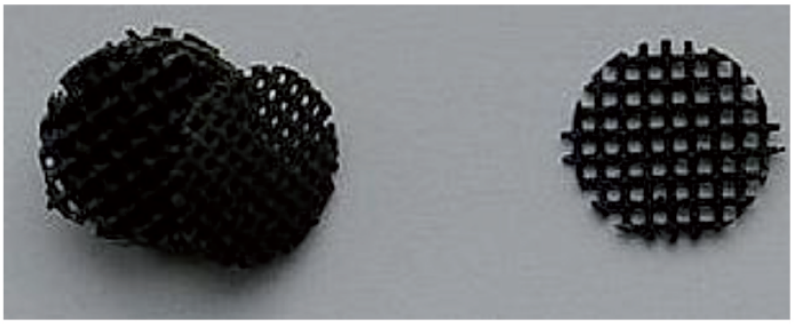

Figure 2.5: Platinum catalyst supported on steel-ceramic wire mesh, manufactured by Catator. [27]

Granulated or pellet catalysts with a support based on aluminum oxide (Al_2O_3) exhibit enhanced heat resistance allowing use of 95–98% hydrogen peroxide. However those supports suffer of mechanical structure integrity issues. Thermal shocks at startup and shutdown reach 200 – 300 K/s and cause cracks in pellets (Fig. 2.6) and can make them break apart and leave the bed [12].

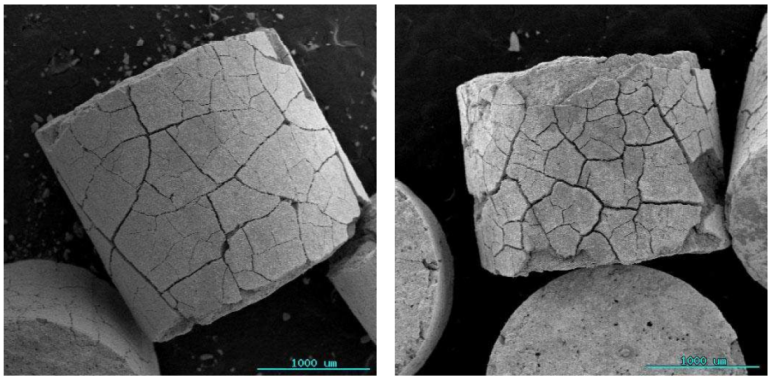

Figure 2.6: Degradation of pellets: images before and after test. [28]

Manganese oxides (Mn_xO_y) are used as active phases on those aluminium oxide supports. Those pellet catalysts (Mn_xO_y/Al_2O_3) provide higher contact surface than described above platinum-grid catalysts. This is mostly due to the fact that their surface area is highly developed (Fig. 2.7) at about 250 m^2/g [27][6]. This means that they may require only a fraction of residence time for sufficient HTP decomposition compared to platinum-grid catalysts.

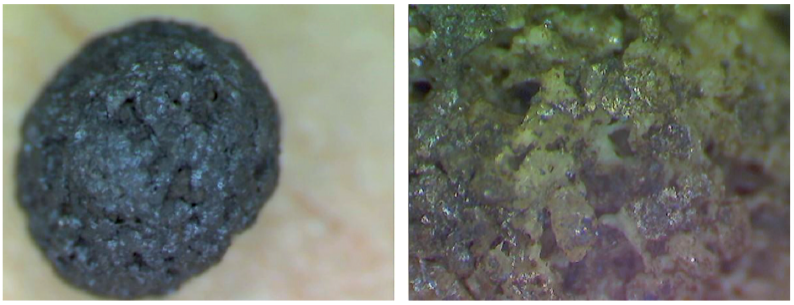

Figure 2.7: Single Mn_xO_y catalyst pellet of 3mm diameter (left, 50x magnification) and its surface structure (right, 250x magnification). [6]

While a simple stacking of silver mesh sheets is ideal to decompose HP with a mass concentration of 90% and below, heterogeneous configurations (Fig. 2.8) are used to decompose high grades of HP. They take advantage of both the good mechanical resistance and long operation life of platinum-grid and the high efficiency and activity of Mn_xO_y/Al_2O_3 pellets. Heterogeneous packed catalyst beds consist of supported (on alpha aluminium oxide) manganese oxides and metal-ceramic grid catalysts (with platinum nano-crystals as an active phase).

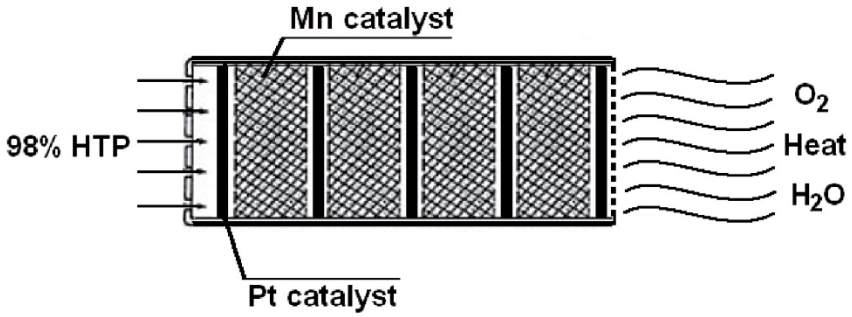

Figure 2.8: Heterogeneous packed catalyst bed scheme.[27]

The catalyst bed loading (i.e. the HP mass flux through the bed) is an important parameter of the performance and degradation of the catalytic bed. The general rule is that the higher bed loading the higher pressure drop, better starting performance and shorter life time [27]. Typical bed loads for HP catalysts are reported [29] to range from a lower limit of 20 kg/(m^2s) to a maximum of 280 kg/(m^2s) even though [30] claimed to have successfully tested a catalytic bed with a mass flux of 976 kg/(m^2s) but no information about the catalyst used in this specific case are provided. In the case of low mass flux (< 50 kg/(m^2s)), packed catalysts are widely used. However, in higher bed loading cases, catalysts with others structures are required to reduced the pressure drop and to resist to the mechanical loads: the monolithic catalysts.

Monolithic catalysts for hydrogen peroxide decomposition have been less studied than catalyst beds consisting of pellets and were under development in the United States and Europe only in the past decade. Monolithic catalysts (using a ceramic honeycomb substrate) do not exhibit the mechanical integrity issues reported above for pellets, as they are made of just one piece of material (Fig. 2.9).

Monolithic catalysts exhibit high mechanical strength allowing their use under the conditions of rapid alternating changes in the pressure and temperature in the catalyst. As compared to common gauze catalysts and granulated catalysts, monolithic catalysts have a number of advantages:

- pressure drop in the catalyst bed stabilizes the flow and so the combustion;
- higher resistance to thermal shock and wear resistance compared to pellets;
- uniform distribution of HP flow and better conditions for the mass and heat transfer;
- shorter diffusion path length, because the catalyst is present in the form of a very thin layer.

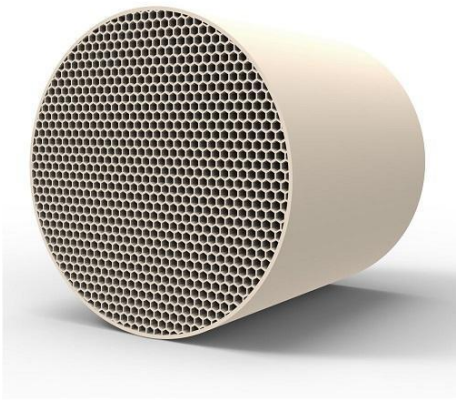

Figure 2.9: Ceramic honeycomb monolithic catalytic bed. [31]

All these properties allow such supports to be used under the conditions of rapid pressure and temperature changes in the catalyst bed. In addition, monoliths with definite flow-through channels increase the active surface area, allowing the catalyst bed volume to be decreased. Thus, monolithic catalysts are an attractive alternative to traditional systems, allowing the development of catalyst beds for micro-engines.

The structure is usually made of ceramics on which a wash-coat layer is deposited to increase the specific surface area. In order to maximize the active area to volume ratio, various channel sizes and geometries (square, circular, and hexagonal) have been investigated in [32]. The choice of the channel shape influences the total necessary monolith volume which again influences the possible number of channels in the monolith. The performance of the hexagonal and the square channels are about the same (hexagonal > square) and they perform much better than the circular one. This is mainly due to the fact that the square and hexagonal shaped channels can be arranged in a much higher density than the circular ones. Hexagonal channels are slightly more difficult and more expensive to produce than square cross sections. Typical size of a channel for the best efficiency and good enough mechanical strength is about 1 mm [32].

Details about performances, data, design impacts, models, and results of tests of those catalyst solutions for hydrogen peroxide decomposition are presented in section 2.3 Monopropellant applications.

2.2.4 Storage and material compatibility

A wide variety of materials has a catalytic activity on hydrogen peroxide decomposition but some of those materials can be poisoned by the stabilizers in HP solution. These aspect makes long-term storability of hydrogen peroxide challenging. Thus, material compatibility for storage of hydrogen peroxide has been widely studied.

According to Davies et al.[33], there are four classes of material compatibility with hydrogen peroxide and only the class-1 materials after additional surface treatment, may be used for long-term storage of hydrogen peroxide so for satellite propulsion. The most commonly used materials are pure aluminium, aluminum alloys, polyethylene, halogenated polyethylene, and PTFE plastics.

2.3 Monopropellant applications

This section exhibits results of model simulations and tests that are present in the open literature about the use of hydrogen peroxide in monopropellant engines. Attention is given to parameters that are influenced by the use of hydrogen peroxide and its impacts in the system, such as temperatures, pressures, decomposition efficiency, specific impulse and thrust.

2.3.1 Catalyst beds performances

Physical and chemical phenomena involved in the decomposition of liquid hydrogen peroxide in a catalytic bed are numerous and very complex, so its modeling is scarce in the open literature. Only Pasini et al.[34][35] provide a detailed description of those phenomena in term of equations. In particular, they refer to the rocket grade HP decomposition through pellet bed reactors.

The two-phase liquid-gas-vapor flow in the bed is treated as an homogeneous, adiabatic, chemically reacting flow, whose properties depend on the local composition, assumed equal in both phases, and on the advancement of the evaporation process.

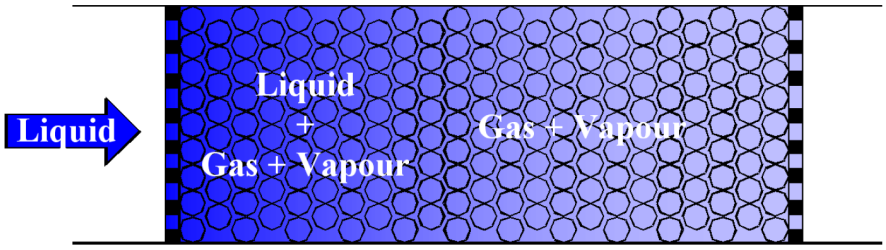

Figure 2.10: Qualitative flow path inside the catalytic bed [34].

Inlet parameters are pressure and temperature at inlet, HP mass concentration and mass flow rate. Catalytic bed parameters are the chemical nature of pellets, shape diameter and porosity of pellets, specific surface area, and loading ratio. Parameters of interest are temperatures, pressures and the advancement of decomposition along the catalytic bed and at outlet.

By introducing suitable simplifications, the mass, momentum and energy conservation equations for the reacting flow through a pellet bed reactor are specialized into a system of two first order, coupled, quasi-linear ordinary differential equations (ODEs) for the pressure (Eq. 2.7) and reaction advancement parameter (Eq. 2.6). The solution for the imposed values of the inlet properties of the HP flow allows to determine the evolution of the entire flow as a function of the distance from the inlet section of the catalytic bed. Temperature can then be calculated from the pressure and the reaction advancement parameter through the evaluation of the constant pressure specific heat [34].

$$\frac{d\lambda}{dx} = \frac{\dot{V}_l + \dot{V}_g}{u} A\, \mathrm{e}^{-E_a/RT}\, N_s \frac{K_1 C_{H_2O_2}}{1 + K_1 C_{H_2O_2}} \quad \text{with } \lambda(0) = 0 \tag{2.6}$$

$$\frac{dp}{dx} = -\left(150\frac{1-\tilde{\epsilon}}{Re_p} + 1.75\right)\frac{1-\tilde{\epsilon}}{\tilde{\epsilon}^3}\frac{\rho u^2}{D_p} \quad \text{with } p(0) = p_i \tag{2.7}$$

Where λ is the reaction advancement parameter, p is the pressure, x is the distance from the inlet section of the catalytic bed, u is the flow velocity, $\tilde{\epsilon}$ is the bed porosity, K_1 is the equilibrium adsorption constant, $\dot{V}$ is the volumetric flow rate, N_s is number of active adsorption sites per unit volume of the catalytic bed, C is the molar concentration, Re_p is the pellet Reynolds number, and D_p is pellet diameter.

Good agreement has been attained between the observed data and the model results [35]. The model provides in this way a rational framework for identifying the main operational parameters of catalytic pellet beds, understanding their interactions, and efficiently guiding the preliminary reactor sizing and design based on the indications readily obtained from sensitivity analyses.

Based on the data reported in Table 2.4, Pasini et al. have observed how the parameters of interests at the outlet vary with pellet diameter, bed loading, bed length, HP mass fraction, and imposed chamber pressure.

Catalyst	FC-LR-87 ($Pt - Al_2O_3$)
H_2O_2 mass concentration	85.7%
Pellet diameter D_p [mm]	0.6
Bed diameter [mm]	18
Bed length [mm]	60
Bed load [kg/s m^2]	19.02
Mass flow rate [g/s]	4.84
Chamber pressure [bar]	17.65

Table 2.4: Model settings of Pasini et al. simulations

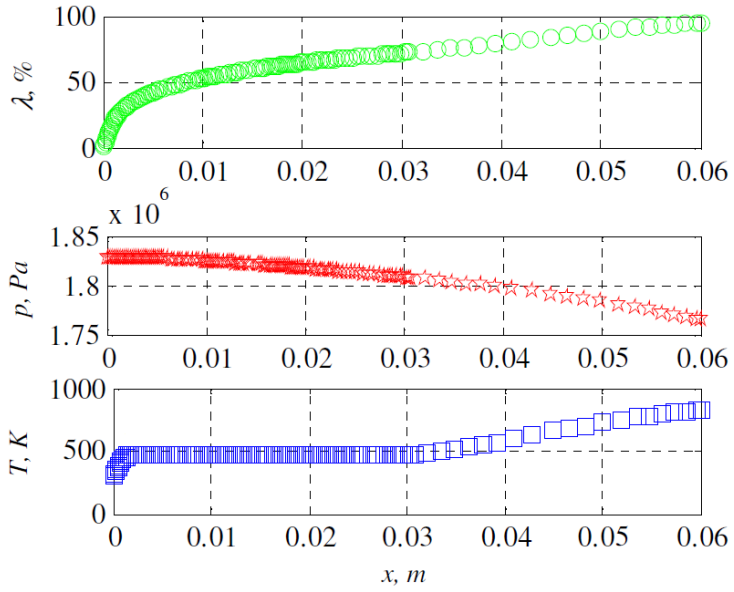

Figure 2.11: Axial profiles of the reaction advancement parameter and of the flow pressure and temperature predicted by the model for the reference catalytic bed configuration [34].

The inlet pressure parameter influences the chamber pressure so an imposed chamber pressure is seen as a parameter which replaces the inlet pressure. Results are reported below in Fig. 2.12.

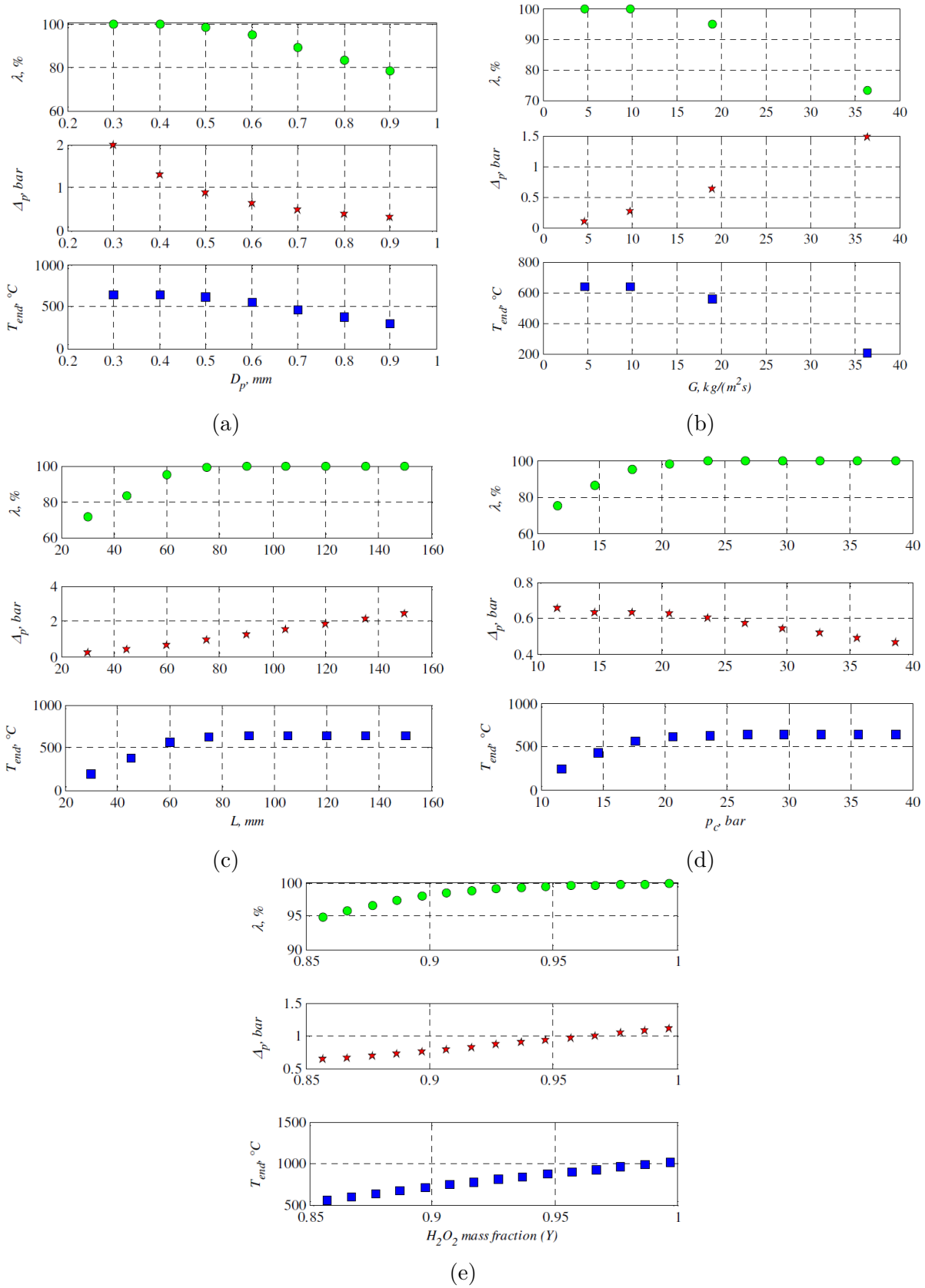

Figure 2.12: Advancement parameter λ, pressure drop Δp, and exit temperature T_{end} as functions of the (a) pellet diameter D_p, (b) bed loading G, (c) bed length L, (d) imposed chamber pressure, and (e) peroxide hydrogen mass concentration Y [34].

Relevant results on preliminary bed sizing and design are [34]:

- Reduction of pellet size improves the decomposition efficiency by increasing the active catalytic surface per unit bed volume and by raising the operational pressure of the reactor, thus accelerating its catalytic activity. Smaller pellets can also be use to maintain the level of performance while reducing the bed volume. The pressure drop increase and the volume reduction will improve the typical raise time of the thrust;

- Reduction of bed load increases the decomposition and reduces the pressure drop. But high pressure drop is important to maintain flow stability. An excessive reduction of the bed load, in the attempt to increase the thrust chamber pressure, reduces the fluid dynamic damping in the bed, exposing the chamber to the risk of development of self-sustained flow oscillations;

- Increase in bed length improves decomposition efficiency but increases the volume. It also increases the pressure drop, and as with reduction of pellet size, higher pressure drop means higher operational pressure in the bed so a better decomposition. This also contributes for the flow stability;

- Higher chamber pressure means higher operational pressure so a better decomposition. However, the increase in the chamber pressure is limited by the mechanical properties of materials;

- Higher hydrogen peroxide concentration increases the temperature and so the kinetics of the reaction.

Any further improvements of the decomposition kinetics must rely on more efficient catalyst/substrate combinations. The catalyst bed performance strongly depends on the type of catalyst applied as well as the active phase content so a characterization of catalytic bed materials performances is performed.

Despite high cost and the development of new catalysts for hydrogen peroxide decomposition, silver catalysts are still widely used in the existing and newly developed thrusters. The main advantages of silver catalysts are high efficiency of hydrogen peroxide decomposition, small size, relatively easy fabrication, and availability of numerous shapes. However, silver catalysts are limited to hydrogen peroxide of 90 wt%. Such a limitation is due to the temperature of decomposition that becomes higher than melting temperature of silver at higher HP concentration. Also silver is poisoned by stabilizers present in HP solution, thus limiting life time of those catalysts at good efficiency. High (up to 95–100%) degree of decomposition of 90% hydrogen peroxide [36] and a specific impulse of 101 s with a c* efficiency of 0.9 [37] and 104.4 s with a c* efficiency of almost 1 [38] have been reported for catalysts based on silver gauzes. Silver catalysts are mainly used for the development of 0.5–1 N thrusters [39].

The previously developed catalysts based on silver gauzes start to be inferior to granulated and monolithic catalysts. Granulated catalysts with a support based on aluminum oxide exhibit enhanced heat resistance allowing use of 95–98% hydrogen peroxide. Porous aluminum oxide is the most widely used support (due to its high specific surface area), and platinum metal and manganese oxides are the most widely active phases.

The most frequently used materials for preparing granulated catalyst supports are γ-alumina because of its high specific surface area and α-alumina because of its high heat resistance [27]. However, their use for preparing the catalyst depends on the concentration of the hydrogen peroxide used. $\gamma - Al_2O_3$ was found to be more sensitive to the thermal shock than the $\alpha - Al_2O_3$. When using 98% hydrogen peroxide, high temperature causes phase changes in $\gamma - Al_2O_3$, leading to a decrease in the specific surface area. The specific surface area of the more heat resistant $\alpha - Al_2O_3$ is lower by two orders of magnitude than that of $\gamma - Al_2O_3$ for the same particle size, and the performance of catalysts based on it is somewhat lower [40]. Surmacz [27][41] has compared the influence of the aluminium supports on the temperature obtained with HP 98% in a manganese oxides catalytic bed. Results are reported in Fig. 2.13.

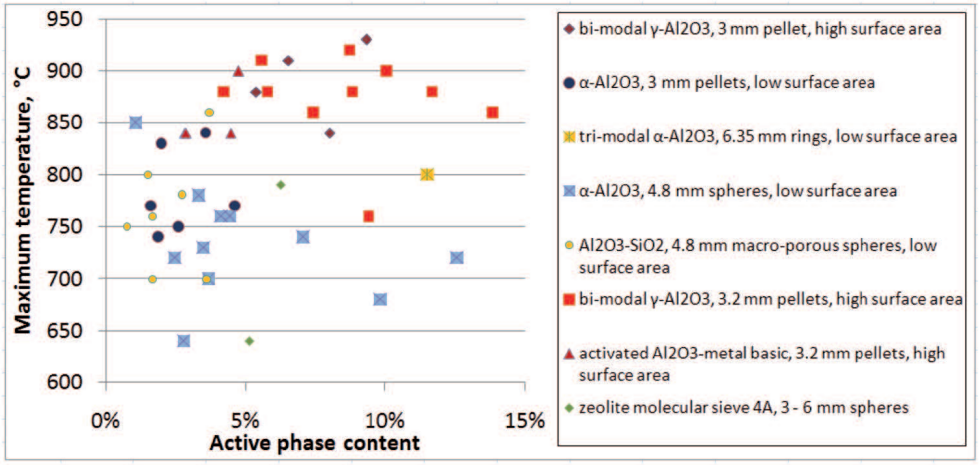

Figure 2.13: Maximum temperature obtained after five-second HTP flow (cold start) for various tests and types of support [27].

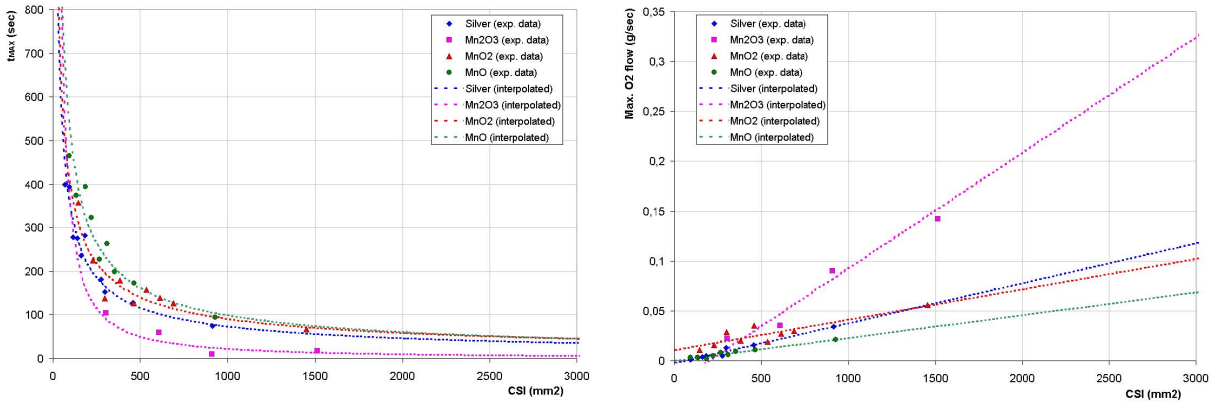

(a) (b)

Figure 2.14: (a) Time needed by the liquid mixture to reach the peak temperature and (b) maximum mass flow of exhaust oxygen, as a function of CSI (Contact Surface Index), for four different powders [41].

Catalysts based on the active phase of manganese oxides are being widely tested and are used in monopropellant thrusters and hybrid engines. Preliminary heating of the catalyst to 420 K-470 K appreciably improves the process stability and decreases the

decomposition onset time. Bramanti and Torre et al.[41] have studied the performance of silver powders and of different manganese oxide powders: MnO, MnO_2, and Mn_2O_3. This, in order to determine which of those materials are the most active with hydrogen peroxide.

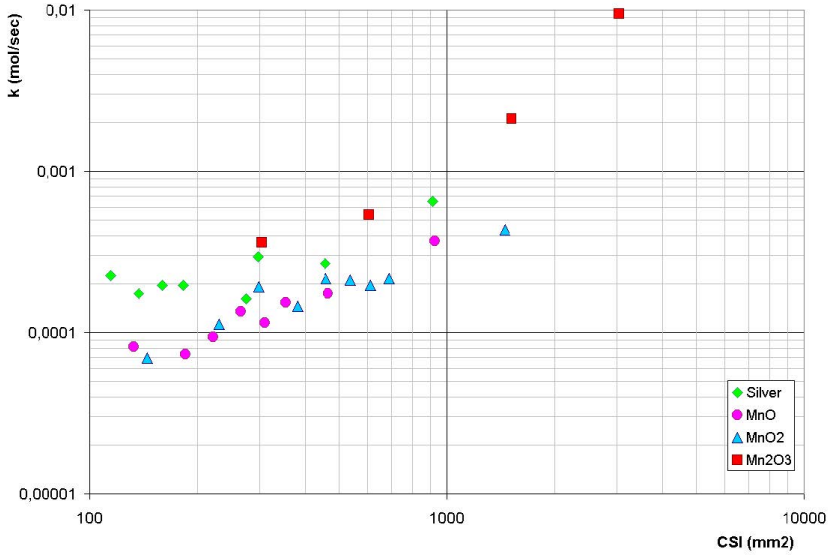

Figure 2.15: Reaction rate, as a function of CSI, for different powders at 300 K liquid mixture temperature [41].

Experiments on powders show that Mn_2O_3 is the most effective catalytic material, followed by silver and MnO_2 (the last two show a very similar catalytic activity) and, as the less active material, MnO (Fig. 2.14 and Fig. 2.15). In particular, the performance of Mn_2O_3 is significantly better than that of all the other tested materials. High performance is obtained in both transient (response time < 1 s during start) and steady (c* efficiency up to 96%) conditions.

Platinum metal is also used on aluminum oxide support. Experiments have been conducted by both Alta and DELTACAT [41] to compare activity of metallic gold, platinum, palladium and silver on HP. Results show that silver seems to be the most active catalytic metal, followed by platinum, palladium and gold. However, in some of the tests carried out by DELTACAT it has been noted that silver wire dissolved with time due to the already mentioned poisoning. Platinum catalysts are commonly used in 5–50N thrusters. High activity of the catalyst ensures 95–98% decomposition of 98% hydrogen peroxide [42] and up to 99% c* efficiency [43]. The thruster developed in [42] has a specific impulse on the sea level of 130s, which corresponds to 185s in vacuum.

Monolithic catalysts exhibit high mechanical strength allowing their use under the conditions of rapid alternating changes in the pressure and temperature in the catalyst bed [40]. Monolithic catalysts are an attractive alternative to traditional systems, allowing the development of catalyst beds for micro-engines. Their surface area is considerably larger than that of gauzes, and the foams made of active metals do not require deposition of the active phase. One of the drawbacks is large pressure drop in the catalyst bed due to irregular structure. Monolithic catalysts for hydrogen peroxide decomposition have been less studied than catalyst beds consisting of pellets and data comparing their efficiency are not actually existent in the open literature.

The performance of hydrogen peroxide decomposition catalysts are compared in several papers; the results are often contradictory.

Pirault-Roy et al.[44] and Amrousse et al.[45] studied the catalytic activity of silver, platinum, and manganese dioxide in hydrogen peroxide decomposition and found that the catalysts could be ranked in the following order: $Mn_2O_3 > Ag > MnO_2 > Pt$.

Romeo et al.[46] compared the performance of two types of catalysts on ceramic support. The following activity series was obtained: $Pt > Ag > Mn_xO_y$. The performance of silver was equal to that of platinum; however, after 15 runs the performance suddenly sharply decreased.

Surmacz [27] presented published data on the experimental qualitative evaluation of the activity exhibited in the decomposition of hydrogen peroxide by some types of catalysts deposited onto $\gamma - Al_2O_3$ by impregnation. The catalysts can be ranked in the following order with respect to the catalytic activity: $Pt/Al_2O_3 > Mn_xO_y/Al_2O_3$. However, according to [47], granulated catalysts based on manganese and aluminum oxides surpass in performance silver gauze and platinum on aluminum oxide. On the other hand, in [48] pellets of a platinum catalyst on an aluminum oxide support surpassed in performance pellets of manganese oxide on the same support.

The above data and all other studies with other materials show that manganese oxide and platinum catalysts exhibit the highest performance irrespective of the support.

No information about the toxicity and environmental impacts of the catalyst materials have been found. Probably these impacts are negligible or nonexistent because the catalyst materials are not expelled in the atmosphere and are not in direct contact with human (no fluid phase).

2.3.2 Relevant realizations

This section briefly revises open literature data on the performance of monopropellant systems using hydrogen peroxide. Relevant data that can be found concern thrusters using Pt/Al_2O_3 [49][50][29] or monolithic [12][32] catalysts. Performances are measured by means of the characteristic velocity efficiency ("c* efficiency") and the "temperature efficiency". In the c* efficiency, the experimental characteristic velocity computed from the measurements of the propellant mass flow rate, the chamber pressure and the nozzle throat cross-sectional area is compared to the theoretical characteristic velocity corresponding to the ideal case of complete adiabatic decomposition: Eq. 2.8.

$$\eta_{c^*} = \frac{c^*_{exp}}{c^*_{th}} = \frac{\frac{p_c^{exp} A_t}{\dot{m}_{exp}}}{\sqrt{\frac{RT_{ad}}{\gamma}} \left(\frac{\gamma+1}{2}\right)^{\frac{\gamma+1}{2(\gamma-1)}}} \tag{2.8}$$

The temperature efficiency just highlights the first cause of degradation of the characteristic velocity, expressing how close the measured chamber temperature is to the adiabatic temperature corresponding to complete decomposition: Eq. 2.9.

$$\eta_{\Delta T} = \frac{T_{dec} - T_{inj}}{T_{ad} - T_{inj}} \tag{2.9}$$

Where T_{dec} is the measured temperature of decomposition, T_{inj} is the injection temperature of the liquid HP and T_{ad} is the adiabatic decomposition temperature.

Finally, the thrust balance allows for the measurement of the thrust history, and therefore of the experimental thrust coefficient.

$$C_F^{exp} = \frac{F_{exp}}{p_c^{exp} A_t} \tag{2.10}$$

Together with the experimental characteristic velocity, the thrust coefficient allows for the evaluation of the specific impulse.

$$I_{sp}^{exp} = \frac{c_{exp}^* C_F^{exp}}{g_0} \tag{2.11}$$

Pt/Al_2O_3 catalysts

In 2008, Pasini and Torre et al.[50][51] have compared the performances of three 5N thrusters using different Pt/Al_2O_3 catalysts identified FC-LR-87 or Pt/Al_2O_3-COM at different bed loads. Hydrogen peroxide at 87.5 wt% is considered in the study. Results are reported in Table 2.5.

	Thruster 1	**Thruster 2**	**Thruster 3**
Catalyst	FC-LR-87	FC-LR-87	Pt/Al_2O_3
Bed load [kg/s m^2]	19.02	9.92	19.26
Dwell time [s]	4.34	8.32	4.28
Mass flow rate actual [g/s]	4.84	4.87	4.90
Mass flow rate calculated [g/s]	4.84	4.87	4.90
Chamber pressure actual [bar]	17.5	18	19.6
Chamber pressure calculated [bar]	18.7	19.5	21.5
Chamber temperature actual [K]	831	900	870
Chamber temperature calculated [K]	906	945	958
Characteristic velocity c* actual [m/s]	822	840	840
Characteristic velocity c* calc. [m/s]	883	900	900
Thrust actual [N]	5.2	5.3	5.2
Thrust calculated [N]	5.9	6.1	6.2
Thrust coefficient actual	1.31	1.31	1.30
Thrust coefficient calculated	1.38	1.38	1.40
Specific impulse actual [s]	110	110	110
Specific impulse calculated [s]	124	127	130
Vacuum Specific impulse actual [s]	145	145	142
Vacuum Specific impulse calculated [s]	164	167	168
Catalytic bed pressure drop [bar]	0.65	0.30	1.0
c* efficiency	0.94	0.93	0.90
Temperature efficiency	0.88	0.93	0.865

Table 2.5: Results of Pasini et al. tests [50]. Calculated values are obtained with ideal adiabatic decomposition.

Despite the long initial transient, the steady-state propulsive performance of the thrusters have been satisfactory. In particular, both the temperature and c* efficiencies exceeded the value of 90%. Furthermore, the catalytic bed activity has not shown any degradation and demonstrated a good repeatability even after the decomposition of about 2 kg of high grade HP. The thermo-mechanical resistance of the $\alpha - Al_2O_3$ substrate seems to be compatible with typical rocket thruster applications without danger of rupture and powdering of the ceramic pellets. High decomposition efficiencies have been obtained with a platinum-deposed surface of the same order of magnitude of the geometrical surface area of the substrate pellets.

Other discussions on the bed load are presented in [29].

In 2016, Lestarde et al.[49] at ONERA laboratory have performed a monopropellant test campaign as a preliminary step for an hybrid use. Test lasted 10 s under an 87.5% HP mass flow rate of 90 g/s in 4 different Pt/Al_2O_3 catalysts. The goal is to determine the transient phase duration for temperature rise and temperature obtained.

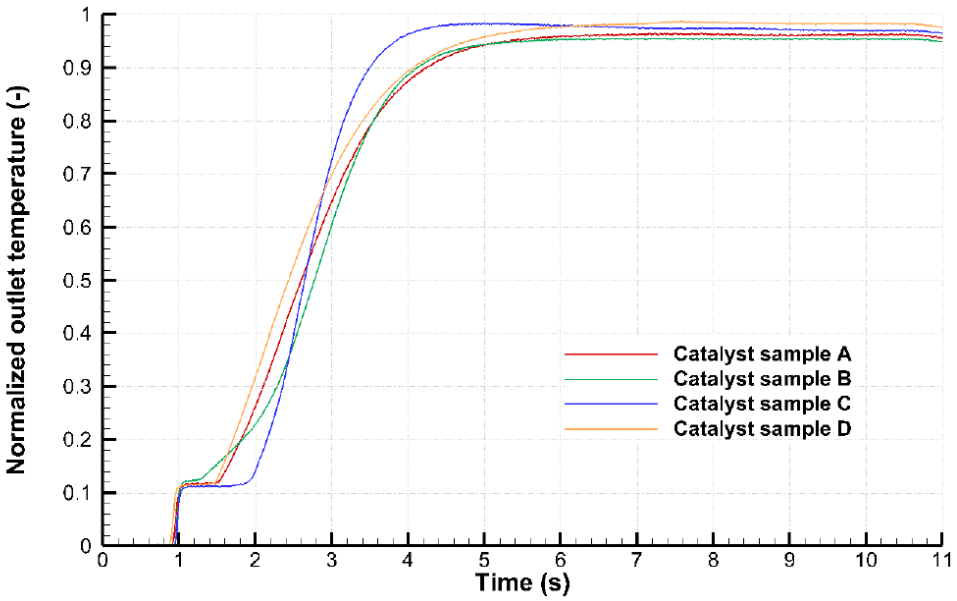

Figure 2.16: Comparison between the decomposition temperatures of the four catalyst samples [49].

It can be noticed that the smaller the catalyst particles are, the lower is the transient phase duration and the higher is the efficiency based of the normalized temperature. It reaches an efficiency based on the normalized temperature of 97.4% and a response time of about 3 s. Application of this monopropellant thruster to an hybrid rocket engine in reported in section 2.4.3.

Monolithic catalysts

Bonifacio et al.[12] have performed tests using honeycomb catalysts based on manganese, with an outer diameter of 13 mm, a cell density of 400 cells per square inch and two different lengths (30 and 60 mm); each cell has a square cross section, with a side length of 1.1 mm. The thruster uses 87.5% HP and is pressured by nitrogen. The goal was to evaluate the limitation of such catalyst in term of HP mass flow rate. Results are reported in Table 2.6

Catalyst length [mm]	30	30	30	60	60	60
Mass flow rate [g/s]	6.7	10.7	14.7	5.0	6.8	8.7
Chamber pressure [bar]	4.02	5.93	6.93	3.34	4.66	3.35
Temperature max [K]	812	851	455	950	897	916
c* efficiency [%]	84.3	77.8	65.9	93.2	95.6	54.1

Table 2.6: Results of Bonifacio et al. tests with monolithic catalysts.

As the hydrogen peroxide mass flow rate increases, the c* efficiency decreases: this finding is likely due to the flooding phenomenon: the inability of the catalyst to decompose a hydrogen peroxide mass flow rate above a certain threshold. For the configuration under examination in [12], the catalysts are able to operate at very high decomposition efficiencies if the total mass flow rate is kept at values below 7 g/s.

Time evolution of mass flow rate, thrust and post-chamber pressure and temperature of the thruster with the best efficiency (catalyst length of 60 mm and mass flow rate of 6.8 g/s) are represented in Fig. 2.17. Thrust generated is about 5.5 N.

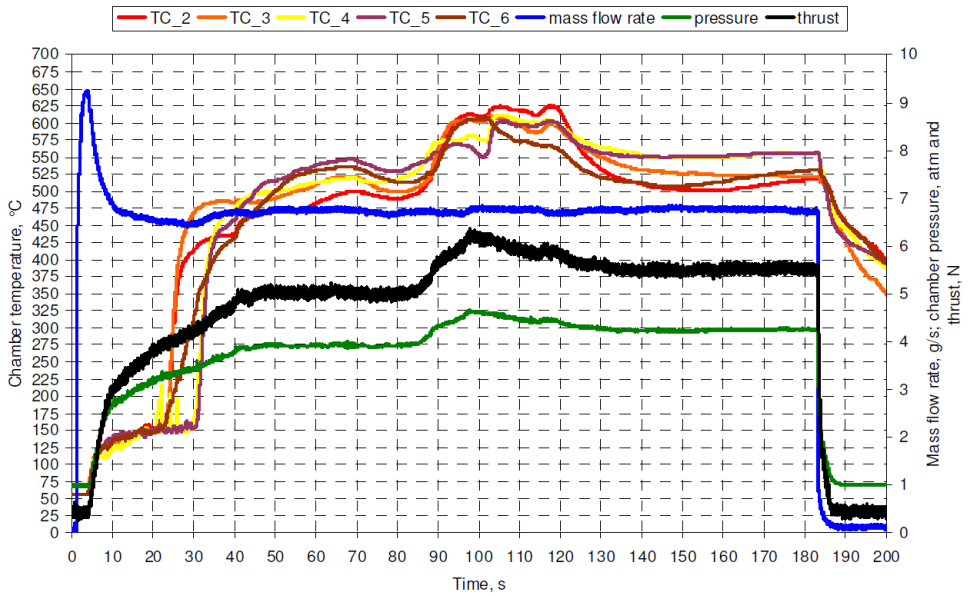

Figure 2.17: Time evolution of mass flow rate, thrust and post-chamber pressure and temperature. Catalyst length of 60 mm and mass flow rate of 6.8 g/s [12].

This test campaign has confirmed the high potential of the monolithic catalysts, with c* efficiencies as high as 96%. However mass flow rate is limited. This constraint is extremely important not only for the monopropellant thruster, as it limits the thrust that can be delivered for a given thruster cross section, but also for the hybrid configuration. In such case mass flow rate is kept at 7 g/s to maximise temperature of products until the fuel is ignited. Once the hybrid rocket engine is ignited, the mass flow rate can be increased because the HP not decomposed in the catalysts will be thermally decomposed in the chamber by the continuous combustion. Nevertheless, working at mass flow rates too important for a good catalytic decomposition can degrades the catalyst bed. It can also disturb the re-ignition because of non decomposed liquid hydrogen peroxide present in the system. Application of this thruster to an hybrid rocket engine will be explained in section 2.4.3.

2.4 Hybrid rocket engine applications

During the development on a hydrogen peroxide HRE, HP is first used and tested in monopropellant thrusters because the monopropellant scenario faces the major issues of the catalysis and of the oxidizer decomposition path. However the main interest of hydrogen peroxide is for its application in hybrid rocket engines.

The development of hybrid rocket engines using hydrogen peroxide first uses the results, reported before, of monopropellant thrusters developments based on the analysis the catalysis and decomposition of the HP. In order to create a self-ignitable and restartable hybrid rocket engine, the high-performance catalyst bed is the critical technology to obtain rapid self-ignition of the fuel and is responsible for the performances and the flexibility of the engine. Indeed, the oxidizer mass flux provided to the solid fuel depends on the decomposition quality. Also the heat released during the decomposition plays a crucial role and is a main reason of the interest of using HP in hybrid rocket engines.

Then, in the hybrid scenario, the issue of predict and improve the regression rate vs oxidizer mass flux is studied. This works focus on results with paraffin-based fuels with brief discussions of other combinations. Paraffin-based fuels are characterised by a high regression rate, low cost, safety features, reliability, and low environmental impact. However, casting a large-scale paraffin engine is difficult because paraffin wax has poor mechanical properties. So paraffin wax is usually mixed with common solid fuel to improve its mechanical properties, thus creating paraffin-based fuels.

2.4.1 Ignition

Removing the classic pyrotechnic igniter provides more safety and is necessary for a multi-pulsed operation. In order to have a self ignition (no ignition device needed) the temperature of decomposed products during the monopropellant phase should be sufficient to pyrolysis the fuel and auto-ignite the combustion between the liquefied fuel and the oxygen from the decomposition.

Using high grade of hydrogen peroxide (98%) is recommended to obtain sufficient temperature and a minimum delay to ignition. Thus, catalysts made of Pt/Al_2O_3 are commonly used to obtain an auto-ignition. Important to remember that the smaller the pellets with sufficient mechanical and thermal resistance, the shorter the transient phase duration and the higher the efficiency. Static firing tests [1] have shown that specific impulse is improved by 8 s going from 87.5% grade to 98% grade of hydrogen peroxide.

Injection also plays a role to maintain temperature high enough by influencing the combustion efficiency. A catalytic injection with a swirl gaseous injector injects a swirling oxidizing gaseous stream which improves mixing between the two propellants. A well designed catalytic bed with a swirl gaseous injector gives 98% combustion efficiency [1] and allows the self ignition of the hybrid engine.

Pressure drop between catalytic bed and combustion chamber should be minimize as the temperature drops too following Eq. 2.12

$$T_{cc} = T_{dec} \left(\frac{P_{cc}}{P_{bed}} \right)^{\frac{\gamma-1}{\gamma}} \tag{2.12}$$

Fig. 2.18 illustrates this issue by giving the maximum pressure drop allowed for a given fuel.

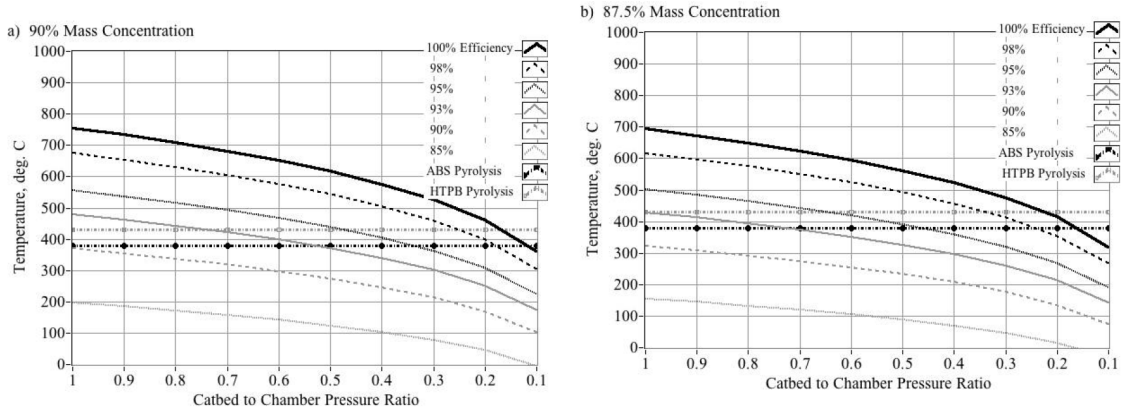

Figure 2.18: HP plume pre-combustion temperature T_{cc}, as a function of catalytic bed to chamber pressure ratios P_{cc}/P_{bed} at various decomposition efficiencies, for 90% and 87.5% solution concentrations [13].

Extra ignition devices have to be indispensable when the auto ignition of solid fuel comes in difficult. As already discussed in section 2.2.2 on thermal decomposition, an alternative ignition method that thermally-decomposes the injected HP stream is in development [13][9]. This approach eliminates the need for expensive and mass inefficient catalytic systems. With this novel approach the HP flow is pre-lead by a small flow of gaseous oxygen injected into a combustion chamber lined with the 3-D printed ABS fuel. USU propulsion research laboratory's patented arc-ignition system weakly initiates combustion between the injected oxygen and the fuel source, and is followed by the HP flow. Released heat from burning fuel is sufficient to initial thermal decomposition of the injected HP stream. Heat liberated by thermal decomposition of the hydrogen peroxide subsequently pyrolyzes sufficient fuel material to allow combustion with the oxygen liberated by the thermal decomposition of the HP. Full ignition latencies after initiation of the HP flow are typically less that 1 second. Multiple on-demand relights and higher specific impulse are provided with this system. The technology is potentially market disruptive: peroxide/ABS system outperforms the other propellants in every measureable category [13]. However the ignition is more dangerous and re-ignition is not infinite due to the need of a O_2 tank. Actually this technology is only possible with 3-D printed fuels as ABS.

2.4.2 Fuel regression rate and oxidizer mass flux

In hybrid rocket engines, the oxidizer burns with the pyrolysis gases (resulting from the solid fuel regression) through a diffusion flame located in a turbulent boundary layer. The convective and radiative heat fluxes stemming from the diffusion flame provide the energy needed for the solid grain pyrolysis in order to sustain heterogeneous combustion. Such a cycle makes hybrid combustion a self-sustained phenomenon which occurs as a macroscopic diffusion flame (Fig. 2.19). This implies a dependency of the fuel regression rate on the heat and mass transfer processes. This stabilized combustion continues as long as the oxidizer is injected and the solid fuel grain is regressing. The engine extinction can be obtained by closing the oxidizer valve [1].

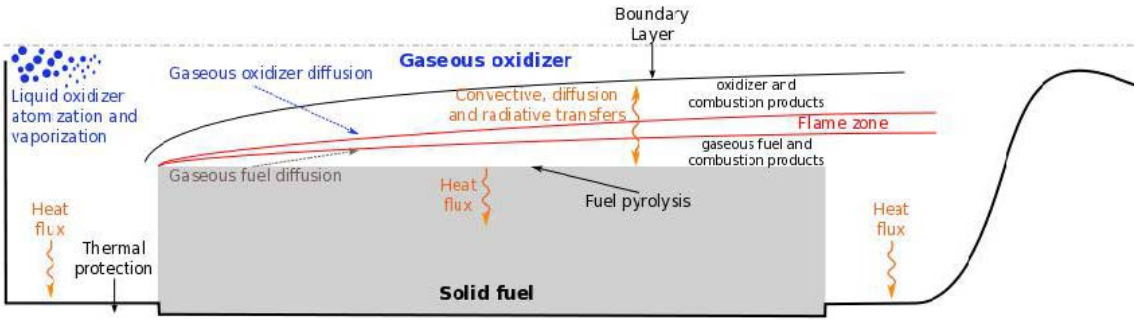

Figure 2.19: Hybrid propulsion diffusive flame scheme [1].

The average solid fuel burning surface regression rate is considered proportional to heat transfer rate and expressed as:

$$\dot{r} = a\, G_{ox}{}^{n} \tag{2.13}$$

where $\dot{r}$ is the fuel regression rate in mm/s, G_{ox} is the oxidizer mass flux in kg/m^2s, and a and n are the regression rate constants which depend on the specific oxidizer/fuel combination. a and n, also called scale factor and burn exponent are determined for each oxidizer/fuel pair from results of tests and simulations. They characterize the combustion and the performance of an hybrid engine and so they are the object of interest of this section.

Wernimont and Heister [3] have studied the combustion behavior of various PE formulations including low-density PE (LDPE), HDPE, and ultra-high molecular weight (UHMW) materials. At 825 K all of the PE materials exhibited the same general characteristics of endothermic melting and depolymerization because the basic chemistry involved in depolymerization of the PE is roughly the same. Depolymerization begins at approximately 625 K and finishes at roughly 745 K. During the depolymerization regime, the melted material becomes a short-chain molecule, which is gaseous at ambient pressure. This depolymerization process continues as the temperature is increased until the entire polymer has become gaseous. The degree of polymer crystallinity corresponds directly to the integrated amount of endothermic behavior exhibited during melting. The crystallinity is greatest for HDPE, followed by UHMW and LDPE in that order.

Tests on PE combustion highlight dependence of regression rate on flux level and chamber pressure. Whereas the low pressure (7 bar) data appear to behave a classical regression law (Eq. 2.13) consistent with turbulent convection-dominated behavior, the higher pressure results show a distinct insensitivity to total mass flux. In this lower flux region (70 kg/m^{2}s), regression rates at the higher pressures tested (14 and 28 bar) are as much as 75% greater than those at low pressures. The data are consistent with a radiation-based regression law that has been theorized, but infrequently observed for low mass flux conditions. In fact, this behavior is ideal because regression rates would no longer be influenced by changes in port geometry (either shape or size) [3].

Research in developing hybrid propulsion systems strongly depends on lab-scale firing tests. These experiments do not allow to fully understand the complex physics within their combustion chambers. Hybrid chemical propulsion physics indeed include many complex phenomena: fluid dynamics coupled with combustion, turbulence, spray atomization and vaporization processes, soot formation and radiation, fuel surface pyrolysis and fuel liquid

film for liquefying fuels as paraffin. The knowledge of the complex interactions between these wide-ranging physical phenomena is however fundamental for hybrid rocket engines design and performance prediction. Numerical simulations are the only mean to obtain a good knowledge and understanding of the gaseous flow inside of the combustion chamber in order to optimize this kind of chemical engine. However this work provides almost only results of firing tests because numerical simulation codes and results with hydrogen peroxide are not available in the open literature.

Tests with paraffin-based fuels are scarce as hydrogen peroxide in propulsive system is a recent trend and paraffins are less used for preliminary tests than others solid fuels because of their poor mechanical properties (difficult to cast). Thus, test results reported below with paraffin-based fuels are mainly with gaseous oxygen as oxidizers. Data of regression rate constants for HP with HTPB [52], PMMA [11], PE [3][12][53], ABS[13] and a bunch of paraffin-based fuels [54][55][56] have been found in the indicated references.

Regression rate constants available in the open literature are resumed in Table 2.7. n is dimensionless and a is reported in $[mm/s]/[kg/m^2s]^n$. The resulted regression rate $\dot{r}$ is then in mm/s. The composition of paraffin-based fuels investigated are reported in Table 2.8.

Fuel	**Oxidizer**	**Reference**	**Coefficient** a	**Exponent** n
LDPE	HP 85%	[3]	0.0294	0.52
HDPE	HP 90%	[53]	0.00737	0.53
HDPE	HP 98%	[53]	0.032	0.53
PE	HP 85%	[12]	0.0223	0.58
PE	HP 90%	[11]	0.01	0.67
PMMA	HP 90%	[11]	0.0075	0.67
HTPB	HP 90%	[52]	0.094	0.53
HTPB	HP 98%	[52]	0.098	0.53
ABS	HP 90%	[13]	0.060	0.59
P-CB+	HP 90%	[56]	0.034	0.96
Paraffin SP-1a	GOX	[55]	0.117	0.62
Paraffin pure	GOX	[54]	0.086	0.71
P-PE	GOX	[54]	0.036	0.81
P-Al	GOX	[54]	0.132	0.62
P-B	GOX	[54]	0.087	0.66
P-CB	GOX	[54]	0.075	0.66

Table 2.7: Regression rate data of solid fuels with HP or GOX as oxidizer.

Fuel name	Paraffin	Polyethylene	Aluminium	Boron	Carbon Black
Paraffin pure	100 %	-	-	-	-
P-PE	90 %	10 %	-	-	-
P-Al	75 %	10 %	15 %	-	-
P-B	75 %	10 %	-	15 %	-
P-CB	88.5 %	10 %	-	-	1.5 %
P-CB+	95 %	-	-	-	5 %

Table 2.8: Composition in mass % of paraffin-based fuels.

Paraffin-based fuels are characterised by high regression rates. However, paraffin wax is a brittle material and exhibits poor mechanical strength. The addition of polymers and metallic additives to paraffin wax can considerably enhance mechanical performance. The ballistic results indicate that the regression rate decrease when 10% mass polyethylene is added to the paraffin wax (P-PE), and such depreciation of regression rate due to polymer addition is compensated by the addition of the aluminium (P-Al), boron (P-B), and carbon black (P-CB) additives. The average regression rates of those paraffin fuels formulations are presented in Fig. 2.20.

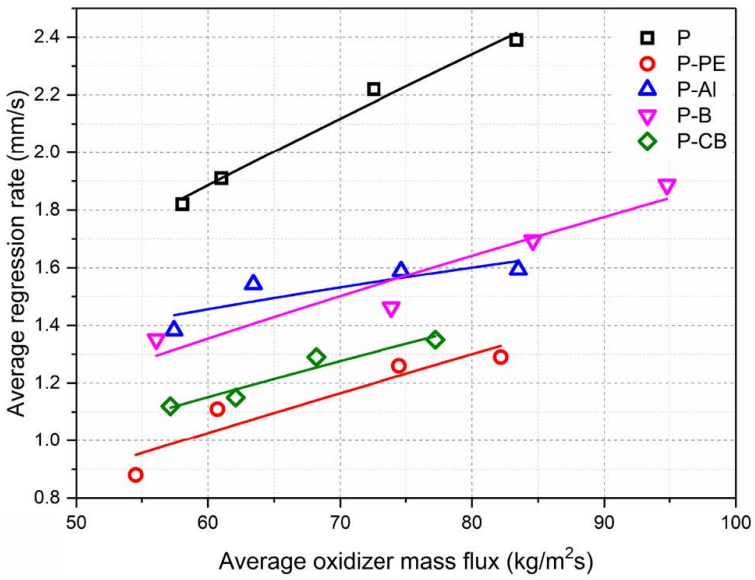

Figure 2.20: Average regression rates of paraffin fuels under gaseous oxygen [54].

The pure paraffin fuel formulation has the highest regression rate among the paraffin-based fuels. However, the combustion efficiency of paraffin is poor and could be improved by blending paraffin with PE. The Al, B, and CB additives are added to the P–PE blend to increase the energy density of the fuel. The addition of these additives could compensate for the depletion of regression rates with PE addition. The Al and B metallic additives have higher regression rates than do the P–PE blended fuel. However, the regression rates are lower than that of pure paraffin wax. Adding CB to the P–PE blend improves the regression rate compared with that of P–PE, but this regression rate is lower than that of the other metallic additives. The increase is attributed to high heat released from the metallic additives during the combustion process. The heat feedback from the additive

to the fuel surface increases the vaporisation and entrainment processes and engenders higher regression rates [57].

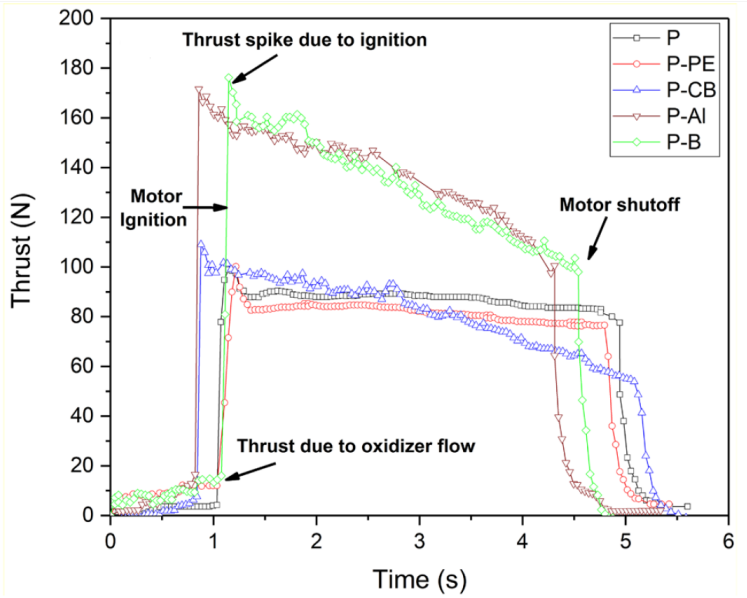

Figure 2.21: Thrust versus time traces of paraffin-based fuels [54].

Finally, the thrust-time traces observed for those paraffin-based fuels are illustrated in Fig. 2.21.

The average thrust produced by the pure paraffin wax is 88 N. At the same oxidiser mass flux range, the average thrust produced by the P–PE fuel engine is 81 N. The addition of PE to the paraffin wax reduces the average thrust and can be attributed to the improved thermal stability of the P–PE blend. The thrust data for the P–CB formulation reveal an average thrust of 83 N, in contrast, the P–B and P–Al formulations produce the highest average thrusts of 130 and 136 N. Specific characteristics of the engines used can be found in reference [54].

It also has to be noted that in HRE combustion, the length of diffusion flame formed on the solid fuel burning surface L_{DF} has to be nearly equal or longer than solid fuel length L_{SF}. For satisfying the requirement, oxidizer mass flow rate has to be such that: [11][9]

$$G_{ox} \geq \left(\frac{1}{4} a \, \rho_f (O/F)_{st} \frac{L_{SF}}{D_{port}} \right)^{1/(1-n)} \tag{2.14}$$

where ρ_f is the solid fuel density, D_{port} the solid fuel burning port diameter, and $(O/F)_{st}$ the stoichiometric mixture ratio.

The HP oxidizer flow rate has to satisfy the oxidizer mass flux needed (Eq. 2.14) for sustaining stable diffusion flame formed on the solid fuel burning port inner surface. This constraint of minimum HP mass flow rate imposed by the fuel can go against the constraint of maximum HP mass flow rate imposed by the catalytic bed for a good decomposition.

2.4.3 Relevant realizations

Monopropellant mode to hybrid mode

Bonifacio et al.[12] have designed an hybrid thruster to deliver a 200N thrust in vacuum (140N at sea level) using the monopropellant thruster discussed in 2.3.2 as the feed line for the 87.5% HP oxidizer. HDPE fuel have been chosen. The required hydrogen peroxide mass flow rate is approximately 60 g/s. This value is one order of magnitude higher than the threshold identified during testing on the monopropellant configuration: maximum 7 g/s. If the mass flow rate were set at 60 g/s since the start of a firing, the catalysts would not be able to decompose the hydrogen peroxide and it would exit almost completely in liquid phase, with little or no temperature increase and no chance to ignite the fuel grain. For this reason, a lower set point is selected as starting point: once the fuel grain has been ignited, the oxidizer mass flow rate is increased.

Swirl injection and high HP concentration

Jérôme Anthoine, Jean-Yves Lestrade and Jérôme Messineo [1][49] have performed tests at ONERA on HP/HDPE hybrid engines. Especially they have compared the performances of 87.5% HP to 98% HP, and the performances of axial gaseous injector to swirl gaseous injector. The catalysts are Pt/Al_2O_3 granules. Results are reported in Table 2.9.

	87.5% HP axial gaseous injector	**87.5% HP swirl gaseous injector**	**98% HP swirl gaseous injector**
Monopropellant phase duration[s]	1.8	1.6	1.1
Oxidizer mass flow rate [g/s]	98	102	102
Chamber pressure [MPa]	3.6	4.7	4.8
Thrust [N]	201	261	273
Specific impulse [s]	193	226	234
Combustion efficiency [%]	91	98	94
Engine efficiency [%]	87	91	88

Table 2.9: Averaged results of ONERA hybrid tests performed with the axial and swirl gaseous injectors for two different concentrations of HP.

When using a swirl gaseous injector in order to improve mixing between the two propellants, the combustion efficiency reaches 98% which is close to the value obtained for solid and liquid rocket engines. A complementary solution to further increase the propulsive performances consists of using HP at the highest concentration possible. Even if the combustion and engine efficiencies are lower with 98% HP, the much higher temperature provided by its decomposition improves the propulsive performances. Static firing test showed that specific impulse is improved by 8 s for 98% HP compared to 87.5% HP and this value could be probably larger since experiments were performed with used catalyst materials which had already reduced performances. Also, swirl injection and higher hydrogen peroxide concentration enable a faster ignition of the solid fuel.

Electrical Arc-Ignition Technology

An alternative, but still in development, technology to the catalytic decomposition for the ignition of hybrid engine using HP is the arc-ignition technology [13]. The arc-ignition technology derives from the electrical breakdown properties of certain 3-D printed thermoplastics like ABS, LDPE, and HIPS.

The hydrogen peroxide flow is pre-lead by a small flow of gaseous oxygen injected into a combustion chamber lined with the 3-D printed fuel. The arc-ignition system weakly initiates combustion between the injected oxygen and the fuel source, and is followed by the HP flow. Previous studies have demonstrated that GOX/ABS combustion generates temperatures exceeding 3070 K, and specific enthalpies greater than 8.5 MJ/kg.

Thus, with the properly tuned GOX pre-lead mass flow, there exists sufficient energy to thermally decompose the incoming HP flow, while simultaneously initiating full-length hybrid combustion. Once hydrogen peroxide decomposition begins, the additional energy of decomposition contributes to the overall combustion process. After the GOX pre-lead ends, the combustion is sustained by the oxygen liberated by the thermal decomposition of the HP.

A example of design is given in Fig. 2.22.

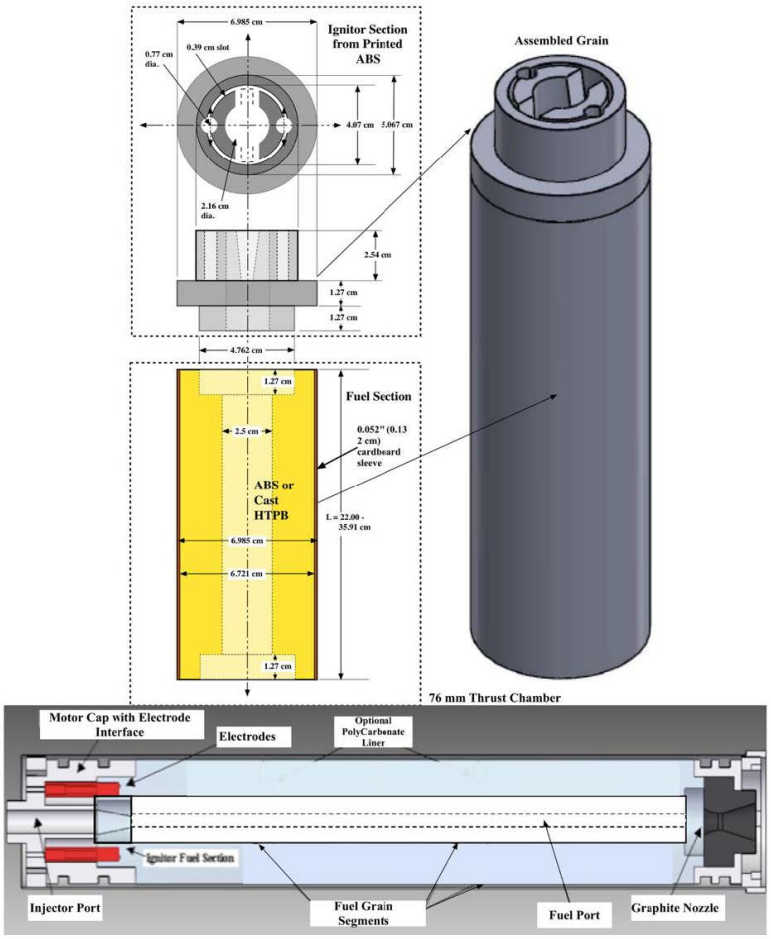

Figure 2.22: Schematic of 3-D Printed Ignitor, Extruded ABS Lower Grain Segment, and Thrust Chamber [13]

T4i

T4i [58] is developing a range of engines for space propulsion using hydrogen peroxide at concentration level up to 95%. Those engines are actually at TRL > 5. Monopropellant systems will provide from 1 to 500 N of thrust and hybrid systems based on paraffin wax fuel will provide from 100 N to 10 kN of thrust. They are also developing liquid bi-propellant engine based on HP/Kerosene.

Preliminary analysis for nanosats launches with HP/paraffin HRE

A preliminary analysis of hybrid rockets, using 98% HP and $C_{20}H_{42}$ paraffin mixed with 10% aluminum in mass as propellants, for launching nanosats into LEO is performed in [59]. Three stages air launched hybrid rockets and ground launched hybrid rockets are compared to put a 20 kg nanosat into a low Earth circular equatorial orbit at 300 km. The results have indicated that the total initial mass is about 7800 kg for a ground launched hybrid rocket and 4700 kg for an air launched hybrid rocket. Such a low mass in the case of air launched rockets would permit the use of relatively light airplanes for placing nanosats into orbit, with great flexibility on launching schedule and launching sites at the equator line.

High thrust facilities and project

In order to improve the TRL of hybrid rocket engines using hydrogen peroxide and upscale them, a large scale test facility have been especially built at Nammo Test Centre [60]. The test stand is dimensioned for hybrid rocket engine firings up to 500 kN of thrust and a long term storage capacity of 20.000 liters of HP. This unique installation is capable of supporting high thrust rocket development programs as the SPARTAN project and the Future Launcher Preparatory Program funded by the ESA to upscale the hybrid technology to a 100 kN-class engine. All those projects and others [60] help the development of large hybrid rocket engines with hydrogen peroxide by improving the TRL of the related technologies.

2.5 Conclusion on Hydrogen Peroxide

Research, completed by many space related entities, indicate rocket grade hydrogen peroxide as one of the most promising propellant for the future. Comprehensive experimental activities, performed by the Institute of Aviation, found many problems connected to the highest-grade hydrogen peroxide, including: production, material compatibility, handling and usage of this chemical in rocket propulsion. The concern about production of 98%+ HP is related to the safety issue. Compatibility matter makes a very limited list of structural materials possible to use with hydrogen peroxide. Handling requires special care mainly associated to clean environment. The main issue for hydrogen peroxide application as monopropellant for spacecraft reaction control systems is that it gives 20% lower performance than commonly used hydrazine. This significant drawback is a barrier in the process of replacing hydrazine by this green propellant.

The catalytic decomposition of HTP is identified as the common topic connecting all types of chemical rocket propulsion using this chemical. However, decomposition of 98% HP is very challenging due to the thermal conditions inside a catalyst bed. On the contrary, numerous advantages of green propulsion create significant perspectives for new researchers aiming to join the space community. It may find application in future green propulsion systems for spacecrafts as well as for launch vehicles. High level of maturity of catalyst related technologies might guarantee the further success in green propulsion development and usage for launch services and satellites. Test results, obtained up to date, confirm the potential to develop these technologies.

Hydrogen peroxide-based hybrid systems could revolutionize the commercial space industry by offering a high-performing, but inherently safe, space propulsion option for ride-share payloads.

Chapter 3

Nitrous Oxide

This chapter is based on the same structure as the previous one but with another oxidizer: Nitrous oxide with the chemical formula N_2O. Nytrox, mixtures of N_2O and O_2, are also studied in this chapter as a variant of the pure nitrous oxide.

Nitrous oxide is the second most commonly used oxidizer in hybrid rocket systems after liquid oxygen. This is primarily due to its low cost, safety, availability, relatively benign nature, and handling advantages compared to the other liquid oxidizers that can be used in propulsion applications. Nitrous oxide benefits from a very high vapor pressure allowing its self-pressurization. Despite its moderate Isp performance and poor impulse density at room temperature, its self-pressurization makes N_2O the ideal choice for small engines for which the systems and operational simplicity are the dominant driving forces. This fact explains the extensive use of N_2O in amateur rocketry and in many sounding rocket programs.

3.1 Characteristics

3.1.1 Physical properties

Nitrous oxide is a colorless gas at standard temperature and pressure with a slightly sweet odor [61]. It is a widely used substance with very interesting physical, chemical and biological properties. The general characteristics and relevant performances to propulsion systems of N_2O are detailed in the Table 3.1. They are compared to the one of LOX and HP 90%.

Nitrous oxide has a vapor pressure of 56 bar at 293 K which allows for self-pressurization. Self-pressurization can be useful because it eliminates the additional weight, complexity and cost of the pressurization system or the turbo pump system needed to feed a liquid oxidizer into the combustion chamber at high pressures. The other advantages of N_2O can be listed as:

- Stable and efficient combustion is easier to attain due to the exothermic decomposition reaction of the oxidizer molecule;
- Extensive experience base exists in the hybrid propulsion field;
- Easily accessible chemical commonly used in several other industries;
- Modest cost.

	LOX	**N_2O**	**HP 90%**
Active O_2 content [%]	100	36	42
Boiling point at 1 atm [k]	90	185	414
Freezing point [K]	54	182	261
Density (293 K liquid) [g / cm^3]	1.141	0.793	1.395
Vapour pressure [Pa]	5200 ($89K$)	5.6x10^6 ($293\ K$)	200 ($293K$)
Molar mass [g / mol]	32	44	32.4
Monopropellant			
Impulsion specific [s]	-	153	160
Density specific impulse x10^3 [kg.s/m^3]	-	222	265

Table 3.1: Physical properties and average performances of nitrous oxide compared to liquid oxygen, and HP 90% [62].

With only 36% active O_2 in the molecule by mass, it is not a highly effective oxidizer. It has a moderate Isp performance which is approximately 30s lower than LOX when they are burned with most common fuels [61].

The disadvantages of N_2O can be listed as:

- Low Isp performance and low density impulse;
- Low density (when self-pressurization is needed). At low temperatures the density can be improved but the pressure drops significantly;
- High dependence of density and pressure on the temperature. Temperature conditioning is required for most practical applications which is not the case of hydrogen peroxide. Despite, the constraints on temperature are way less demanding than with liquid oxygen;
- System optimizes at high oxidizer to fuel ratios requiring a high mass fraction of liquid.

The two last disadvantages listed above can find a solution in the so called nytrox discussed later.

Nitrous oxide decomposes into the reference species N_2 and O_2 by releasing substantial heat following the chemical Eq. 3.1.

$$N_2O \longrightarrow N_2 + \frac{1}{2} O_2 + q\,; \quad q = -82\,\mathrm{kJ\,/\,mol} \tag{3.1}$$

The heat released during the reaction is equal to 1.865 MJ/kg which is 35% lower than H_2O_2 decomposition. Even though this inherent feature of N_2O helps the Isp performance and allows for use in the monopropellant mode, it also introduces the most important safety hazard associated with this substance. In contrast to liquid HP, the heat released to gaseous or near boiling point N_2O can quickly and dangerously increase the pressure. Self decomposition in the tank, feed lines and the combustion chamber is possible and might result in catastrophic failure and explosion.

It can be noted that N_2O is an highly effective solvent and this characteristic introduces significant material compatibility problems.

3.1.2 Nytrox properties

Nitrous oxide and oxygen are highly miscible in the liquid phase [63] which opens up the possibility of using the mixture as an oxidizer for chemical propulsion systems. A new class of oxidizers which are composed of equilibrium or non-equilibrium mixtures of nitrous oxide and oxygen are so formulated in order to maximize the benefits of the pure components and eliminate the shortcomings of the individual components. Those mixtures are called nytrox. In the mixture O_2 serves as the pressurizing agent, whereas N_2O is the densifiying component. Unlike the pure oxidizers, the mixture allows for two independent control variables (temperature and pressure) which can be finely tuned to optimize the system for a particular application.

A simplistic explanation of the nytrox concept is given in Fig. 3.1 which shows the oxygen, nitrous oxide and the mixture of the two as a function of temperature in the oxidizer tank. At deep cryogenic temperatures, oxidizer is liquid oxygen in its pure form. As the temperature is increased, mixture of the two substances becomes feasible and the nytrox oxidizer is formulated. As the temperature increases, oxygen content of nytrox decreases and finally at temperatures close to the room temperature, pure nitrous oxide becomes the practical oxidizer [63]. A qualitative comparison of nytrox with N_2O and O_2 given in Table 3.2 shows the interests of nytrox over the pure substances.

	O_2	**N_2O**	**Nytrox**
Isp Performance	5	3	4
Density	4	2	4
Impulse Density	4	1	3
Chemical stability	5	4	4
Toxicity	5	4	4
Storability	1	5	3
Self Pressurization Capability	1	5	3
Gas Phase Combustion	1	3	5
Hypergolicity	1	1	1
Ease of handling	3	5	4
Material Cost	5	4	4
Chemical compatibility	5	5	5
Performance tuning capability	1	2	5
Engine Stability/Efficiency	2	5	4
Overall Safety	3	2	5

Table 3.2: Comparison of pure O_2, N_2O and nytrox as oxidizers [63]. 1: Worst performance, 5: Best performance.

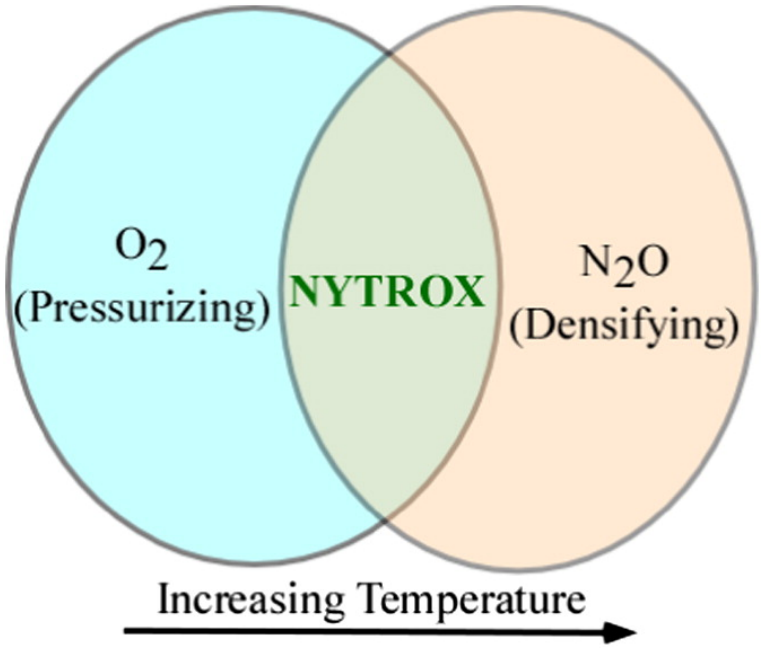

Figure 3.1: Nytrox concept [63].

The primary advantages of this new system over the pure oxidizers can be listed as [63]:

- Partial self pressurization possible at high densities which eliminates or minimizes the use of pressurant gas;
- High density and density impulse and higher Isp performance compared to N_2O;
- Non-cryogenic operational temperature, much easier to manage than LOX and pure N_2O (composite tank can be used);
- Efficient gas phase combustion;
- Easier development of stable and efficient engines compared to liquid oxygen due to the exothermic decomposition of the N_2O molecule;
- Optimization based on mission requirements is possible. The critical control variables are the temperature and pressure which determine the oxidizer mass fraction in the liquid and vapor phases of the mixture;
- Improved safety. A typical nytrox system with 70% oxygen in the vapor phase requires 4 to 5 orders of magnitude larger ignition energy compared to pure nitrous oxide. In summary, nytrox vapor is virtually impossible to ignite with any conceivable ignition source.

Fig. 3.2 shows that at a selected self-pressurization level, the densities of the nytrox mixtures are significantly higher than the densities of the pure substances. Also, at a given temperature, the liquid density is not sensitive to the system pressure as long as the pressure is not close to the critical value at that temperature. This feature of the nytrox mixture gives the designer the flexibility of selecting the system pressure without affecting the liquid oxidizer density significantly.

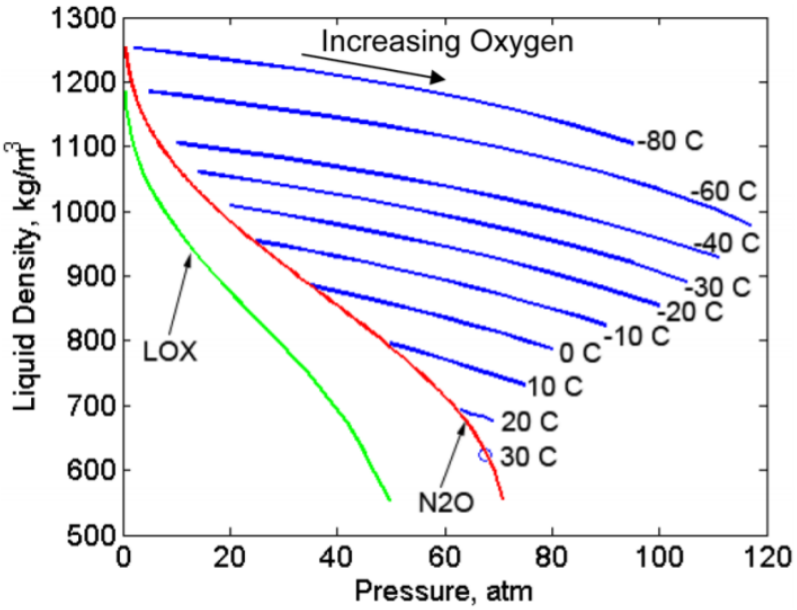

Figure 3.2: Liquid density as a function of pressure at various temperatures for the O_2/N_2O mixtures [63].

Nytrox can also be done with other oxidizers than O_2 but it is non common and open literature information about those mixtures are scare. N_2O_4 or mixtures of nitrogen oxides exhibit similar density and pressure characteristics as the baseline N_2O/O_2 nytrox system at higher temperatures. The important shortcoming is their toxicity. Note that some of the mixtures with practical significance are N_2O_4/O_2, $N_2O/O_2/NO$, $N_2O/O_2/O_3$ or $N_2O/O_2/NO/O_3$. The addition of NO into the baseline Nytrox would add some extra pressurization capability, enhance the Isp performance and improve the reactivity of the oxidizer. Addition of small quantities of O_3 into baseline nytrox would also be beneficial in terms of enhancing the decomposition rate of nitrous oxide and the Isp performance, possibly improving engine stability and efficiency. Helium could be added to reduce the sensitivity of nytrox to chemical decomposition. Small amounts of organic or inorganic fuel components can be incorporated to enhance the reactivity of the baseline nytrox. Addition of higher concentrations of fuels would result in a highly sensitive but also a high performance monopropellant that could be beneficial for certain propulsion applications. Note that the fuel components should be selected such that it would be highly miscible with Nytrox but would have a low vapor pressure at nytrox temperatures to minimize the possibility of the vapor phase explosion. The other types of additives that could prove to be beneficial are gelling agents [63].

3.1.3 Environmental and toxicity considerations

At low concentrations nitrous oxide is mildly toxic. Neurotoxic effects of N_2O occur after acute exposure. Effects include slowed reaction time and performance decrements. Long-term occupational exposure has been associated with numbness, difficulty in concentrating, paresthesias, and impairment of equilibrium [64].

It is widely accepted that nitrous oxide is a highly effective global anthropogenic green house gas which is 300 times more effective than carbon dioxide in trapping heat. However, the level of nitrous oxide used in rocket propulsion applications is quite limited compared

to the other industries and thus, its effect on the global warming is negligible [65].

The toxicity and polluting impact of N_2O can then be considered as higher than HP but it is still much less toxic and pollutant than hydrazine usually used in monopropellant thrusters.

3.1.4 Safety

N_2O is widely used since a long time in a lot industries but at concentration and quantities much lower and than in rocket propulsion. Rocket propulsion is unique in the sense that large quantities of nitrous oxide are stored at room temperature and consumed at a very fast rate. A particularly dangerous mode of failure is the decomposition of the N_2O vapor in the oxidizer tank. Due to the large quantities of N_2O in the tank ullage, a decomposition process in the tank could potentially produces large explosions. Unfortunately, at larger scales the situation gets worse since the surface to volume ratio reduces as the tank size grows. This is especially a problem in propulsion systems because the combustion chamber is closely coupled with the oxidizer tank. At the end of the liquid burn, the hot injector could potentially heat the nitrous vapor in its vicinity and start a deflagration wave that could propagate in the tank. Note that for pure nitrous oxide in a closed vessel at ambient temperature, complete decomposition could result in a 25 fold increase in the tank pressure [61]. This indicates that even a partial decomposition could lead to a structural tank failure.

Nytrox is used to improve the safety by reducing this risk. The minimum energy to start a self sustaining deflagration wave in nitrous oxide with varying initial concentration of oxygen is shown in Fig. 3.3. A nytrox system, even at a relatively low oxygen concentration of 35% by mass in the vapor phase, requires more than 4,000 times more ignition energy compared to pure nitrous oxide.

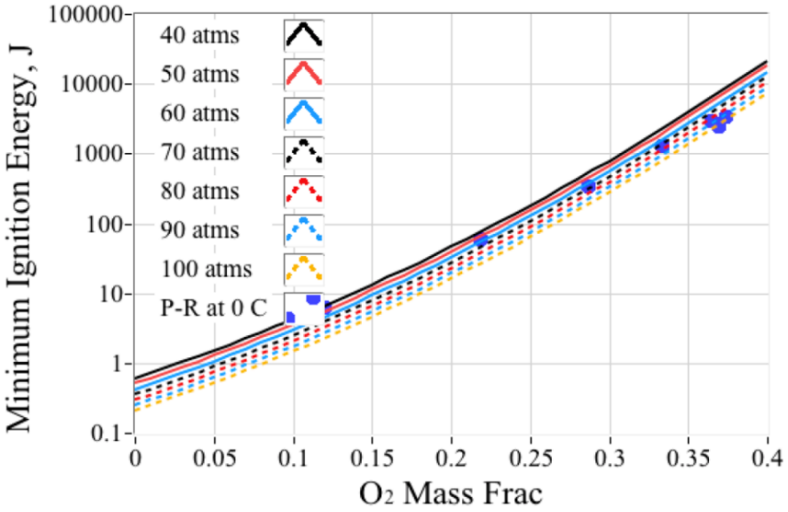

Figure 3.3: Minimum ignition energy for nytrox mixtures at different storage pressure levels [66].

Nytrox vapor is practically impossible to ignite with any ignition source that might exist in the tank [66]. The effect of pressure is small compared to the effect of dilution.

3.2 Decomposition and catalysis

Modeling and testing of the decomposition chemistry of nitrous oxide is highly problematic since it introduces unknown risks in the development of large scale N_2O propulsion systems.

3.2.1 Decomposition path: spin forbidden unimolecular decomposition

Nitrous oxide is a triatomic linear molecule with the asymmetrical NNO configuration. The electronic structure involves single charges to be stable. The two main structures described in Fig. 3.4 are essentially equivalent and contribute equally to the normal state [67]. The particular structure of nitrous oxide has an impact on its decomposition.

Figure 3.4: Stable electronic structures of nitrous oxide [66].

Nitrogen atoms are not formed during the decomposition process, which indicates that the decomposition takes place by the break-up of the NO bond. This feature is why nitrous oxide can be used in hybrid propulsive applications because it allows the generation of O_2 molecules needed for the combustion with the solid fuel.

It is well established that nitrous oxide exothermally decomposes into the reference species, O_2 and N_2, following the global reaction in Eq. 3.1. The measured activation energy for the nitrous oxide decomposition is of approximately 240 kJ/mol.

Note that this reaction requires a change in the multiplicity (from the singlet ground state for the N_2O molecule to a triplet state in atomic oxygen) which is a forbidden transition in quantum mechanics. Due to the interesting spin forbidden nature and also the relatively simple structure of N_2O, this reaction does not strictly follow the classical unimolecular theory and has been the subject of many theoretical studies [68][69][70]. The reaction rate is determined to be 2 orders of magnitude slower compared to a normal unimolecular reaction due to the necessary change from the singlet state to the triple state.

The abnormally low unimolecular reaction rate for N_2O, partly induced by the spin-forbidden processes, plays an important role in its relative safety compared to the other substances that decompose following unimolecular exothermic reactions as hydrogen peroxide. Nitrous oxide decomposition rate is six orders of magnitude slower than the decomposition of hydrogen peroxide, making it a much safer propellant. This difference is originated by the spin forbidden transition of N_2O and the lower activation energy of HP decomposition. Fig. 3.5 clearly shows the relative safety of nitrous oxide compared to hydrogen peroxide. Even though both materials release comparable levels of energy as they decompose, the significantly reduced rate of decomposition makes nitrous oxide a much less sensitive material. The other major safety related distinction between these two commonly used oxidizers is the fact that the decomposition reaction in liquid phase HP is possible, whereas all attempts, as they have been reported in the open literature, to ignite liquid N_2O have failed even with the use of blasting caps [71][72].

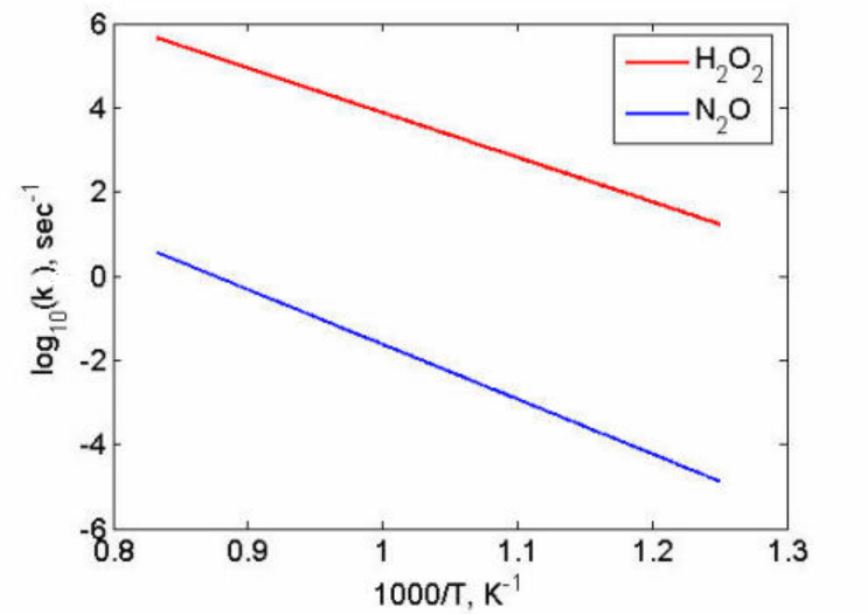

Figure 3.5: Decomposition reaction rate constant for N_2O and HP [61].

However, ignition of gaseous N_2O increases significantly and almost immediately the pressure and can result in an explosion. If handled properly, nitrous oxide (and nytrox) is one of the safest oxidizer used in chemical propulsion systems.

The kinetics of nitrous oxide decomposition is very complex to model but at pressure higher than 40 bar, which correspond to rocket propulsion applications, the kinetic model can be simplified to a first order kinetic [73][74][75][76]. Fig. 3.6 shows that no appreciable decomposition takes place for temperatures less than 850 K. The time scale for decomposition reduces exponentially with temperature and it reaches the millisecond scale at temperatures larger than 1500 K.

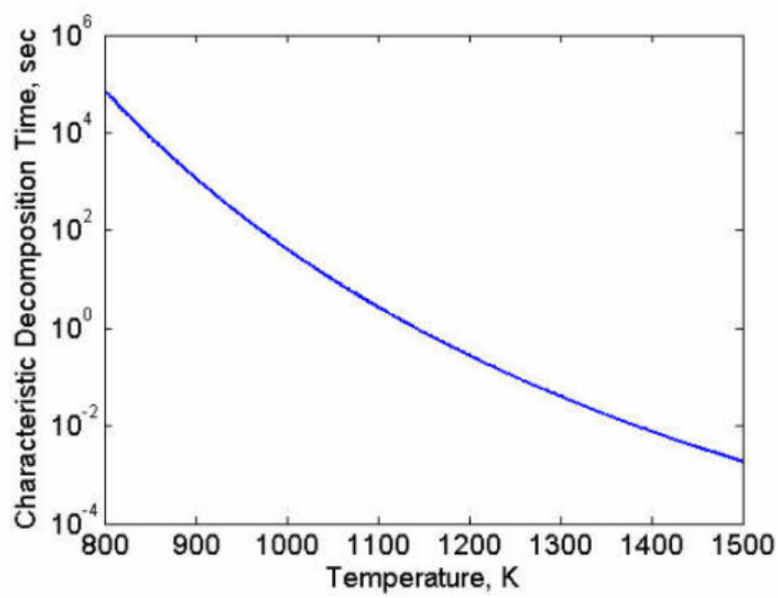

Figure 3.6: Characteristic decomposition time as a function of temperature at pressures larger than 40 bar. [61].

3.2.2 Thermal ignition of decomposition

The ignition of nitrous oxide vapor can take place homogeneously when the material is uniformly heated to a temperature larger than its auto-ignition temperature or locally when enough energy is locally introduced to the vapor at lower temperatures such that a self sustaining deflagration wave can start to propagate in the medium.

At a certain temperature, the heat produced by the exothermic reaction exceeds the heat loss to the surroundings and an increase in the temperature is observed. The homogeneous ignition characteristics of nitrous oxide are modeled in [61]. This mode of ignition is highly unlikely in the oxidizer tank ullage since elevating the ullage temperature to the relatively high auto-ignition temperature of nitrous oxide requires vast amount of heat which is not usually available in a typical system. The areas where the homogeneous ignition is likely to play a significant role are the dead volumes in the feed lines which could be subject to appreciable increase in temperature due to gas compression effects. A slow increase in temperature (induction period) is typically followed by an exponential growth period (explosion). The inflection point of the system is when the system temperature exceeds T_M given by:

$$T_M = T_0 + \frac{RT_0^2}{E_a} \tag{3.2}$$

As shown by Fig. 3.7a the critical temperature at which the homogeneous ignition of N_2O vapor takes place within a reasonable time period to have time to stop the incoming explosion is around 850 K. Considering high length over diameter ratio of vessels, explosion boundary can be seen in the P-T plan reported in Fig. 3.7b.

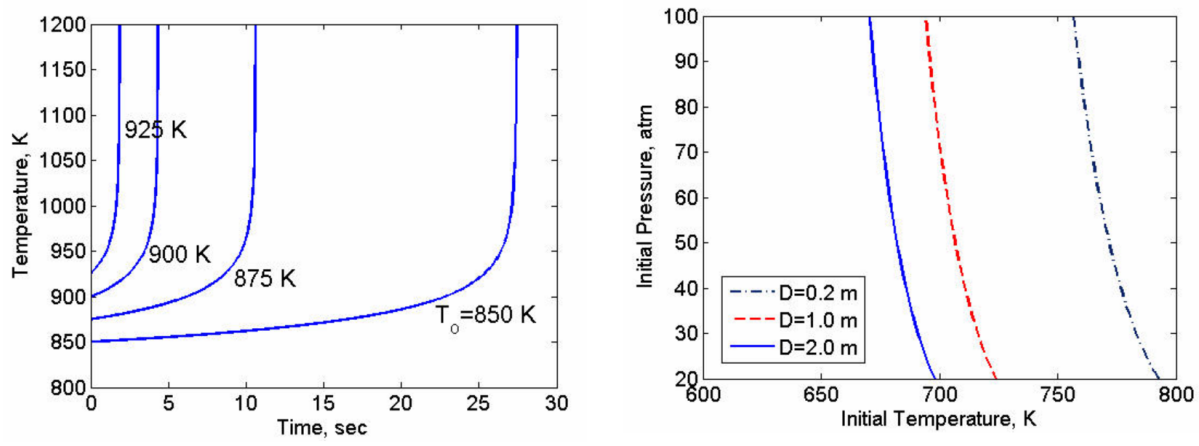

(a) (b)

Figure 3.7: (a) Induction time as a function of initial temperature, no heat loss case. (b) Ignition boundary for cylindrical vessels with varying diameters. [61]

Finally the effect of dilution on the explosion boundary has been demonstrated in Fig. 3.8, which shows the explosion boundaries for a cylindrical vessel with a diameter of 2 m at three oxygen concentration levels, 0%, 50% and 80% by mass. The interesting observation is that the effect of dilution on the ignition boundary is relatively small, approximately a 30 K change for a jump from the 0% to the 80% level.

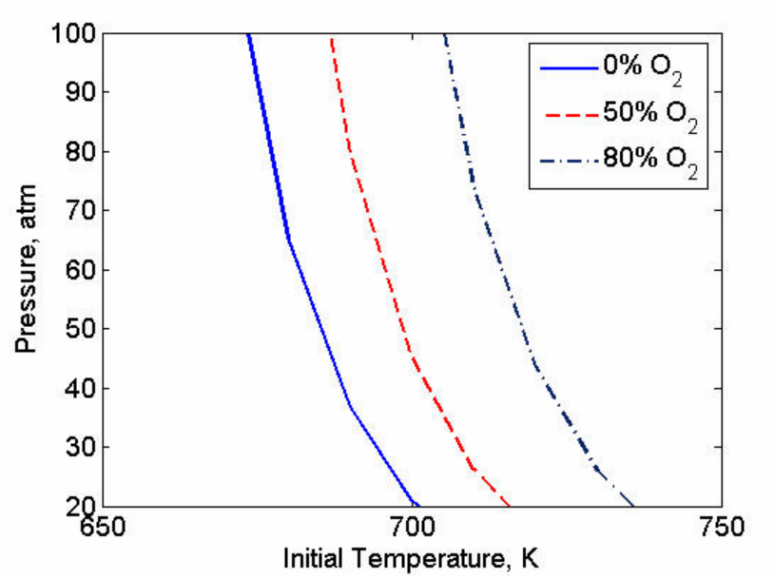

Figure 3.8: Effect of nytrox concentration on the ignition boundary. Vessel diameter 2 m. [61].

Local thermal ignition is the most common ignition mode expected in rocket propulsion applications, since it only requires small quantities of highly localized thermal energy which are readily available in all practical systems. A local ignition would start a self sustained deflagration wave in the N_2O vapor which result in an over-pressurization of the pressure vessel. The rate of increase in pressure (the violence of the explosion) depends on the speed of the laminar deflagration wave, S_L, which can be calculated using the Zeldovich theory [77]. The laminar flame speeds, which are plotted in Fig. 3.9, show a decreasing trend with increasing oxygen mass fraction primarily due to the reduction in the adiabatic flame temperature with dilution. The flame speeds are fairly low (15 cm/s) because of the slow kinetics for the decomposition of N_2O. It can also be noted that $S_L \propto 1/\sqrt{P_0}$.

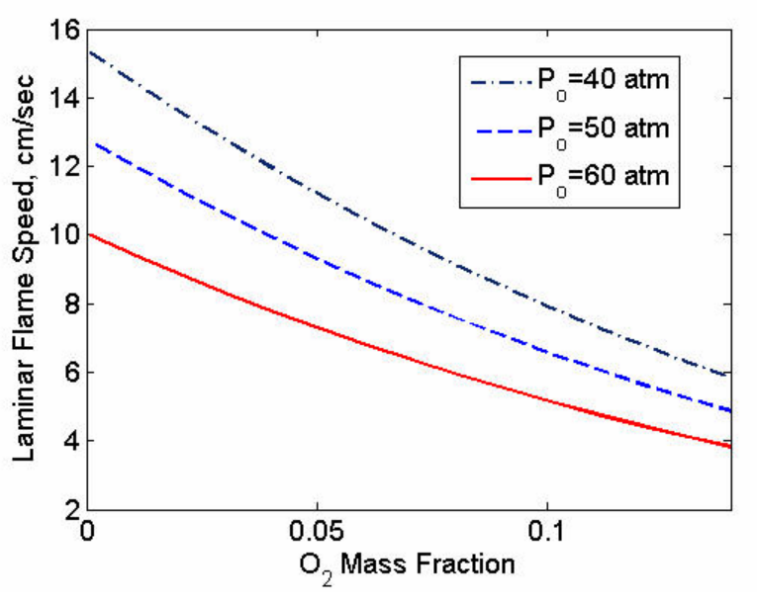

Figure 3.9: Laminar flame speed for nytrox at three pressure levels [61].

As already mentioned with Fig. 3.3, the influence of dilution on the ignition energy is significant. Minimum ignition energy for pure nitrous oxide is approximately 450 mJ but nytrox becomes extremely difficult to ignite at dilution levels higher than 30%.

At the end of the liquid burn, the hot injector could potentially heat the nitrous vapor in its vicinity and start a deflagration wave that would over-pressurize the feed lines and propagate freely in the tank. The decomposition hazard increases with increasing system scale due the unfavorable surface to volume ratio scaling. Also, if a large quantity of nitrous oxide is accumulated in the combustion chamber before the igniter action, a subsequent ignition could result in a chemical explosion and an extreme over-pressurization in the combustion chamber ("Hard start").

The recommendations to avoid those thermal decomposition hazards can be listed as [61]:

- Dilution of the ullage with an inert gas such as helium or O_2 is highly recommended to reduce the pressure increase and avoid structural failure;
- Incorporation of a properly designed burst disk to limit the over-pressurization in the case of ignition in the ullage;
- Minimize the dead volumes in the feed lines;
- Slow down the valve opening rate;
- Prevent hot gases from the igniter from flowing back into the feed lines;
- Adjust the delay between the oxidizer valve opening and ignition signals in the control system to avoid a "Hard start" (the N_2O flow should always lag the igniter action);
- N_2O systems should be tested at full scale;
- Nitrous oxide is a reasonably effective solvent for a number of hydrocarbons including a lot of common polymers, so any materials should be carefully tested for compatibility with N_2O. Catalytic materials in N_2O systems should be avoided. A comprehensive list of catalytic materials for N_2O is given in [65] and [78] and in the next sections.

3.2.3 Catalytic decomposition

As already mentioned, nitrous oxide decomposition is highly exothermic (1865 kJ/kg) and yields high temperature nitrogen and oxygen (approximately 1920 K) but the energy barrier is huge, requiring temperature over 850 K to achieve appreciable decomposition rates. One solution is to use a catalyst to enable decomposition at significantly lower temperatures. N_2O conversion versus temperature profiles and specific reaction rate, with different catalysts have been researched in the open literature for comparison as performance parameters for N_2O decomposition. For comparison purposes, the light-off temperature T_{50} is defined as the temperature required for 50% N_2O conversion.

A large variety of catalysts for N_2O have been studied for reducing its emissions in industrial applications. But those studied face a different problem than in propulsive applications because N_2O concentration in the gas flux is about few % and the main discussion are about the activity of the existent catalysts for N_2O in presence of other

gas such as CH_4, H_2O and CO_2 [78][79]. Kapteijn et al. [78] have studied the catalytic activity of many materials over nitrous oxide. Some of the relevant results are reported in Fig. 3.10a and Fig. 3.10b for comparison purpose.

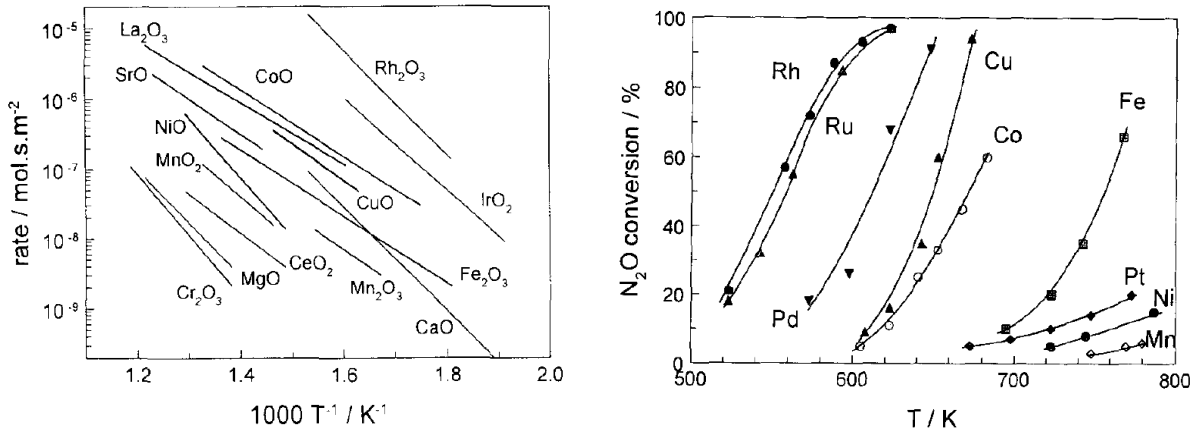

(a) (b)

Figure 3.10: (a) Decomposition rates of selected pure oxide catalysts for N_2O decomposition. (b) Comparison of N_2O conversion over several catalysts based on noble metals. [78]

Noble metal-based catalysts as rhodium, ruthenium, iridium and palladium demonstrate satisfactory N_2O decomposition performance and at low temperature ($T_{50} \sim 500 - 600K$). Although their high cost and sensitivity to H_2O, CO_2, and high concentration of O_2 limit their industrial applications [80], they fit for propulsion applications. The temperature in a catalyst bed can be as high as 1920 K during decomposition. Compounds stable at high temperatures are usually obtained in the form of a wire 0.2 mm in diameter made of Rhodium alloy (10% Rh), Iridium alloy (10% Ir), chromium alloy (20% Cr), and others platinum metals. Active phase activity of metals can be sorted by the light-off temperature T_{50} as: Rh (530 K) > Ru (595 K) > Ir (605 K) > Pt (705 K) > Pd (765 K) [81]. Rhodium is the most stable and the most used in propulsion applications. Rhodium catalysts with a modified zirconia-alumina support are among the most effective catalysts for the N_2O decomposition [82].

Oxides can be used as a basis for developing low-cost catalysts. The experimental data [81] conclude that Co, Cu, Mn, and Cr oxides can be recommended as active components for developing catalysts based on non-noble metals. They exhibit fairly high activity in the decomposition of N_2O and are thermally and chemically stable. The most used and active ones can be sorted as: Co_3O_4 (690 K) > NiO (700 K) > MnO_2 (705 K) > CuO (715 K) > Cr_2O_3 (720 K).

More recently, spinel-type oxide catalysts based on Cobalt have been developed [83][84]. They show promising performances even in presence of oxygen but their activity is still inferior to noble metal-based catalysts. The three most active spinels are: $MgCo_2O_4$ (715 K) > $ZnCo_2O_4$ (755 K) >$CoCo_2O_4$ (765 K).

A more detailed analysis of the activity of the most common materials for the decomposition of nitrous oxide in monopropellant applications is performed in the next section.

3.3 Monopropellant applications

Similar to hydrogen peroxide or hydrazine, nitrous oxide can be regarded as a monopropellant since its decomposition reaction is exothermic. The theoretical specific impulse performance for a N_2O monopropellant thruster can reach up to 206 s when the decomposition temperature is maximal at about 1920 K. This performance makes N_2O monopropellant thrusters suitable for spacecraft station-keeping and small orbit manoeuvres.

This section first provides a modeling effort from Vadim Zakirov and Hai-yun Zhang [85] of the simulation of nitrous oxide monopropellant thruster operation. Then an analysis of the activity of the most common materials for the decomposition of nitrous oxide in monopropellant applications is performed. Finally, some relevant realizations are reported.

3.3.1 Model of nitrous oxide decomposition in monopropellant thrusters

As discussed previously, existent catalysts are enable to decompose nitrous oxide at its storage temperature so the most common and safest solution is to electrically preheat the catalyst. The heat generation from the decomposition self-sustains the reaction so that the electrical power input is no longer required once the engine in ignited and at nominal temperature.

In the model of Vadim Zakirov and Hai-yun Zhang [85], the nitrous oxide gas flows through the thruster that is considered an open system divided in six control volumes (Fig. 3.11) in which the physical and thermal properties are uniform.

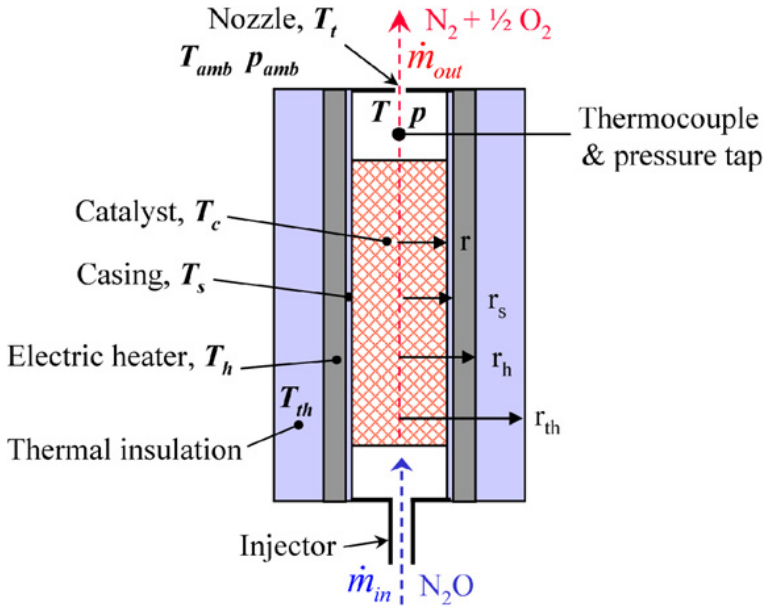

Figure 3.11: Nitrous oxide monopropellant thruster schematic. [85]

- **Chamber:** the heat generation by decomposition is balanced by flow heating, and heat transfer with catalyst and casing;
- **Catalyst:** the catalyst in the pellet form is considered being a porous medium for which heating rate is determined by thermal conductivity with thruster casing and convective heat transfer with gas;

- **Casing:** the heat rate absorbed by the casing is equal to the difference among the rates transferred through the control volumes by conductivity between heater and catalyst, convection from gas inside the chamber, and radiation to the ambient;
- **Electric heater:** the electric power input is converted to heat by the heater, and is dissipated by thermal conductivity to the thruster's casing and thermal insulation;
- **Thermal insulation:** the thermal insulation is for reduction of heat losses out of the thruster. Its heating rate is determined by heat transfer from the heater by conductivity and heat removal to the ambient;
- **Nozzle:** isentropic flow of ideal gas is assumed for the nozzle flow calculation.

For simplification, the problem is divided into 2 parts: simulation of N_2O decomposition inside the reaction chamber, and choked flow of reaction products through the nozzle. Since decomposition reaction rate inside the chamber depends on the N_2O mass flow rate that is restricted by the nozzle, and vice versa, the flow rate through the nozzle relies on conditions inside the chamber determined by the reaction rate, an iterative approach is used for solution. The analytic equations of the flow and the heat transfers, as well as details about the algorithms of this model can be found in reference [85].

Three cases have been studied and the comparison of results between experiments and simulations are reported in Fig. 3.12, Fig. 3.13, and Fig. 3.14.

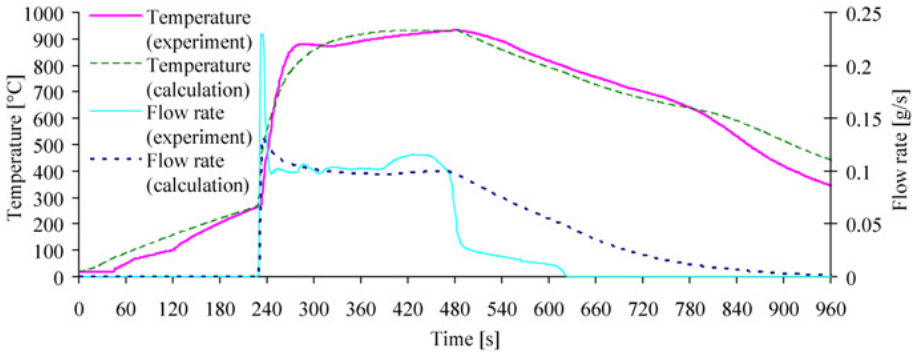

Figure 3.12: Comparison of experimental and computational results for a typical run test. [85]

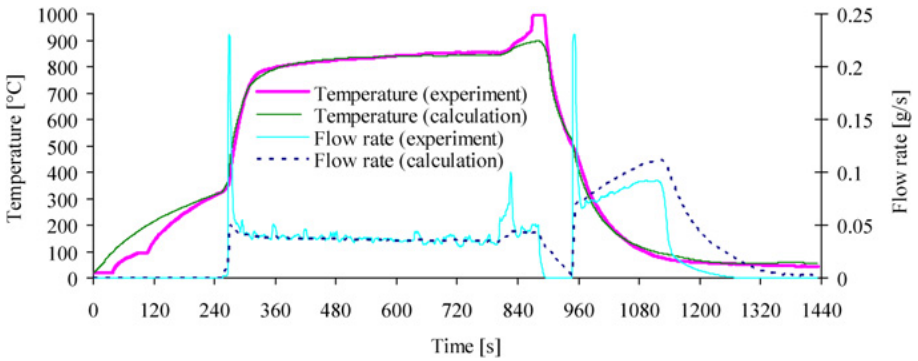

Figure 3.13: Comparison of experimental and computational results for a test with cooling through an excessive amount of nitrous oxide. [85]

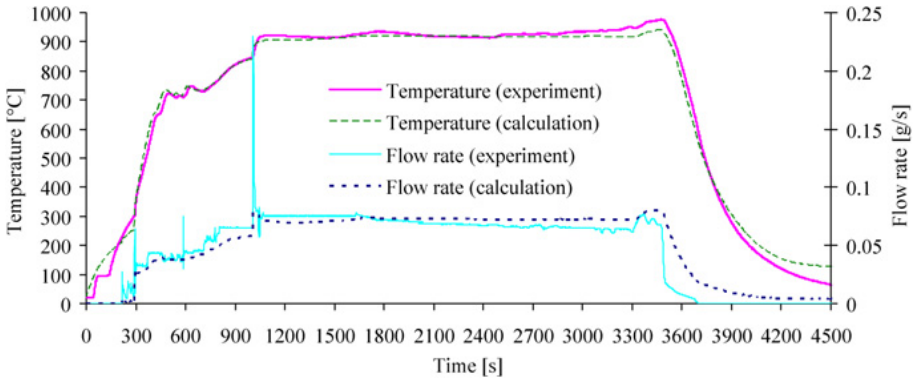

Figure 3.14: Comparison of experimental and computational results for a long duration test. [85]

A satisfactory correlation achieved between experiment and simulation during model validation suggests this model can be used for solution of practical N_2O monopropellant thruster design problems.

3.3.2 Catalysts performances

As seen previously in 3.2.3, it is not difficult to find a catalyst to be active enough to initiate the N_2O decomposition at a low temperature [80][81][78][83][79][84] for removing N_2O from exhaust gas. Unfortunately, these catalysts can not survive in a high-temperature environment. Open literature publications about N_2O decomposition catalysts for high-temperature applications such as propulsion are rarer. Catalysts performances reported here focus on catalysts actually used for propulsive applications in monopropellant or hybrid rocket engines. Catalyst materials should be both active at a low temperature and thermally stable at a very high temperature. Those catalysts with satisfactory or promising performances are based on rhodium (Rh), ruthenium (Ru) or iridium (Ir).

Hendley et al. [86] have studied the activity of Rh et Ru (wt 0.5% loading) catalysts supported on Al_2O_3 pellets (3.3 mm diameter and 3.6 mm length).

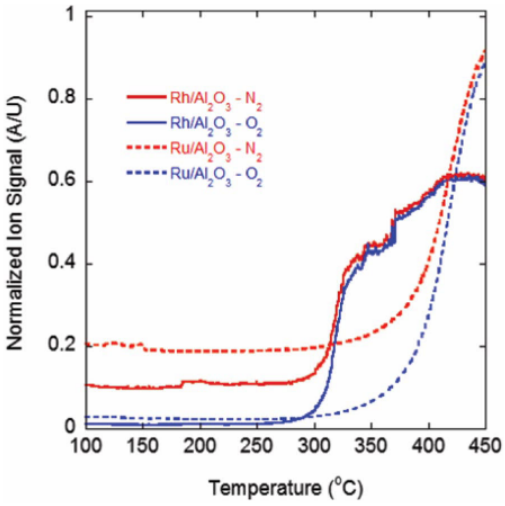

Figure 3.15: EGA of nitrous oxide flow over rhodium and ruthenium catalyst. [86]

They use the Evolved Gas Analysis (EGA) technique to identify the nitrous oxide decomposition onset in the presence of ruthenium and rhodium catalysts. Results in Fig. 3.15 show that oxygen and nitrogen decomposition species were detected when the chamber reached approximately 550 K for the rhodium and 600 K for the ruthenium catalysts.

Reducing the decomposition onset temperature is preferable in a practical application, thus rhodium based catalysts are the most studied for N_2O as a propellant. No more relevant study about ruthenium based catalysts have been found.

As rhodium catalysts support on Al_2O_3 pellets show good performances, Haber et al.[87] have studied catalysts composed of rhodium supported on $\gamma - Al_2O_3$ doped with alkali metals lithium (Li), sodium (Na), potassium (K), and caesium (Cs).

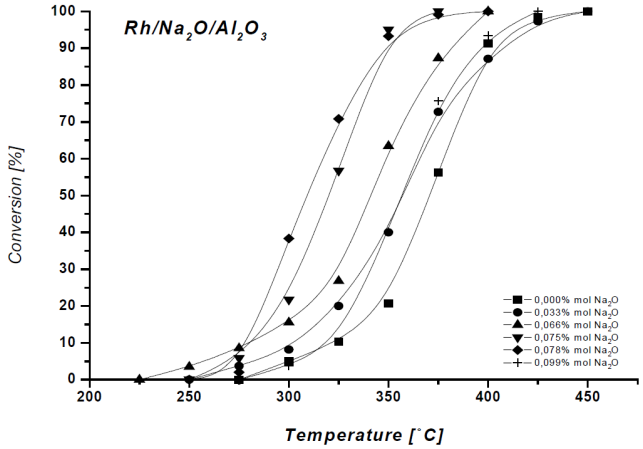

Figure 3.16: Temperature dependence of N_2O conversion for $Rh/Na_2O/Al_2O_3$ catalysts containing different sodium contents.[87]

It has been found that doping with alkali metals influences the catalytic activity, in particular N_2O decomposition strongly depends on the sodium content in Al_2O_3 as shown in Fig. 3.16. In case of undoped sample the reaction starts around 575 K and attains 100% conversion at 700 K. Doping with small amounts of Na_2O increases the activity, so that, for the sample containing 0.078 mol% Na_2O the reaction starts at 50 K and 100% conversion is attained at 650 K.

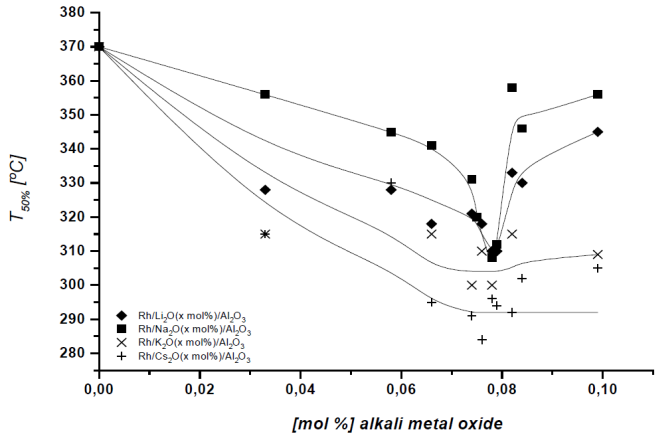

Figure 3.17: T_{50} as a function of the amount of Li, Na, K and Cs supported on Al_2O_3 for Rh catalysts.[87]

Fig. 3.17 shows that a sharp maximum of catalytic activity is attained at the concentration of about 0.08 mol% for lithium and sodium, whereas a plateau is attained around this concentration for potassium and cesium. For concentration of sodium higher than 0.08 mol% the catalyst activity becomes poor. It can also be noted that addition of potassium improves the catalytic activity to the same extent independently of whether it is deposited on pure alumina or alumina containing high amount of sodium. So The detrimental effect of sodium may be compensated by doping with potassium as indicated in Fig. 3.18.

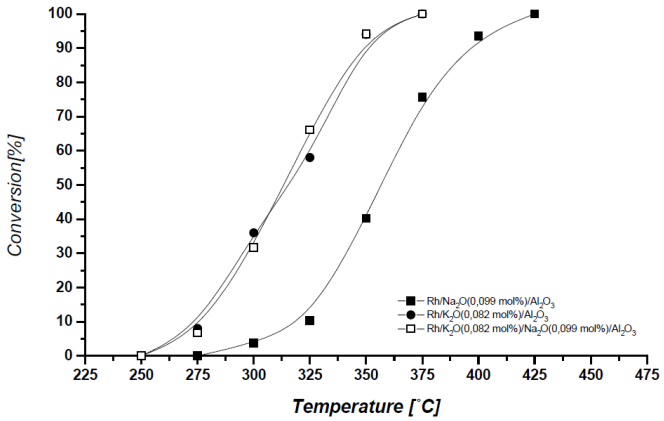

Figure 3.18: N_2O conversion as a function of temperature for Na, K and K/Na containing catalysts.[87]

Gaidei et al.[88] have then studied the catalyst activity of rhodium on other supports than pure alumina. A particular interest is given to zirconium supports (ZrO_2). Alumina based supports show reducing activity after a previous test at 1170 K which is not the case with ZrO_2 supports. The catalyst of 12% Rh/ZrO_2 composition shows the highest thermal stability during the process of cyclic tests. However, Al_2O_3 supports have an higher activity because they can contain higher quantity of rhodium (up to 19% by mass) due to their higher surface development. All those high performances rhodium-based catalysts offer high dynamic characteristics with a response time of around 0.2 s.

Finally, catalysts based on Iridium benefit from an increasing interest in the last decade.

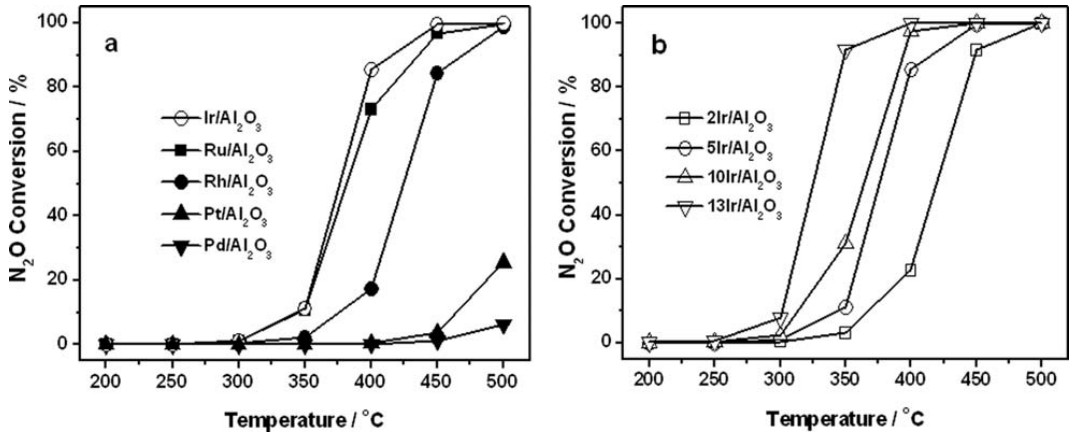

Figure 3.19: N_2O conversions for (a) different noble metal catalysts with 5% loading and (b) on Ir/Al2O3 catalysts with different loading (b).[89]

As indicated by Jian Lin et al.[89] in Fig. 3.19 Ir-based catalysts could outperform Rh-based catalysts.

Shaomin Zhu et al.[90] have particularly studied novel iridium-based catalysts for N_2O decomposition as a propellant: the Ir-hexaaluminate catalysts. With the chemical formula $BaIr_xFe_{1-x}Al_{11}O_{19-\alpha}$ (x equals to 0.2, 0.5, or 0.8), they are denoted as BIFA. Fig. 3.20 and Fig. 3.21 indicate that BIFA can initiate N_2O decomposition at lower temperature than Ir/Al_2O_3 (620 K) and can sustain the stability at 1200 K which offer higher operating temperatures than Ir/Al_2O_3 and Rh/Al_2O_3 catalysts.

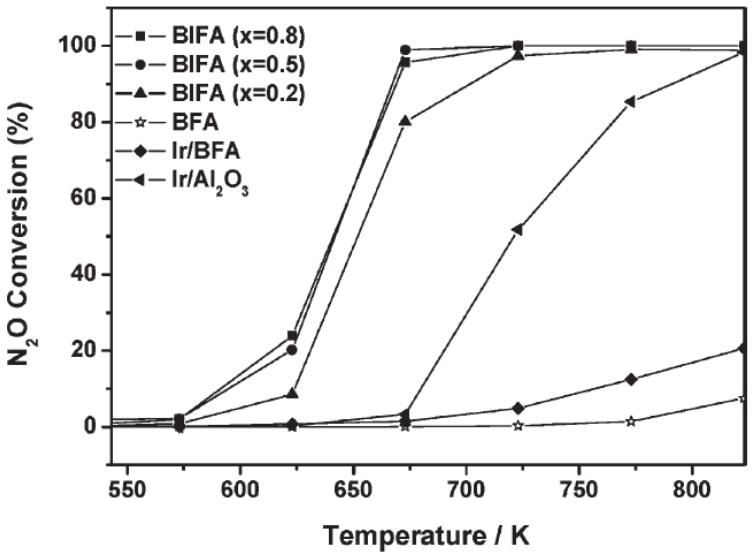

Figure 3.20: N_2O conversion as a function of temperature over BIFA and Ir/Al_2O_3 catalysts.[90]

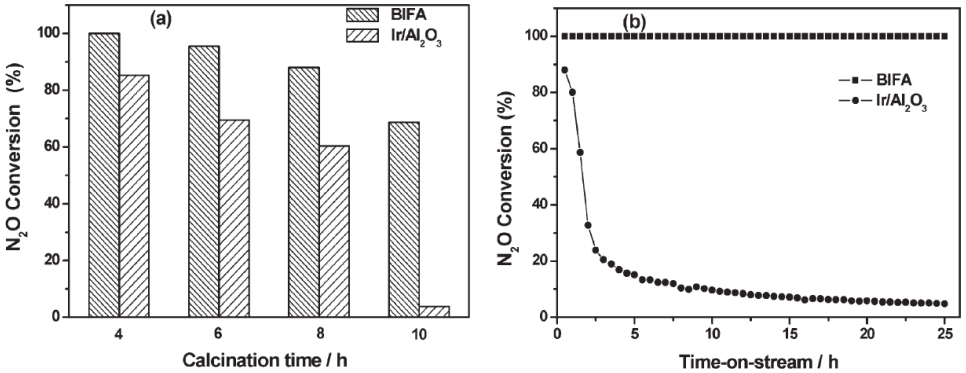

Figure 3.21: (a) Effect of calcination time at 1470 K on catalytic activities of BIFA and Ir/Al_2O_3 catalysts at 770 K. (b) Evolution of N_2O conversions at 770 K as a function of the time-on-stream over BIFA and Ir/Al_2O_3 catalysts.[90]

Ir-hexaaluminate catalysts can be act as promising catalysts for N_2O decomposition applicable in propulsion systems. Those new catalysts are promising but no more published result of tests in a propulsion system have been found.

3.3.3 Relevant realizations

As discussed in [91], a test facility has been constructed to test nitrous oxide monopropellant thrusters working with noble metal on alumina catalyst and providing thrust levels up to 2 N. The typical design for those thrusters is shown in Fig. 3.22.

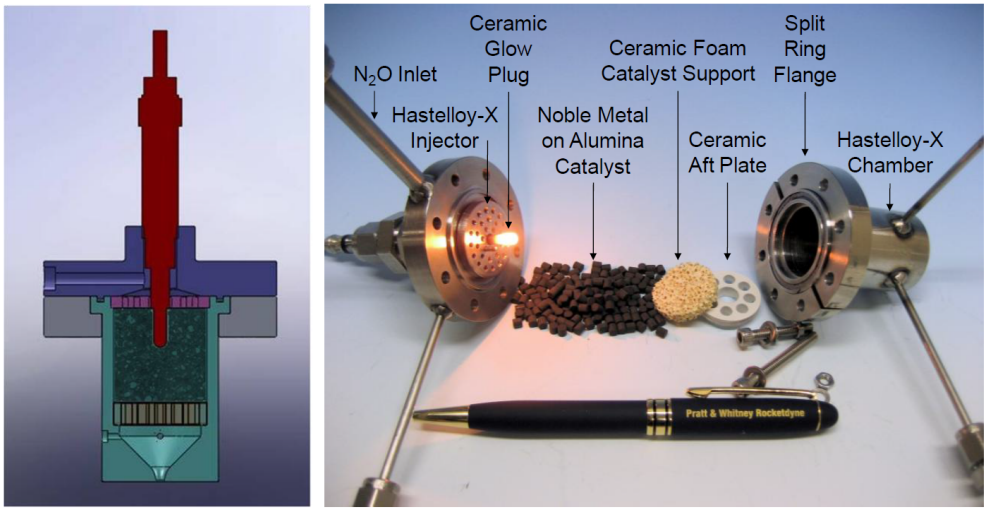

Figure 3.22: Design and pre-assembly of the catalyst gas generator (2.54 cm diameter).[91]

The ceramic glow plug has provided a successful means for initiating the self-sustaining reaction with as little as 30 W supply power and local catalyst temperature as low as 570 K. Critical aspects of a 2 N nitrous oxide monopropellant thruster from results of [91] are:

- Steady-state hot fire on a single catalyst of over 1 hour shows no sign of degradation;
- Multiple re-starts and thermal cycles on a single catalyst bed is possible. Hot re-starts require no additional pre-heat;
- Bed loadings up to 15 kg/m^2/s and chamber temperatures up to 1500 K provide a good decomposition efficiency. Higher bed loadings show a decrease in performances and higher chamber temperatures will degrade the catalyst;
- Catalyst bed pressure drop is low, typically 10% of chamber pressure. Efficient operation are found at chamber pressures over 5 atm.

N_2O thruster with palladium catalyst

Several experimental tests were carried out by G. Gallo, G.D. Di Martino et al.[92][93] in order to investigate the capability to decompose nitrous oxide with $Pd(5\%)/Al_2O_3$ cylindrical pellets catalyst in a 0.8 N monopropellant thruster. They concluded that the optimum operating condition exists for a loading value around 1.4 kg/m^2/s and that the catalysts should be heated up by means of a glow plug up to an initial temperature of around 570 K. A combined increase of the catalytic bed length and the catalysts' initial temperature allows to obtain very high decomposition efficiency.

N_2O thruster with rhodium catalyst

Hennemann et al.[94] present experimental results with a 2 N thruster prototype employing nitrous oxide decomposed by a Rh/Al_2O_3 catalyst. Cylindrical pellets of 2 mm diameter and 3 mm length and containing 5% by mass of rhodium oxide were used.

Results of a sequence of 5 pulses with 25 s on and 10s off followed by sequences of 3 pulses with 15 s on and 10s off are shown in Fig. 3.23a and Fig. 3.23b.

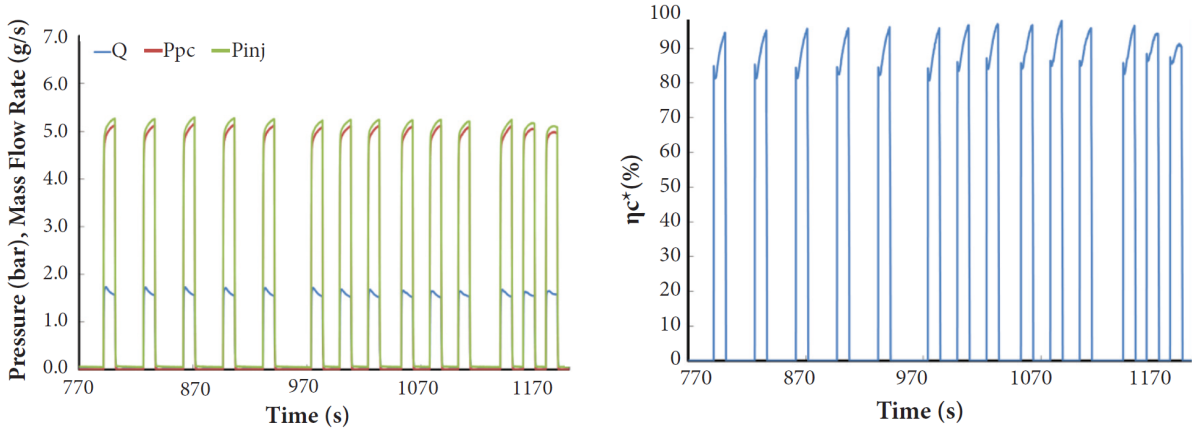

(a) (b)

Figure 3.23: (a) Pressure and mass flow rate measurements. (b) Characteristic velocity efficiency. [94]

It is observed that the injection pressure (P_{inj}) and post-chamber pressure (P_{pc}) reached respectively 5.29 bar and 5.15 bar, for an average mass flow rate of 1.65 g/s. The temperature at the end of the catalytic bed reached 1670 K and the thrust reached 1.93 N, close to the design value of 2 N. Pulses present similar profiles for several sequences and in different periods. However, a decrease in catalyst efficiency can be observed in the range of 1136 s to 1200 s. This is mainly due to the high temperatures reached in the catalytic bed which cause rhodium oxide loss. Relatively high decomposition efficiency at around 88% and high characteristic velocity efficiency at around 96% were observed prior to catalyst degradation.

N_2O thruster with iridium catalyst

Guobiao Cai et al.[95] describe the development research of a 1 N thruster based on nitrous oxide for fine attitude control of small spacecrafts. A 10 mm diameter and 2 5mm length catalyst bed made of Ir/Al_2O_3 grains of 0.9 mm with 17% iridium content was used. Nickel-chrome wires were wrapped tightly around the reaction chamber as the preheating source. Outside these wires, several layers of glass fiber fabric were wrapped for heat insulation (Fig. 3.11). Aluminum foil with a low surface emissivity was wrapped on the outermost layer, which may help to reduce the preheating energy as well as enhance the reaction temperature.

The vacuum-thrust measuring experiment was firstly conducted at a mass flow-rate of around 0.6 g/s (Fig. 3.24a). By reducing the mass flow rate to around 0.1 g/s, the thrust can reach 140 mN at the lowest (Fig. 3.24b).

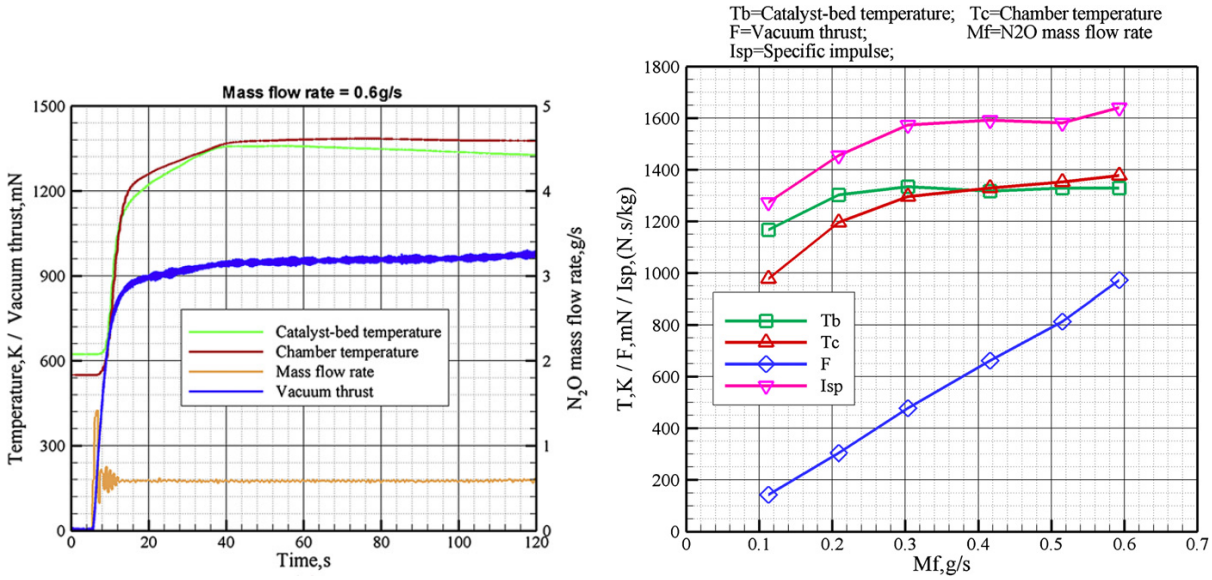

(a) (b)

Figure 3.24: (a) Experimental results of vacuum-thrust measuring at 0.6 g/s mass flow rate. (b) Performance of the thruster at different mass flow rate. [95]

Successful activation and self-sustaining reaction were achieved at 520 K. Static vacuum thrusts ranging from around 140 mN to 970 mN were achieved with the flow rates altering from around 0.1 g/s to 0.6 g/s. The highest specific impulse reached 167 s. It was found that the chamber temperature decreased along with the decrease of the N_2O mass flow rate, which in turn resulted in a gradual decrease of the specific impulse. Although the chamber temperatures were different, the catalyst-bed temperatures were similar.

Considering the high temperature performance of the current catalyst, the mass flow rate between 0.4–0.6 g/s is a suitable range for the 10 mm × 25 mm catalyst bed.

The deterioration of catalyst is rapid at a high temperature. 1420 K is a critical point for this catalyst. When temperature exceeded this limit, the reactors were hard to be restarted. This might be a major limit to the performance improvement of the N_2O monopropellant thruster based on Ir/Al_2O_3 catalysts.

All of the results [95][89] demonstrate the excellent and self-sustaining performance of the Ir/Al_2O_3 catalyst in N_2O decomposition, making it potential to satisfy the long-term run in 1 N scale thruster for orbit adjustment and attitude control of satellite.

Self-pressurization feed system

N_2O liquefied gas is featured for its high vapor pressure at room temperature. This property can be used to self-pressurize an N_2O tank. It can provide a steady supply of gaseous N_2O for the thruster. However, the tank pressure will decrease during N_2O supply process due to the evaporation of the liquid N_2O in the tank. The pressure drop may influence the stability of the N_2O supply if it exceeds the regulating range of the pressure regulator.

Guobiao Cai et al.[95] have also studied the characteristics of the N_2O self-pressurization feeding process. At low mass flow rate up to 18 kg/m^2/s (monopropellant thruster) a N_2O tank can be modeled by three lumped region as shown in Fig. 3.25.

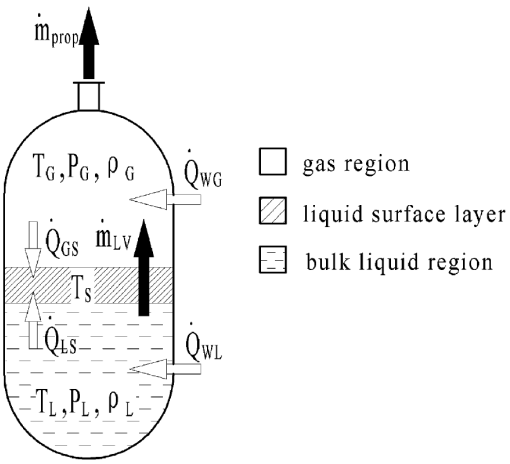

Figure 3.25: Tank model for gaseous N_2O feeding.[95]

The main governing equations, state equation and supplementary equations of the model can be found in [95]. The comparison of the experimental data and the simulated results at 0.7 g/s with 10 L and 3.3 L tanks is shown in Fig. 3.26. The simulation results agreed well with the experimental results. This indicates that the model can be used to predict the N_2O self-pressurization process of a sub-Newton propulsion system.

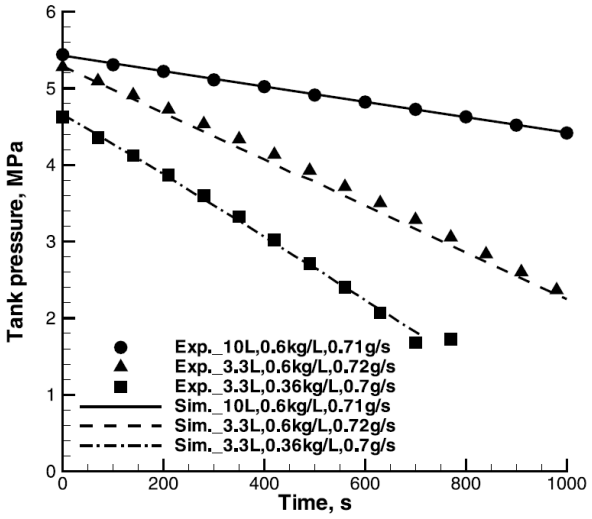

Figure 3.26: Experimental and simulated results of N_2O self-pressurization.[95]

Experimental and simulated results indicate that the tank pressure decreases during the N_2O self-pressurization process due to N_2O evaporation. A faster pressure drop is observed with a smaller volume tank or a lower initial filling factor. A large pressure drop occurs after long-term tank self-pressurization, so N_2O tank may not expel all the propellant at a stable mass flow rate in late stage of tank self-pressurization process, even at low mass flow rate. The phase change rate limits the maximum flow supported by self-pressurising nitrous oxide feed system. This would not be a problem within the operation range of the prospective monopropellant thruster (0.1-2 N). However, in hybrid rocket engines the mass flow rate is higher so the N_2O feeding process is different. Additional heat is required to compensate for the pressure drop by increasing the vaporisation rate of nitrous oxide. This is discussed later in section 3.4.3.

3.4 Hybrid rocket engine applications

The most impressive demonstrations of a N_2O hybrid rocket engine to date are the X-Prize winning SpaceShipOne system and the RocketMotorTwo used in SpaceShipTwo by Virgin Galactic to perform touristic sub-orbital flights.

In this section the performances of nytrox in HRE are discussed, then the fuel regression rate with nitrous oxide are reported focusing on paraffin-based fuels. Finally, some relevant realizations are reported.

3.4.1 Performances and system advantages of nytrox over pure nitrous oxide

The use of nytrox instead of pure nitrous oxide offers more safety and more flexibility in the design on a system while remaining storable as already discussed in 3.1.2. In hybrid rocket engines, nytrox can also improve the performances as shown in Fig. 3.27a and Fig. 3.27b.

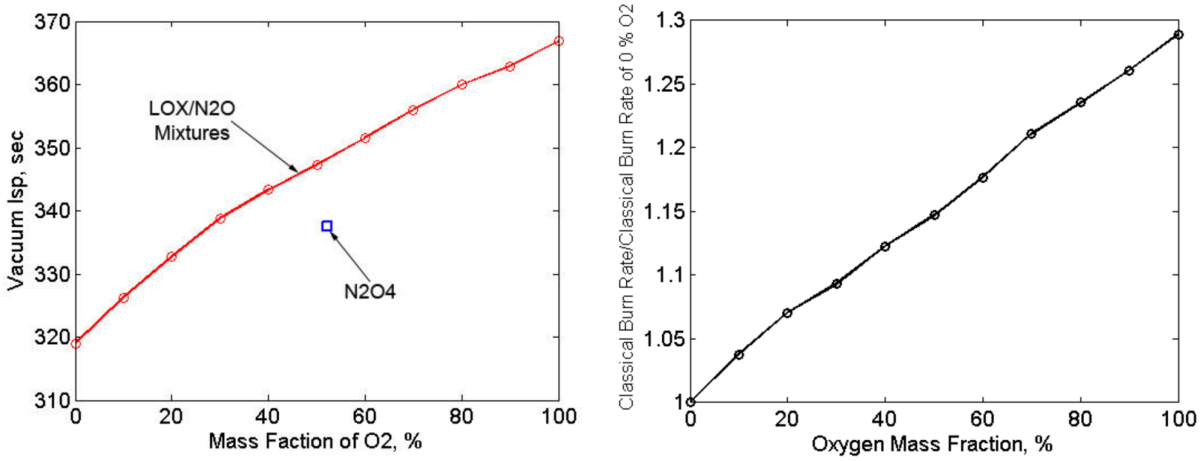

(a) (b)

Figure 3.27: (a) The maximum Isp as a function of the mass fraction of oxygen in the nytrox. (b) Regression rate of nytrox normalized by the regression rate of pure nitrous oxide as a function of the mass fraction of oxygen in the mixture. [63]

The 35% O_2/N_2O mixture matches the Isp performance of N_2O_4 toxic oxidizer and an increase of 29% in the regression rate is predicted as the mass fraction of O_2 is increased from 0% to 100%.

3.4.2 Fuel regression rate

Exploitable regression rate data, characterised by coefficient a in $[mm/s]/[kg/m^2s]^n$ and exponent n constants of Eq. 2.13, found in the open literature are all reported in Table 3.3 for comparison purposes.

Lohner et al.[96] and Doran et al.[97] have studied the regression rate of HTPB, PMMA, HDPE, and paraffin SP1A fuels with nitrous oxide at the Stanford test facility. Ballistic coefficients for SP1A are not reported in Table 3.3 because the 5 cm diameter fuel grains combined with a high regression rate limited test durations to approximately 2 seconds. Thus, the very short steady-state operation of the tests renders the data unreliable for

accurate ballistic coefficients. This example shows the reason why paraffin/N_2O regression rate data are poorly represented in the open literature. The regression rate obtained with paraffin was approximately 3 times greater than with HTPB. They succed to obatin regression rate of 3 mm/s for an oxidizer flux of 200 kg/m^2/s.

Tsong-Sheng Lee and Hsin-Luen Tsai [98] have studied the mixture of 50% paraffin wax and 50% HTPB (so-called 50P) fuel.

A paraffin based fuel composed of paraffin 66%, PE 4%, HTPB 15%, aluminum 10%, and magnesium 5% (denoted as 65P in Table 3.3) have been tested by Liu et al.[99] with GOX and N_2O. The exponent n is larger with GOX as the oxidizer, because of a high oxidation capacity and less heat required during the injection for GOX. Meanwhile, the constant a becomes smaller with GOX as the oxidizer, indicating a lower regression rate. The regression rates are similar under the optimal O/F ratio for both oxidizers.

Leverone et al.[100] report that aluminizing a paraffin wax fuel grain raises the combustion temperature and so increases the regression rate. Worth to be noted that it also radically reduces the engine's O/F ratio, which in turn lowers the amount of nitrous oxide required by the rocket and shortens its flight tank. The vehicle in this study experienced a 6.2% reduction in propellant mass with the addition of 40% aluminum particles by mass, versus a pure paraffin wax grain.

Fuel	**Oxidizer**	**Reference**	**Coefficient** a	**Exponent** n
HDPE	N_2O	[97]	0.116	0.33
PMMA	N_2O	[97]	0.131	0.33
HTPB	N_2O	[97]	0.188	0.35
50P	N_2O	[98]	0.1146	0.50
65P	N_2O	[99]	0.0876	0.40
65P	GOX	[99]	0.0431	0.72
Paraffin SP-1a	N_2O	[101]	0.155	0.50
60SP-1a/40Al	N_2O	[100]	0.175	0.50
ABS	GOX	[66]	0.128	0.52
ABS	Nytrox 87	[66]	0.124	0.46
ABS	N_2O	[66]	0.0118	0.80
HTPB	N_2O	[66]	0.0134	0.77

Table 3.3: Regression rate data of solid fuels with N_2O as oxidizer.

Those data which characterize the combustion can be used to design hybrid rockets corresponding to the systems used in the indicated references. Some contradictory results and unusable data for comparison have been found as in [102] and [103]. The difference of regression rate data for similar configurations is explained by the fact that a lot of other parameters influence the regression rate of a fuel and those parameters are not necessarily mentioned in the studies found in the open literature. The solid fuel geometry, the use of nytrox instead of pure N_2O, the injection of the oxidizer and the use of a diaphragm play a significant role in the regression rate of the fuel.

The combustion process is severely influenced by the incoming oxidizer flow pattern. Bouziane et al.[104] investigate the effects of oxidizer injection on the performance of a 1 kN paraffin-fueled hybrid rocket engine. Showerhead (SH), hollow-cone (HC), pressure-swirl (PSW) and vortex (VOR) injectors have been compared using nitrous oxide as the oxidizer (Fig. 3.28). They are all designed to deliver a mass flow rate of 550 g/s and a pressure drop of 25 bar.

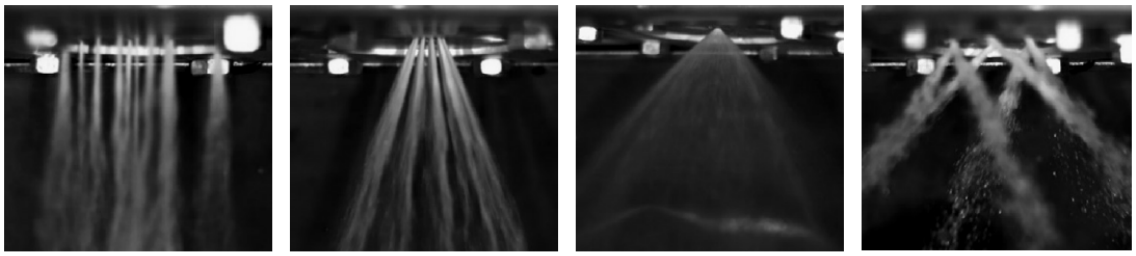

Figure 3.28: Discharge through (a) SH, (b) HC, (c) PSW, and (d) VOR injectors.[104]

Tests have been performed with different injectors but at constant oxidizer mass flux rate so it is impossible to extrapolate regression rate coefficients. Results are reported in Table 3.4.

	SH	**HC**	**PSW**	**VOR**
Regression rate $[mm/s]$	6.2	7.4	4.8	7.6
Specific Impulse $[s]$	160	150	170	185
Thrust coefficient	1.27	1.16	1.35	1.31

Table 3.4: Comparison of injectors performances.

The highest regression rate is achieved with VOR injector, with an increment of 58% and 23% compared to PSW and SH, respectively. This is because the VOR provides a centrifugal force to the injected oxidizer and produces a higher convective heat transfer to the solid fuel. HC also presents a high regression rate, whereas, at the same time, it shows the lowest efficiency and thrust coefficient. This is due to strong recirculation and impingement of the liquid N_2O on the rather soft paraffin fuel. Unburned paraffin fuel is ejected through the engine's nozzle without proper combustion, accounting for an increased regression rate but keeping the specific impulse low.

A diaphragm mixing device located in the midst of the fuel grain can enhance the combustion efficiency and fuel regression rate of a hybrid rocket engine. The diaphragm splits the solid grain in 2 parts as shown in Fig. 3.29.

Matthias Grosse [105] has studied the regression rate of N_2O/paraffin 1 kN hybrid rocket engine with 2 types of diaphragm: 1 and 4-hole perforation. The test results show that the use of a diaphragm positioned at 33% of the paraffin grain length delivers the highest combustion efficiency and regression rate. At this position, test results give a combustion efficiency of 93.7% for the 1-hole diaphragm and 96.6% for the 4-hole diaphragm while it is of only 86.7% without diaphragm. Regression rate results at 33% are reported in Table 3.5.

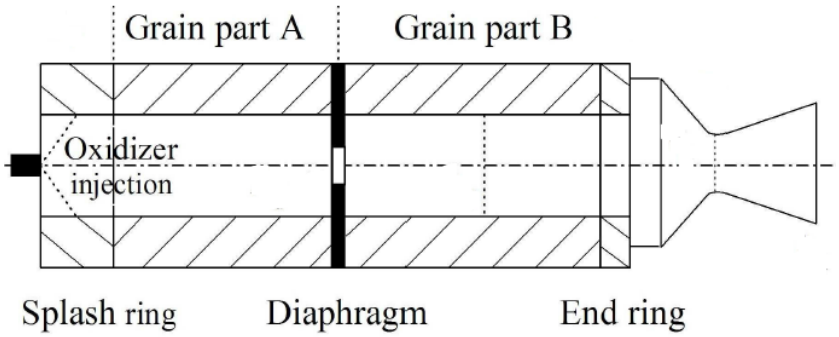

Figure 3.29: Scheme of the hybrid rocket engine with a diaphragm.[105]

	Coefficient a	**Exponent** n
without diaphragm	0.132	0.56
1-hole, part A	0.162	0.49
1-hole, part B	0.539	0.36
4-hole, part A	0.145	0.54
4-hole, part B	0.293	0.52

Table 3.5: Regression rate coefficients for N_2O/paraffin with a diaphragm at 33% of the fuel grain length.

The regression rate downstream of the diaphragm at the 33% position is about 40% higher at 250 kg/m^2/s for the 1-hole diaphragm and about 80% higher at 180 kg/m^2/s for the 4-hole diaphragm compared to the reference without diaphragm.

However, if unburned fuel residuals in the chamber part upstream of the diaphragm shall be avoided, special design are necessary to compensate for different regression rates.

Generally, the use of a mixing device aside from its common position at the end of the grain can be a valuable design alternative to achieve a nearly complete combustion and enhance the overall regression rate by simple means.

3.4.3 Relevant realizations

ABS fuel 3-D printed

As with hydrogen peroxide, Whitmore et al.[13][106][66] have studied electrical arc-ignition technology to ignite 3-D printed ABS fuel with nitrous oxide and with GOX. More especially, nytrox 87 is used and performances are compared with GOX oxidizer. Regression rates for GOX/ABS and nytrox 87/ABS, overlaid with regression rate data for other propellant combinations are reported in Fig. 3.30 and corresponding constants in the previous Table 3.3.

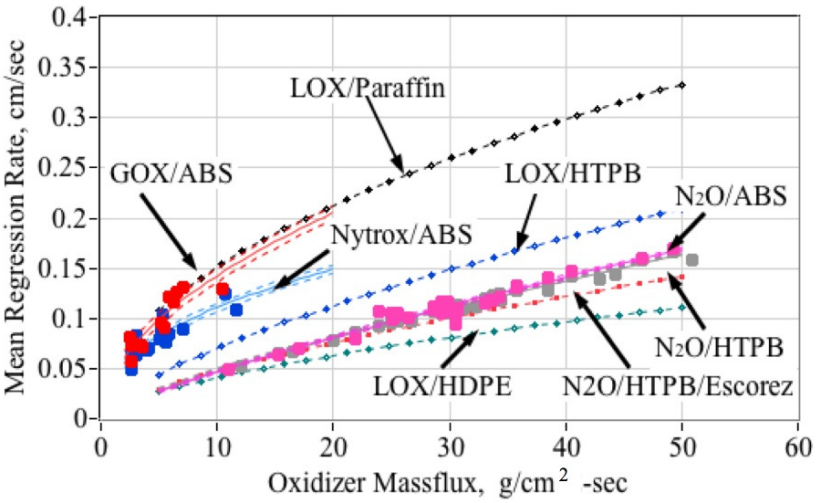

Figure 3.30: GOX/ABS and nytrox 87/ABS fuel regression rates compared to other hybrid propellants.[66]

The nytrox/ABS regression rate is moderately lower than for GOX/ABS and LOX/ paraffin systems, a result that is primarily due to the reduced flame temperature and the associated heat transfer from the flame zone to the fuel surface. However, the resulting nytrox 87/ABS regression rate is clearly higher than with pure nitrous oxide.

Despite its acceptable performances, the nytrox/ABS propellants exhibit mean ignition latencies that are significantly larger than for GOX-ignition: 0.9 s versus 0.3 s. It is hypothesized that the rapid expansion and subsequent phase change super-chills Nytrox fluid entering the combustion chamber. The very cold Nytrox reduces the pyrolysis rate of the fuel material and absorbs some of the spark energy.

Multiple prototype ground-test units with thrust levels varying from 4.5 N to 900 N have been developed and tested by Whitmore et al.[13][106][66]. Thus, with this spaceflight demonstration the TRL of the arc ignition technology must be acknowledged to be at least level 5. This promising technology is effective in igniting the nytrox/ABS propellants. The significantly high ignition latency compared to GOX/ABS could be overcome using a catalyst material which is not common when N_2O is used in a hybrid rocket engine.

Self-pressurization and system advantages

The phase change rate limits the maximum flow supported by self-pressurising nitrous oxide feed systems. This would not be a problem within the operation range of the prospective monopropellant thrusters (0.1-2 N). However, in hybrid rocket engines the mass flow rate is higher so the N_2O feeding process is different. Additional heat is required to compensate for the pressure drop by increasing the vaporisation rate of nitrous oxide. In order to sustain a mass flow rate of 6 g/s an heating of 1 kW is already needed [107].

It is considered that mass flow rates higher than 20 g/s cannot be supported by self-pressurising nitrous oxide feed system for space propulsion applications using only an additional heater. The engineering thermal solutions of the problem can involve:

- Application of additional heating;
- Regenerative cooling of nozzle or the whole thruster by nitrous oxide;

- Application of heat exchangers;
- Application of high thermal conductivity materials in the design;
- Increase in heat transfer exchange surface area;
- Application of nitrous oxide gas accumulators.

Those measures might still not be enough to support required high propellant flows. In such a case propellant expulsion system or pump-feed must be used.

An alternative is to use gaseous oxygen as the supplementary pressurant for the nytrox systems. For such a system, at the end of the liquid burn most of the vapor is composed of oxygen (typically more than 90%). Note that the optimal oxidizer to fuel ratio for the oxygen paraffin system is around 2.2 as opposed to 7.5 in the case of N_2O [63]. The sudden reduction of oxidizer flow rate in late stage of tank self-pressurization process will result in a significant drop in the oxidizer to fuel ratio which is ideal for an oxygen/paraffin hybrid rocket engine.

The elimination or minimization of the external pressurization system and the higher temperature operational capability would favor the nytrox mixture for a wide range of applications where good performance, low cost and operational simplicity are critical.

It can also be noted that the cooling property of nitrous oxide can be turned into a benefit. Active thermal control of the spacecraft can be performed by bleeding nitrous oxide out of the tanks.

HYROPS code

Leverone et al.[100] have studied the performance sensitivity on a blow down N_2O/paraffin hybrid sounding rocket. The influence of various design features on the performance of a 100 km apogee sounding rocket are investigated through a set of parametric trade studies using the Hybrid Rocket Performance Simulator (HYROPS). The results focused on how the chamber pressure, design O/F ratio and content of aluminium in the paraffin wax fuel could be varied so as to improve the design of a hybrid sounding rocket. Relevant results are reported below.

The vehicle's apogee can be markedly improved by increasing the design chamber pressure, but high pressures can also reduce the hydraulic pressure drop in the oxidizer line to below 15% at the end of the burn. Therefore, for stable combustion, the maximum design chamber pressure for the vehicle in this study was found to be 42 bar. An increase in chamber pressure also decreases the amount of propellant mass required, which in this case fell by 22 kg for a 30 bar engine, as compared to 42 bar.

A 6.2% reduction in propellant mass can be achieve with the addition of 40% aluminum particles by mass in the pure paraffin wax fuel.

The results obtained in [100] demonstrate that trade studies with software such as HYROPS can be useful to understand the complex interplay between design parameters in a hybrid rocket, and how they affect overall vehicle performance. Performance gain and mass saving obtained from the performance simulations of HYROPS reduce costs associated with the development of a hybrid rocket. However, it is also necessary to obtain experimental test data to better model the behavior of hybrid rocket engines.

3.5 Conclusion on Nitrous Oxide

Nitrous oxide can be stored as a liquid on board a spacecraft for long periods. Its high vapour pressure eliminates the need for an on board expulsion system. Its non-toxicity and compatibility with common construction materials suggest inexpensive system design and exploitation. The ability of this chemical to exothermically decompose leads towards its use for restartable monopropellant and hybrid engines. Its decomposition can be accelerated by catalyst which suggests low electric power input for the propulsion system. Nitrous oxide can also be used in cold-gas, and resistojet thrusters.

This covers all propulsion functions required for small satellites. Since the whole range of propulsion functions can be covered by one self-pressurising propellant, multi-mode propulsion systems can be envisioned to satisfy a wide variety mission requirements. Such systems would employ different types of thrusters fed by nitrous oxide from a single, simply designed storage tank. Due to its efficient propellant management, this multi-mode propulsion system would be very flexible to small satellite mission scenario changes. In the case of monopropellant mode failure, the thruster can be used in cold-gas mode ($Isp = 59s$).

Nitrous oxide/paraffin hybrid rocket engines have been invented as alternatives to other rocket engines, especially those that burn granular and rubbery solid fuels as HTPB. Originally intended for use in launching spacecraft, these engines would also be suitable for terrestrial use in rocket-assisted takeoff of small airplanes [108]. When fully developed, a nytrox-based hybrid system offers high value to the commercial space industry by offering a high-performing, but inherently safe, space propulsion option for rideshare payloads.

Chapter 4

Hydroxyl-Ammonium Nitrate

This chapter is based on the same structure as the previous one but with hydroxyl-ammonium nitrate (HAN) oxidizer.

HAN is a well-known ionic liquid propellant with low toxicity high density, high specific impulse, and low freezing point used in monopropellant and hybrid rocket engines. HAN-based monopropellants are among the most promising candidates for environmentally friendly rocket engine propellants to substitute hydrazine. HAN is also a powerful oxidizer for hybrid rocket engines.

HAN is an ionic liquid miscible with water up to 95% by mass, its equilibrium structure corresponds to hydroxyl-ammonium (NH_3OH^+) cations and nitrate (NO_3^-) anions. Its formula is $(NH_3OH)^+(NO_3)^-$ which can be summarized as $H_4N_2O_4$.

4.1 Characteristics

4.1.1 Physical properties

In solid form HAN is unstable and potentially explosive [109]. Thus, HAN is used in concentrated aqueous solutions up to 95% by mass in order to limit the explosion potential. HAN is storable in liquid phase. The general characteristics of HAN are detailed in Table 4.1. They are compared to the one of N_2O and HP 90%.

	HAN 95%	**N_2O**	**HP 90%**
Active O_2 content [%]	33	36	42
Boiling point at 1 atm [K]	445	185	414
Freezing point [K]	-258	182	261
Density (293 K liquid) [g / cm^3]	1.68	0.793	1.395
Vapour pressure [Pa] at 293 K	13.8	5.6x10^6	200
Molar mass [g / mol]	96	44	32.4

Table 4.1: Physical properties of HAN compared to nitrous oxide, and HP 90% [110].

Aqueous solutions of HAN possess a very low vapor pressure at room temperature. This low vapor pressure is one of the primary reasons that this propellant is considered to be significantly less hazardous than either hydrazine or hydrogen peroxide. HAN is easy to handle because it has very few toxins and is a stable substance at ordinary temperatures

and pressures. Its high density and its solubility in water makes it versatile by allowing the formulation of safe and efficient monopropellant blends [110].

Several drawbacks of HAN, which are discussed later, are high adiabatic temperature, unstable combustion behavior and incompatibility with different materials. Also HAN has a high viscosity about eight times higher than water, which made it difficult for the HAN flow to penetrate the catalyst.

4.1.2 HAN-based monopropellants properties

In typical applications, a fuel component such as methanol (MeOH) is added to the solution, creating a HAN-based monopropellant, to increase the propellant performance. HAN-based monopropellants are also reported to contain small amounts of ammonium nitrate (AN) [111]. AN is added to HAN solutions in order to decrease the freezing point. The water acts as the desensitizing agent and also serves to provide the necessary cooling to control the flame temperature of the combustion reaction [112]. In the composition of this monopropellant, excess nitric acid coming form the production process could be found [113]. Nitric acid must be kept below 0.1% by mass and iron below 5 ppm for safety purposes as it is discussed later.

The most promising HAN-based monopropellant for rocket propulsion applications is called SHP163 and is made of HAN 74%, methanol 16%, water 6% and AN 4% by mass. The density is reduced to 1.4 which is still 40% higher than hydrazine and the density specific impulse can reach up to 1.7 times the one of hydrazine [114]. Viscosity is also reduced by a factor 4 compared to 95% HAN. This composition corresponds to the stoichiometric ratio between HAN and methanol. SHP163 provides an Isp up to 270 s, which is 20% higher than hydrazine, with an adiabatic flame temperature of around 2400 K [111]. Two other similar formulations are worth to be noted: HAN269MEO15 and HAN284MEO17 [115][116]. Another HAN-based monopropellant for rocket propulsion reported in the open literature is called "AF-M315E" but its composition, its properties and its performances are not widely known due to its proprietary nature [117].

Other HAN-based monopropellants widely spread in the open literature are the liquid gun propellants LGP1845 and LGP1846 [118][113][119]. However their application to artillery guns is not of our interest here.

Majority of studies on HAN and HAN-based monopropellants have been conducted to characterize their ignition and combustion behavior. Methanol combination with HAN can deliver very high levels of temperature up to 2400 K. Flame structures of HAN and HAN-based liquid propellants, how pressure affects their burning rates [120], the phenomenon that occurred between the liquid and gas phase under high pressure and temperature environments, and the droplet combustion are some major subjects of study. The performances of the HAN-based liquid propellants, especially for SHP163, are discussed in section 4.3: Monopropellant applications.

4.2 Decomposition and catalysis

4.2.1 Decomposition path and auto-catalytic reaction

The chemical path of the HAN decomposition is way more complex than with HP and N_2O.

Different gas such as NO, N_2O, NO_2, NH_3, HNO, HNO_2, HNO_3 and other intermediates are involved in the decomposition of HAN. The results of the decomposition of HAN is highly dependent on the temperature and pressure conditions and cannot be resumed in a simple general equation. Fig. 4.1 shows the intermediate reactions involved in HAN decomposition.

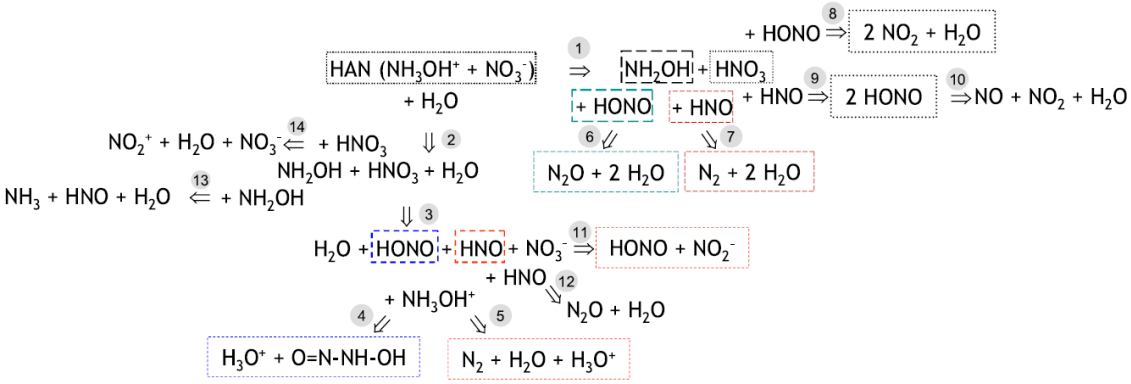

Figure 4.1: Intermediate reactions for HAN decomposition [109].

The first step of HAN decomposition is proton transfer from $(NH_3OH)^+$ to $(NO_3)^-$, producing NH_2OH and HNO_3. Since NH_2OH is a much stronger base than water, any protons that HNO_3 releases will associate with NH_2OH. Therefore, HNO_3 dissociation, releasing H^+, will simply reverse, leading to no net reaction. The second step of HAN decomposition is initiated by the combination of gaseous HNO_3 and NH_2OH, which form HONO and HNO [109].

Later, if the the nitric acid (HNO_3) becomes too concentrated it can produce nitrous acid (HNO_2). Nitrous acid as a reaction product also plays a role as a catalyst with HAN which lead to production of more nitric acid and so more catalyst [121]. This exhibit the auto-catalytic nature of the reaction between HAN and nitric acid. In this case the reaction rate will continuously increase leading to a possible explosion. In conclusion, the presence of nitric acid inside the HAN (coming from the process of production) triggers an auto-catalytic reaction, which represents a critical safety issue. Many accidents are reported by the U.S. Department of Energy in [118].

It is of primary concern to suppress the auto-catalytic reaction, as it is irreversible and very destructive once initiated. This is why HAN is usually blend with hydrocarbon fuels as methanol as seen previously. The fuel will burn with the nitric acid and then prevent the auto-catalytic reaction. However, in HRE this method is not favorable with regard to safety because it suppresses the safety advantage of a hybrid rocket engine which is the phase difference between oxidizer and fuel.

Auto-catalytic reaction can also be catalysed by presence of metal ions like iron and this is why it is recommended to keep iron below 5ppm in the composition of HAN-based monopropellants [110].

4.2.2 Thermal decomposition

Thermal decomposition of HAN has been studied by Hwang et al.[122], Courthéoux et al.[123] and Amrousse et al.[109]. The same thermal behavior was observed: first an endothermic reaction corresponding to the evaporation of water below 370 K, then the exothermic thermal decomposition of neat HAN liquid leading to the complete transformation of the propellant into gaseous products.

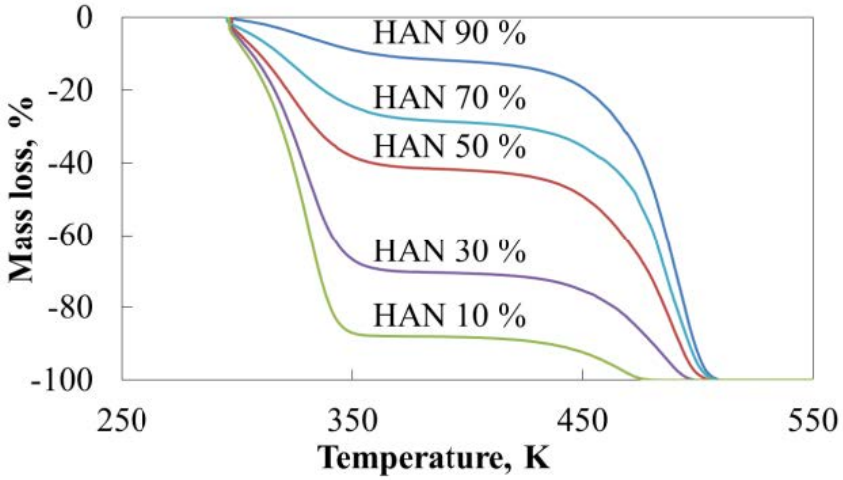

Figure 4.2: Decomposition of HAN solution [124].

Fig. 4.2 shows clearly the water evaporation because the weight loss at 370 K corresponds to the mass % of water in the solution for each tests. Then the remaining HAN decomposes thermally at around 450 K.

Hwang et al.[122] have obtained the same results with HAN solution containing methanol in a stoichiometric proportion with HAN (Fig. 4.3).

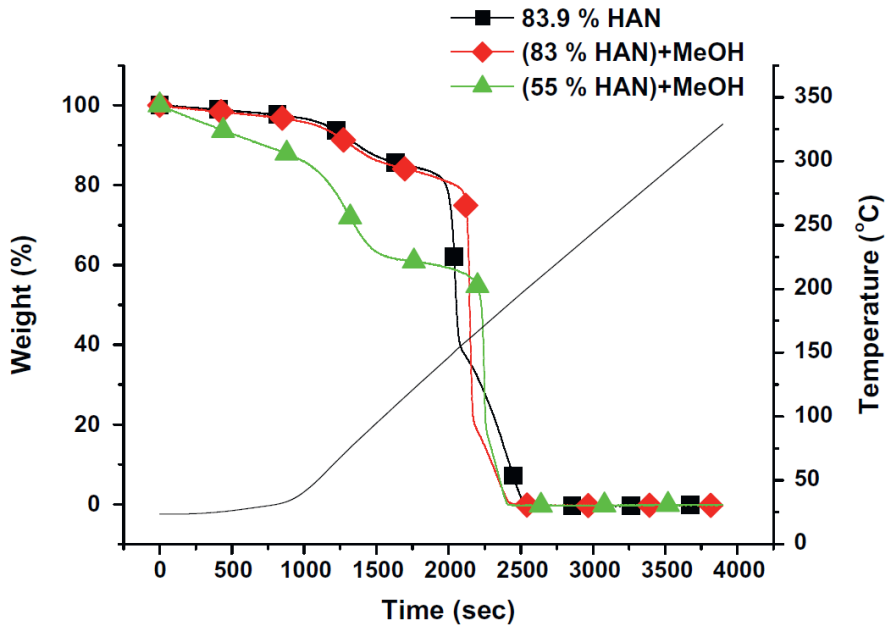

Figure 4.3: Decomposition of HAN-based monopropellants [122].

It can be noted that the presence of methanol does not affect the behavior of the thermal decomposition of HAN. Before the temperature reaches the boiling point of water, methanol evaporates mainly together with some portion of water.

This behavior can create thermal instabilities not desired for the good operation of the engines that demand high level of precision and reliability. Though lowering of decomposition temperature is desirable, the temperature of decomposition should still be above a certain temperature in view of safety during storage and operation. Catalytic materials are usually used to reduce the temperature of decomposition below 370 K.

4.2.3 Catalytic decomposition

Thermal stability and reproducible decomposition behavior are critical for HAN application in space thrusters. However, impurities coming from the production and by-products could change the reaction mechanism of HAN decomposition and start the auto-catalytic reaction in the worst case. A well selected selective catalyst can hinder the auto-catalytic reaction and decrease the ignition delay significantly to a reproducible value of less than 0.2 s as reported by Hoyani et al.[110].

While HAN can decompose even without a catalyst, catalytic decomposition is preferred over thermal as it lowers the decomposition temperature and enhances the rate of reaction. In contrast to the thermal decomposition, the temperature profile is stabilized and programmed to minimise the evaporation of water before that HAN decomposition occurs as it is shown in Fig. 4.4 and Fig. 4.5.

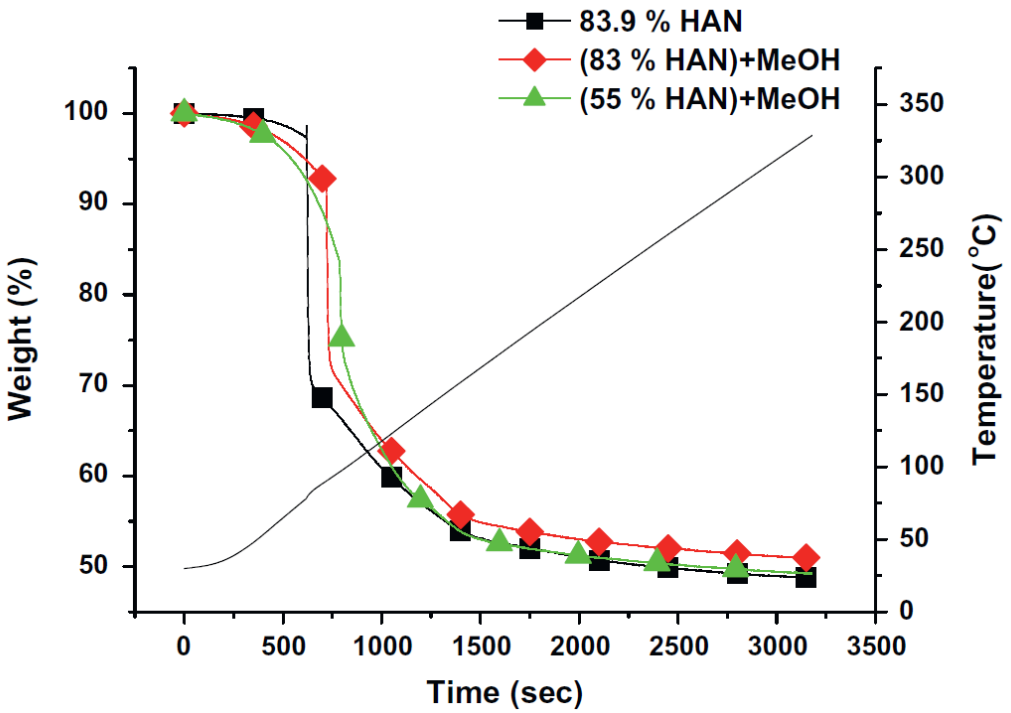

Figure 4.4: Decomposition of HAN-based monopropellants over an Iridium based catalyst [122].

The presence of water and methanol disturbs so little the interaction between HAN molecules and catalysts that the catalytic decomposition kinetics rate are considered similar between HAN-water-methanol and HAN-water mixtures despite the very different energetic content of both mixtures [123].

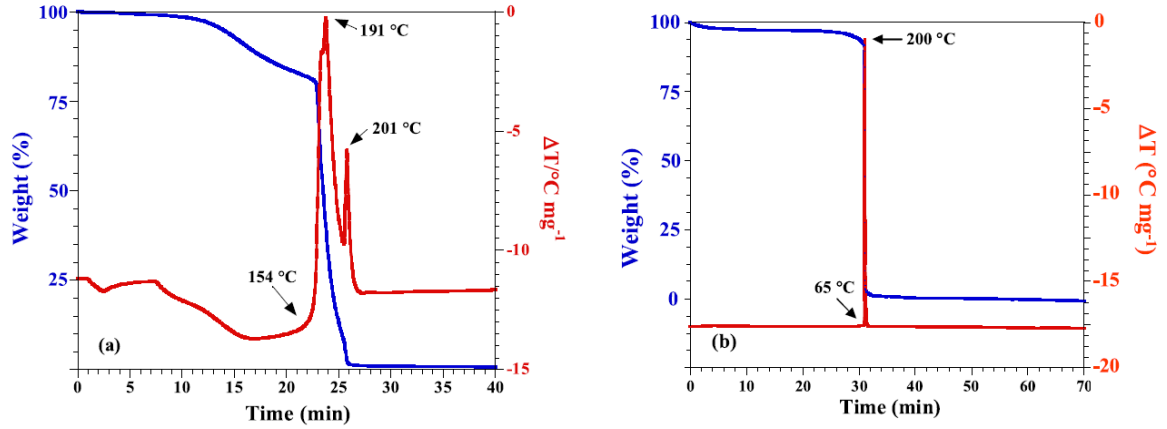

Figure 4.5: (left) Thermal and (right) catalytic (iridium) decomposition of SHP163 [109].

In [109], an Iridium based catalysts was used to reduce the decomposition temperature down to 340 K for SHP163.

Methanol combination with HAN can deliver very high levels of temperature higher than 2400 K so the catalyst materials must withstand those temperatures. Compared to the catalysts stated in the previous chapters, at those temperature the catalysts supported by Al_2O_3 pellets are usually changed to barium hexaaluminate (BHA, $BaO.6Al_2O_3$) grains or monolithic structures. The active materials reported in the open literature are iridium [125][126][127][128][127], platinum [129][130] and cerium [111][131][132]. Doped cerium catalysts was found to be far robust and resistant to any poisoning when compared to iridium catalysts.

The particular performances of those catalyst materials in monopropellant applications are discussed in section 4.3.2.

However, for hybrid rocket engines using HAN, catalytic ignition is usually avoided. Blending HAN with methanol to reduce the risk of auto-catalytic reaction is not suitable for HRE applications because it suppresses the safety advantage of a hybrid rocket engine which is the phase difference between oxidizer and fuel. Without the methanol blending, HAN solution are usually too viscous to go through a catalytic bed. When it does, nitric acid from the HAN decomposition reaction diffuses into the feed line, which triggers the auto-catalytic reaction. The thermal runaway by auto-catalytic reaction damages the system severely as in the tests conducted by Shinjae Kang and Sejin Kwon [121]. It is recommended to employ other ignition devices for the HAN hybrid rocket engines such as torch, spark, or hypergolic cartridge ignition.

4.3 Monopropellant applications

4.3.1 Combustion and burning rate of HAN-based monopropellants

The combustion mode of HAN-based monopropellants is very complex and is dependent upon composition and pressure. The combustion mechanism of HAN solutions still has not been clarified completely.

Fig. 4.6 shows SHP163 combustion at different pressures. Small and white bubbles are observed at 1 MPa due to the evaporation of water. From 3 MPa the bubbles volume increases and the color of transparent solution becomes brown, this phenomenon is caused by the formation of NO_2 gas, evaporation of water, and partial and slow decomposition of HAN. At 4 MPa and 6 MPa, the bubble diameter become smaller. It means that the bubbles of decomposition are generated but the high pressure assumes their decrepitating.

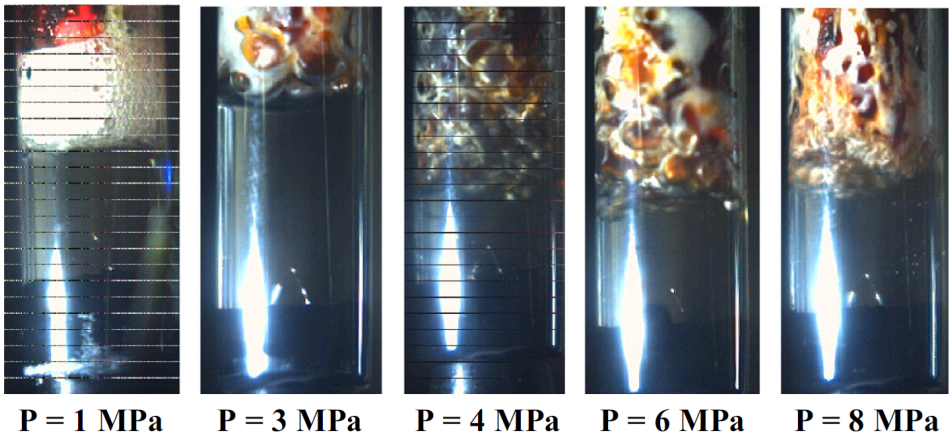

Figure 4.6: Pictures taken by high speed camera during combustion of SHP163 [113].

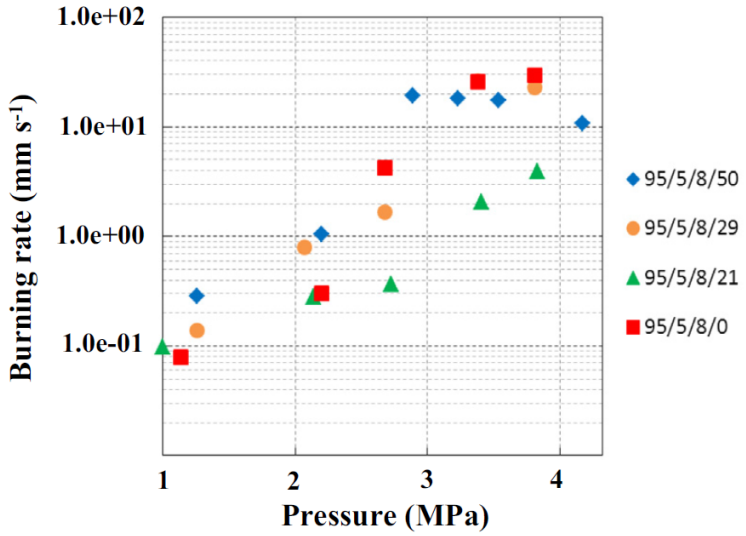

Figure 4.7: Burning rates of HAN-based monopropellants. SHP163 corresponds to the 95/5/8/21 sample [113].

The pressure influences the combustion behavior and so the burning rate as shown in Fig. 4.7. The burning rates have been measured by Amrousse et al.[113] with different mass percents of methanol, the SHP163 corresponding to the HAN-AN-water-MeOh ratio 95/5/8/21. The burning rates of 95/5/8/0, 95/5/8/29 and 95/5/8/50 mixtures jumped from the moderate rates to extremely high rates. The burning jump was absent in the case of SHP163 which present the best linear burning rate equation. The initial mass of methanol has a strong effect on the stability of burning rates. The jump of the burning rates cannot be demonstrated by combustion mechanism, but rather by hydrodynamic instability which changes the combustion mechanism [114]. Chang et al.[116] and Katsumi et al.[133] have conducted the same kind of experiments and they have arisen with the same conclusion that this instability of the liquid-gas interface triggers a sudden increase in the burning rate. According to instability theory [114], the addition of methanol reduces such instability so in the presence of methanol the burning rate decreases due to suppression of the vaporization rate and stabilization of the liquid surface. However, the mechanism whereby methanol suppresses the burning rate is not fully understood.

It is also reported that the boiling of water is responsible for the high burning rate because it increases the vaporization rate [134]. This is why AN is used in the blending of HAN-based monopropellants. In addition to lower the freezing point of the propellant, it minimizes the water content to avoid high burning rate characteristics.

4.3.2 Catalysts performances

Xiaoguang et al.[128] have studied the ignition decomposition temperature of HAN 80% with various catalytic metals on Al_2O_3 and SiO_2 pellets. Results are reported in Table 4.2.

Ignition temperature [K]	Ru	Rh	Pd	Ir	Pt
SiO_2 support	342	357	371	294	363
Al_2O_3 support	351	355	373	350	355

Table 4.2: Ignition temperature of HAN 80% on various metal catalysts supported on SiO_2 or Al_2O_3 [128].

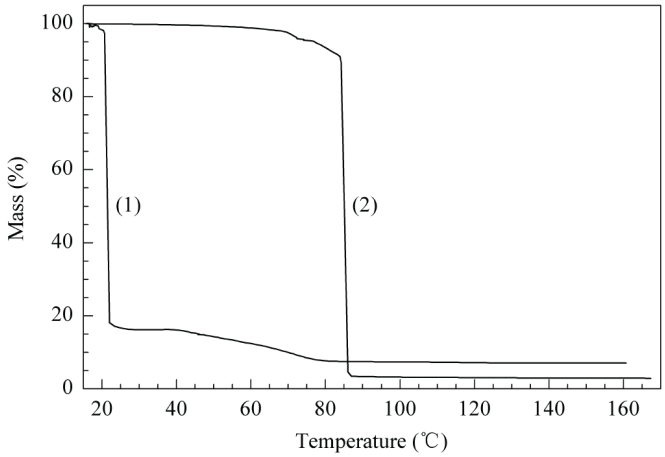

Figure 4.8: Decomposition of 80% HAN with (1) Ir/SiO_2 and (2) Ir/Al_2O_3 catalysts [128].

Iridium is the most active metal. Other metal catalysts such as Pt, Pd, Rh, and Ru have poor activity on HAN. Although a SiO_2 support shows an higher activity than with a Al_2O_3 support to ignite the decomposition, Ir/SiO_2 catalyst does not catalysed well the last reactions of HAN decomposition process as shown by Fig. 4.8.

This can create instabilities so Ir/Al_2O_3 catalysts such as Shell405 are preferred. Based on the decomposition of hydrazine with the well known Shell405 iridium catalyst, iridium is the most tested active phase for HAN decomposition. Iridium reduces the decomposition temperature of SHP163 to 325 K instead of 430 K for the thermal process.

The catalyst support plays a key role in enhancing the overall rate of decomposition of the monopropellant but few comparative studies have been carried out on the efficiency of different catalyst supports. Amrousse et al.[109][113][125][126][135][127] have compared the efficiency of the Shell405 catalyst ($Ir30\%/Al_2O_3$ pellets) with monolithic 30% Ir honeycomb catalysts (Fig. 4.9). A test on a 20 N thruster reported on Fig. 4.10 shows that the pressure slopes with 30% Ir honeycomb catalysts are higher than with Shell405 catalyst.

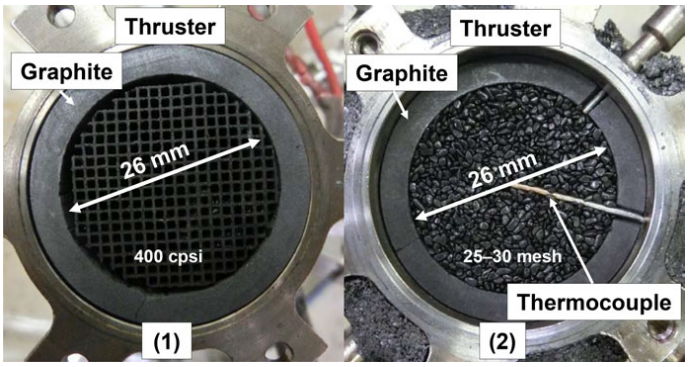

Figure 4.9: (1) Monolith catalyst and (2) grain catalyst [125].

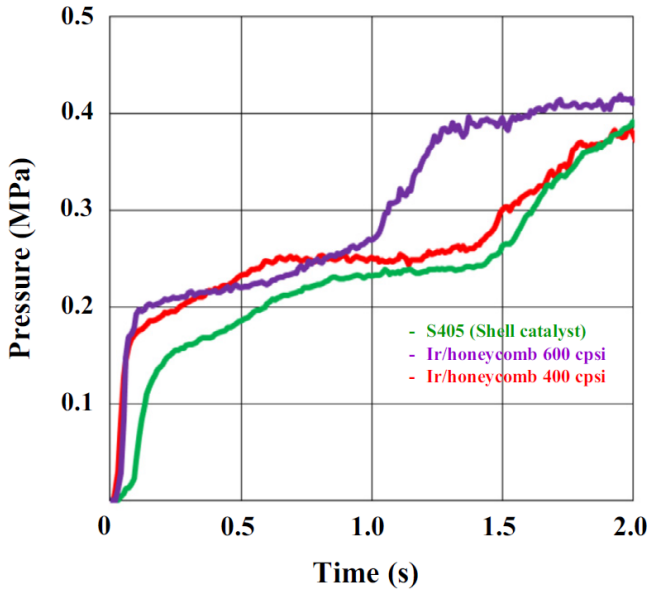

Figure 4.10: Burning reaction tests of SHP163 over 3 different iridium catalysts on a 20 N thruster [113].

Moreover, the pellets of Shell405 catalyst suffer at the high temperature of SHP163 decomposition. Honeycomb catalysts can withstand to higher temperatures than pellet catalysts but their activity are usually reduced due to a lower surface development. Also, the cost of honeycomb catalysts is much lower than pellet catalysts. Even if monolithic structures withstand the high temperature, the iridium starts to oxidize at those temperature and the performance decays with the increasing of reaction timing. The physical integrity and catalyst efficiency over a longer period of operation decline which makes it unfit for long duration mission.

Agnihotri and Oommen [131][132] have studied new active phases based on cerium (Ce) oxide. Different cerium oxide samples containing varying amounts of cobalt (10, 15, 20, 24, 26 and 28 mol%) were prepared. The highest catalytic activity is observed for CeCo 26 composition with signifcantly higher exothermicity (Fig. 4.11). However, further addition of cobalt is found to lower the high catalytic activity observed for CeCo 26.

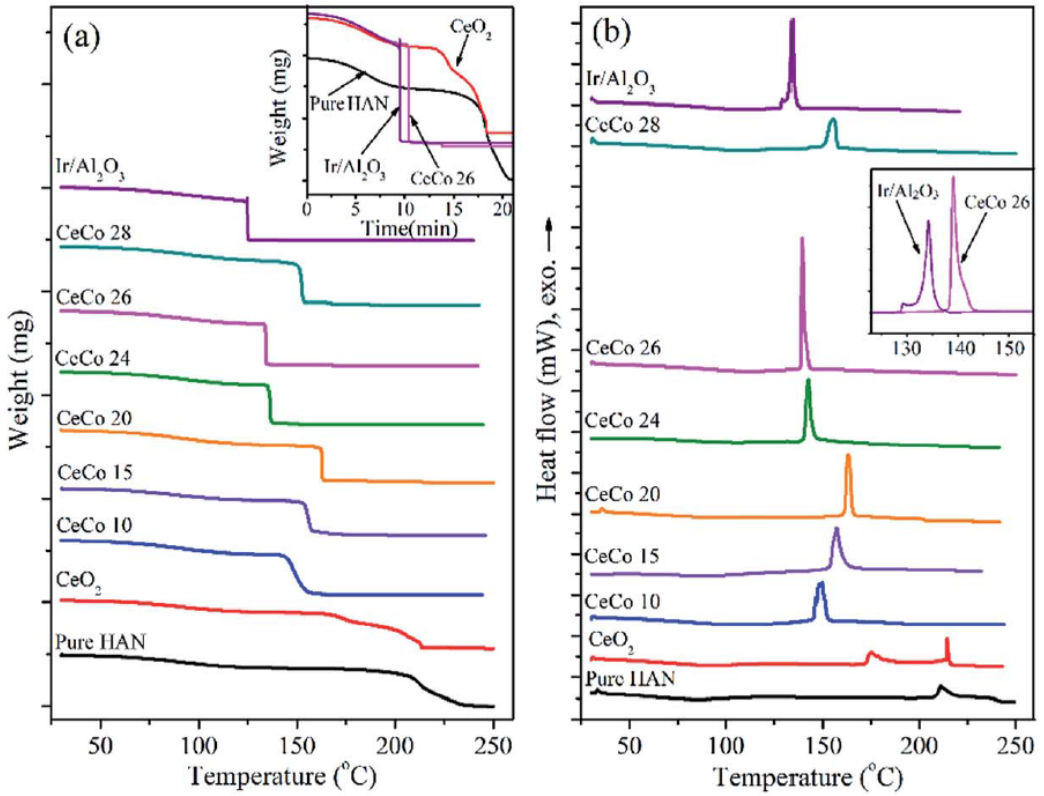

Figure 4.11: (a) Activity and (b) exothermicity of HAN decomposition over cerium and iridium catalysts [131].

Fig. 4.12a shows the product proportions of HAN decomposition without catalyst and with Ir and CeCo catalysts. This suggests distinctively different reaction route for CeCo 26 catalysed system. Lowering of nitrogen oxide and acidic species during decomposition over CeCo 26 suggests enhancement of nitrogen concentration which also implies a lower average molecular weight of the product gases and higher thruster performance. Compared to iridium based catalysts, the cerium oxide catalysts have similar reaction rates, are more durable in terms of physical integrity and more resistant to catalyst poisoning but they have an higher decomposition temperature by 285 K (Fig. 4.12b).

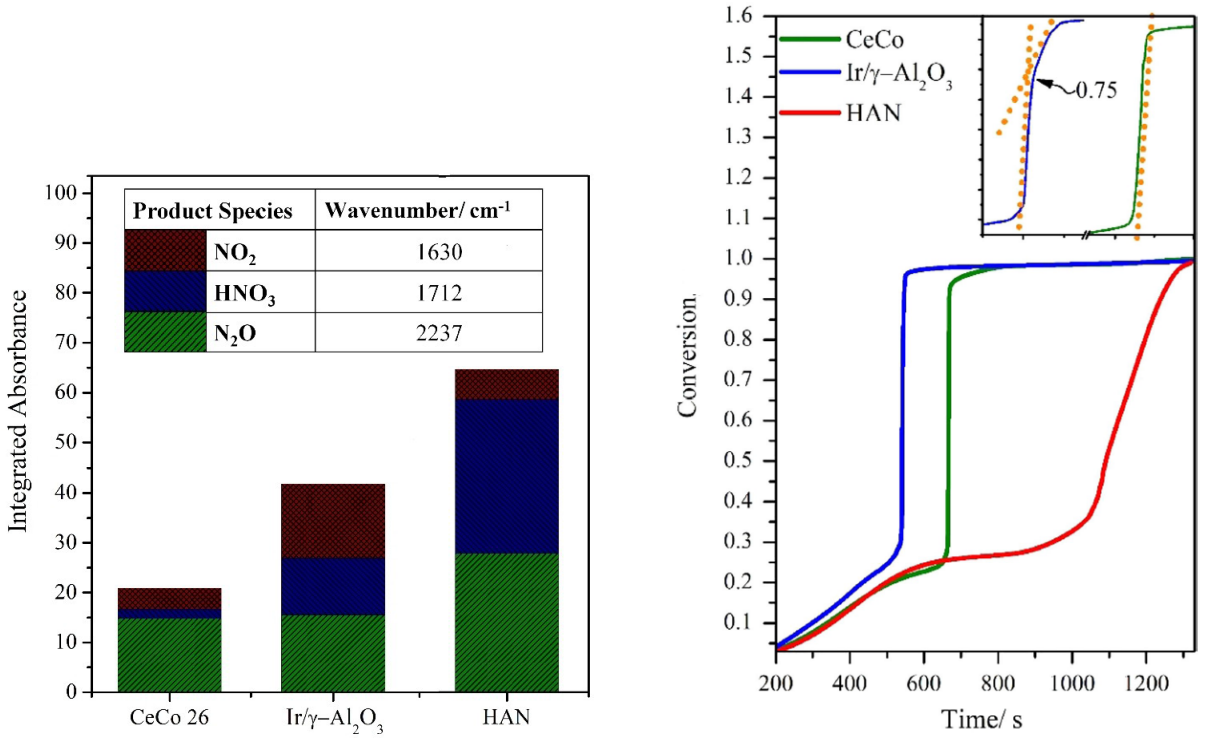

Figure 4.12: (a) Product proportions and (b) activity of HAN decomposition over cerium and iridium catalysts and without catalyst [131][132].

The activity of cerium oxide catalyst is extremely promising but real tests of durability and activity in a high temperature and pressure thruster are still to be conducted.

Finally, in 2021 Kang and Kwon [129] have demonstrated that a new catalyst, a platinum barium hexaaluminate (Pt/BHA) catalyst, could decompose HAN in a thruster. This catalyst takes the form of grains and has the advantage of being resistant to high temperature and insensitive to the possible poisoning of HAN decomposition products. Its main drawback is that its activity is sufficient only at a preheated temperature of at least 625 K. Tests performed on a 1.5 N thruster have shown a characteristic velocity efficiency below 20% when the Pt/BHA catalyst is preheated at 575 K whereas the characteristic velocity efficiency is of 72% when the Pt/BHA catalyst is preheated at 625 K.

This catalyst is obviously less active than the others previously reported but its very high resistant could allow long missions using a HAN-based monopropellant. The idea could be to use two catalysts, a first one based on iridium or cerium oxide to decompose the HAN at low temperature and then a Pt/BHA catalyst to withstand the high temperature decomposition. The Pt/BHA catalyst would be heated by the exothermic decomposition ignited by the first catalyst. A lot of studies and tests are needed to be done to develop this technology.

4.3.3 Relevant realizations

Japan Aerospace Exploration Agency

Japan Aerospace Exploration Agency (JAXA) is one a the major actor involved in the research and development SHP163 for its utilization as an alternative of hydrazine toxic component in monopropellant thrusters. This HAN-based monopropellant have been selected for their "Innovative Satellite Technology" project launched in 2016.

As explained by Hori et al.[136], this project has led to the use of SHP163 in a 1N thruster, the Green Propellant Reaction Control System (GPRCS) which equips the satellite RAPIS-1 launched in 2019.

From the open literrature point of view, this is the most relevant project using HAN in a real application. Around 3000 s of accumulated operation time and 10000 times of pulse mode burn have been recorded. Based on the data received from the RAPIS-1 and the GPRCS until end of 2019, the combustion efficiency in the real use was evaluated at more than 80% and the first factor of the "space proven" is successfully achieved.

Discharge plasma ignition system

In 2018, an ignition system using the discharge plasma of argon noble gas, called a discharge plasma system, has been proposed by Wada et al.[137] in substitution for the conventional solid catalysts.

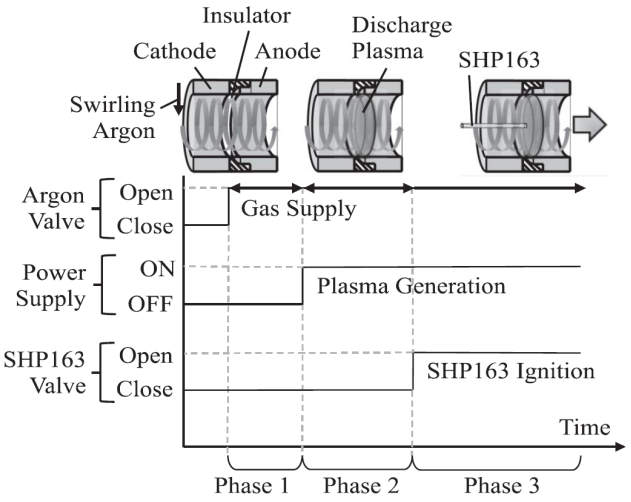

Figure 4.13: SHP163 ignition sequence using a discharge plasma system. [137].

Fig. 4.13 is an illustration of the SHP163 ignition process using the discharge plasma system. In phase 1, the argon gas valve is opened, allowing argon gas to flow into the combustion chamber through a swirl gas injector. In phase 2, a power supply is turned on. An intense electric field forms between the cathode and anode, and a discharge plasma is then generated from ionized argon gas. In phase 3, the propellant valve is opened. The propellant ignites when it comes into contact with the discharge plasma.

With a single-hole injector, at an SHP163 feed pressure of 800kPa, a maximum thrust of 0.37 N was achieved with a power consumption of 527W and a SHP163 mass flow rate of 0.34 g/s, in conjunction with a characteristic velocity efficiency of 98%.

The thruster lifetime is evaluated in terms of electrode degradation. At an accumulated firing time of 1646 s, no effect of electrode degradation on the performance of the 1 N thruster was observed.

4.4 Hybrid rocket engine applications

Publications and discussions about the use of HAN in a hybrid rocket engine in the open literature are extremely rare. Some references previously cited mention that HAN can be used in a hybrid rocket engine configuration but no data, test or existent engine are reported. The main discussion is about the difficulties that will be encounter to ignite such a hybrid rocket engine compared to the monopropellant system described previously.

The few articles that could seem interesting are either inaccessible or unusable (fully written in Japanese with no translation available).

The scarce data reported by Heister and Wernimont [3] and Biddle et al.[138] suggest an Isp performance of the HAN 95%/HTPB system of around 260 s. In the end this performance is not higher that what can achieve a HAN-based monopropellant such as SHP163 in a monopropellant system.

4.4.1 Ignition

Catalytic ignition of HAN in a hybrid rocket engine should be avoided. In the tests performed by Kang and Kwon [121], the catalytic reactor was irreversibly damaged by the auto-catalytic reaction because no blending with a fuel such as methanol was used. As already discussed in section 4.2.3, blending HAN with hydrocarbon fuel can reduce the concentration of nitric acid to avoid the auto-catalytic reaction, but it takes away the HAN hybrid rocket engine's advantage with regard to safety.

It is recommended to employ other ignition devices for the HAN hybrid rocket engine: for instance torch, spark, or hypergolic cartridge ignition.

Loehr [139] suggests that the temperature of decomposition products in the combustion chamber should exceed the auto-ignition temperature of HTPB and may therefore negate the requirement for an ignition grain heating charge typically associated with HTPB hybrid rocket engines. However, ignite the HAN decomposition safely without catalyst is still need to be done.

4.4.2 Fuel regression rate

Theoretically, using HAN as an oxidizer in hybrid propulsion systems would have the advantage of enhancing the regression rate in the turbulent boundary layer because HAN has a much lower vapor pressure and experiences higher heat transfer rates compared to oxygen.

The only data found are provided by Belcher [117] and they indicate this regression rate law for HAN/HTPB: $\dot{r} = 0.05\, G_{ox}^{0.8}$ with $\dot{r}$ expressed in mm/s and G_{ox} in kg/m^2/s. Unfortunately, no other data or test have been found in the open literature.

4.4.3 Relevant realization

The only realization found concerning a hybrid rocket engine using HAN is about a gas-hybrid rocket engine studied by Onodaka et al.[124]. Gas-hybrid rocket engine means that the HAN liquid oxidizer is burnt with a gaseous fuel and not with a solid fuel. A general structure of the gas-hybrid rockets is shown in Fig. 4.14.

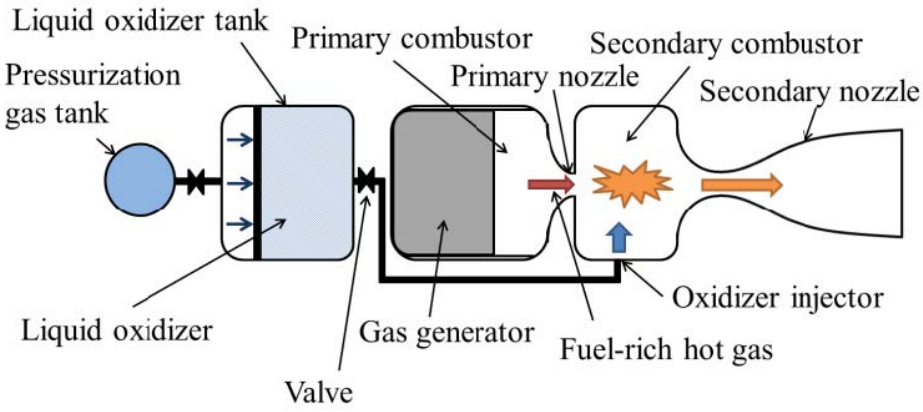

Figure 4.14: Structure of gas-hybrid rocket engine [124].

In fact the fuel-rich hot gas is used to ignite the HAN decomposition. This system called gas-hybrid rocket engine is similar, in terms of working principle, with the discharge plasma ignition system.

Finally, the only realization found in the open literature involving the term hybrid is not a hybrid rocket engine in the sense of this work.

Chapter 5

Thermochemical analysis NASA CEA

This chapter presents an analysis of performances of hydrogen peroxide, nitrous oxide and HAN in hybrid rocket engines using the NASA CEA code. The combustion chamber flame temperature and the vacuum specific impulse are the performance parameters analysed. The fuel investigated with all oxidizers is the paraffin wax of formula $C_{50}H_{102}$. The performances of HTPB with hydrogen peroxide are also computed to provide a comparison with paraffin. The flow is considered in a shifting equilibrium in the nozzle.

Four analysis are performed:

- **Hydrogen peroxide performance analysis with HTPB and paraffin.** HP from 87.5% to 100% (step 2.5%, and also 99%) with HTPB and paraffin $C_{50}H_{102}$ for O/F ratio from 2.5 to 10. Parameters are combustion chamber pressure of 10, 20, 30, 40, 50, 60 and 70 bar for a nozzle expansion ratio of 40;
- **Hydrogen peroxide / paraffin performance analysis at different nozzle expansion ratio.** HP 97.5%, 99% and 100% with paraffin $C_{50}H_{102}$ for O/F ratio from 2.5 to 10. Parameters are combustion chamber pressure of 30 and 70 bar for nozzle expansion ratio of 20, 40 and 80. The flow is considered frozen at throat;
- **Nitrous oxide / paraffin performance analysis.** Liquid N_2O with paraffin $C_{50}H_{102}$ for O/F ratio from 2.5 to 10. Parameters are combustion chamber pressure of 30 and 70 bar for a nozzle expansion ratio of 40. The flow is considered frozen at throat;
- **HAN / paraffin performance analysis.** HAN with paraffin $C_{50}H_{102}$ for O/F ratio from 5 to 12.5. Parameters are combustion chamber pressure of 30 and 70 bar for a nozzle expansion ratio of 40. The flow is considered frozen at throat.

As nitrous oxide and HAN are not included in NASA CEA, the enthalpy of formation of N_2O used is 82.05 kJ/mol [61][62] and the enthalpy of formation of HAN used is 338.7 kJ/mol [140].

5.1 Hydrogen peroxide performance analysis with HTPB and paraffin

Combustion chamber flame temperature and vacuum specific impulse for HP from 87.5% to 99% with HTPB are plotted in Fig. 5.1 and Fig. 5.2; and with paraffin in Fig. 5.3 and Fig. 5.4. The performances of HP 100% with HTPB and paraffin are plotted in Fig. 5.5.

For both fuels the impact of the chamber pressure is more significant on the chamber temperature than on the vacuum specific impulse and it is more significant at higher concentration of hydrogen peroxide. Between chamber pressure of 10 and 70 bar, with both fuels, a difference of 94 K in maximum flame temperature is observed with HP 87.5% while it is of 136 K with HP 100%. Going form 10 bar to 70 bar can provide an increase in chamber temperature of 4%. However this impact of chamber pressure is way less significant on the vacuum specific impulse. Going from 10 bar to 70 bar, the vacuum specific impulse can be increased by maximum 2 s with HP 100% which is less than a 1% increase.

The concentration of hydrogen peroxide is a more influencing parameter than chamber pressure. As expected, the higher the concentration of HP is the higher the performances are. The maximum vacuum specific impulse with a chamber pressure of 70 bar for each cases is reported in Table 5.1.

HP concentration [%]	87.5	90	92.5	95	97.5	99	100
HTPB							
Maximum vacuum Isp [s]	311	314	319	322	326	328	329
Optimum O/F	7.5	7.25	7	6.75	6.5	6.5	6.5
Paraffin							
Maximum vacuum Isp [s]	310	315	318	322	326	328	329
Optimum O/F	8.25	8	7.75	7.5	7.5	7.25	7.25

Table 5.1: Maximum vacuum specific impulse performance of HP/HTPB and HP/paraffin with a chamber pressure of 70 bar and a nozzle expansion ratio of 40.

The maximum performances of the two fuels are identical. The same similarity is observed with the chamber temperature, of around 2750 K for HP 87.5% and 3000 K for pure HP. The main difference between HTPB and paraffin $C_{50}H_{102}$ is the O/F corresponding to the maximum performance which is slightly higher when paraffin is used. The O/F shift in hybrid rocket engines has the same impact either HTPB or paraffin are used because the decrease rate of Isp in the neighbourhood of the optimum O/F are identical with both fuels.

5.1.1 HP 87.5% to 99% with HTPB results

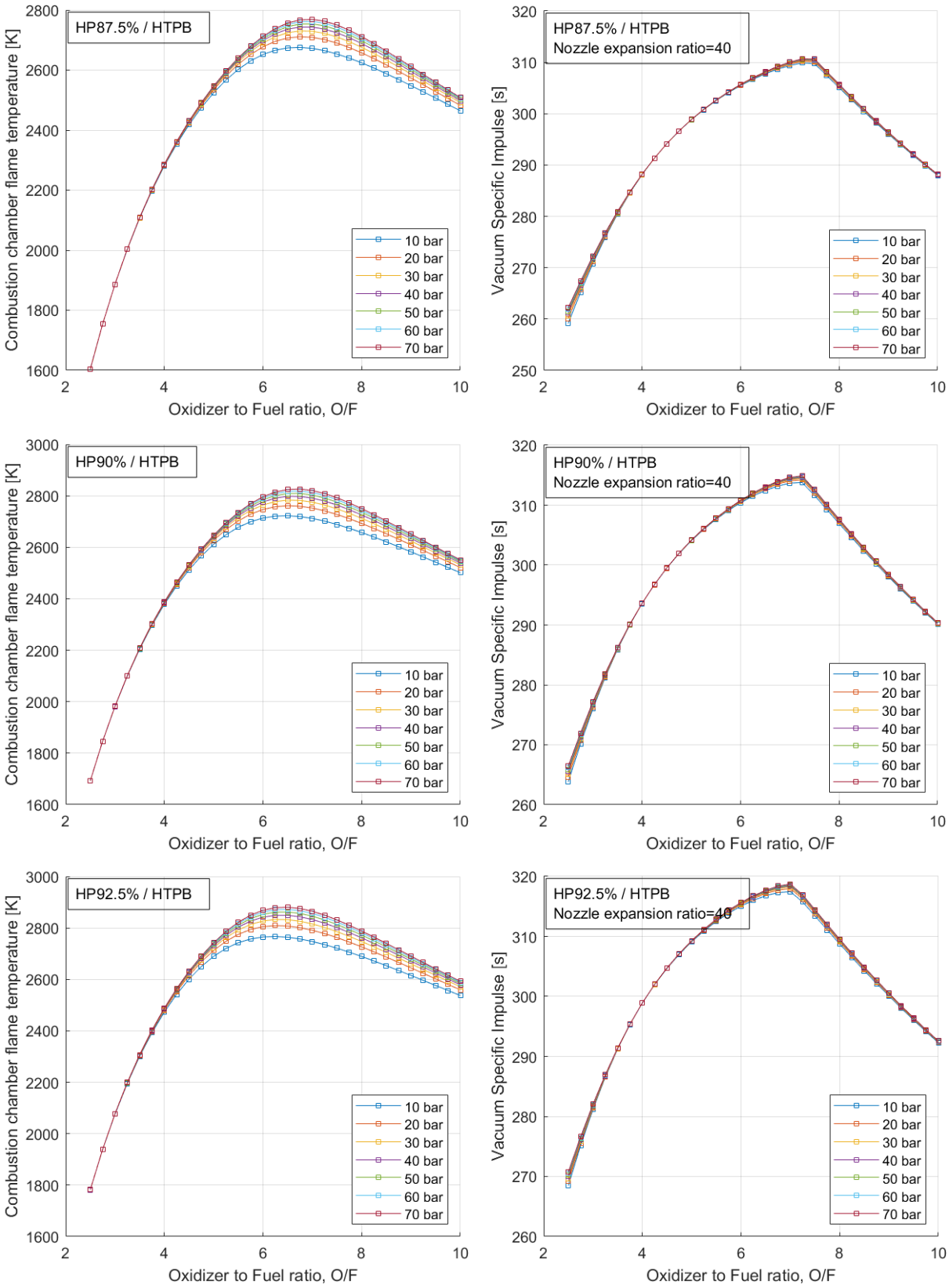

Figure 5.1: NASA CEA results of HTPB with HP at 87.5%, 90% and 92.5%.

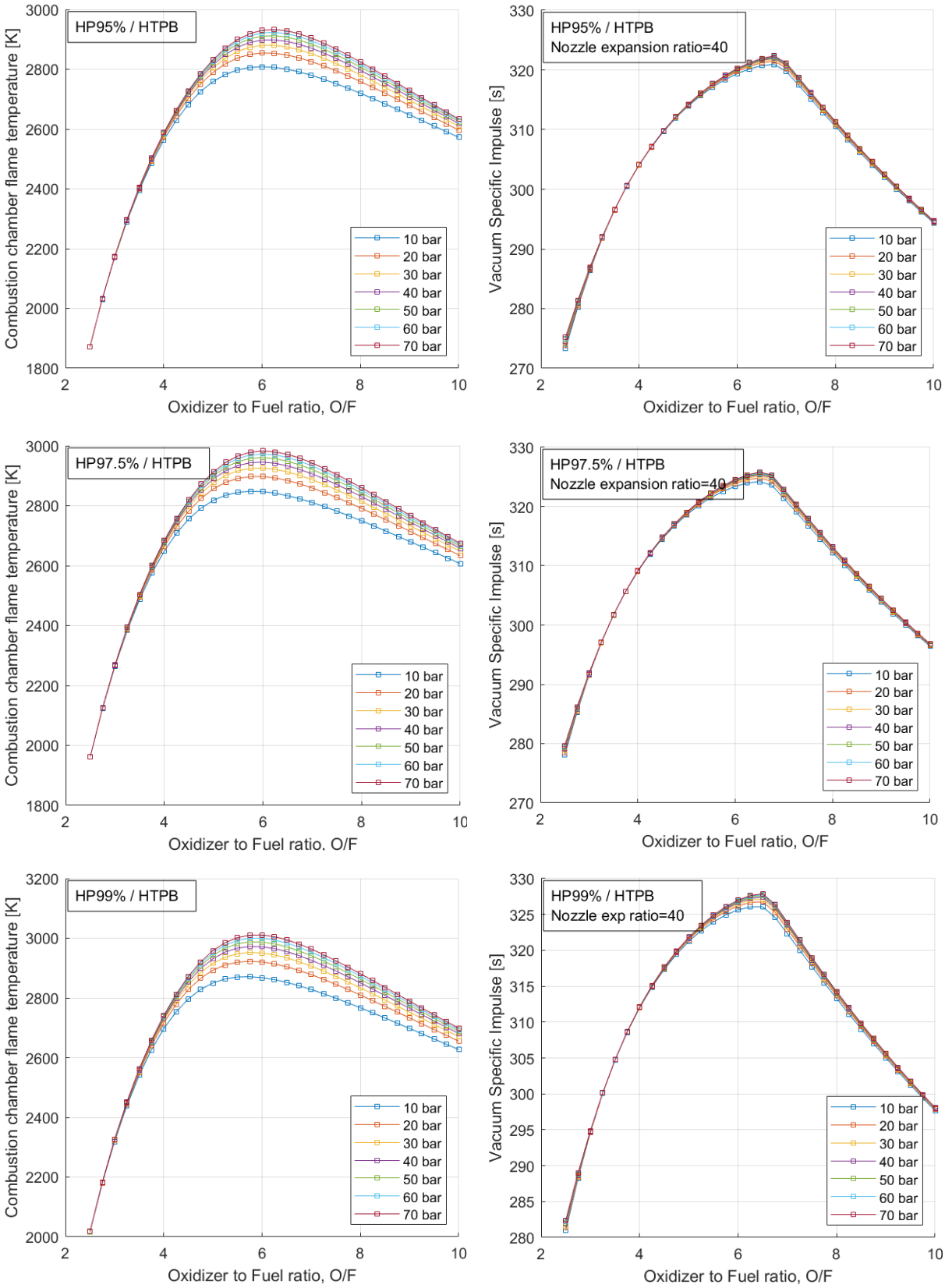

Figure 5.2: NASA CEA results of HTPB with HP at 95%, 97.5% and 99%.

5.1.2 HP 87.5% to 99% with paraffin results

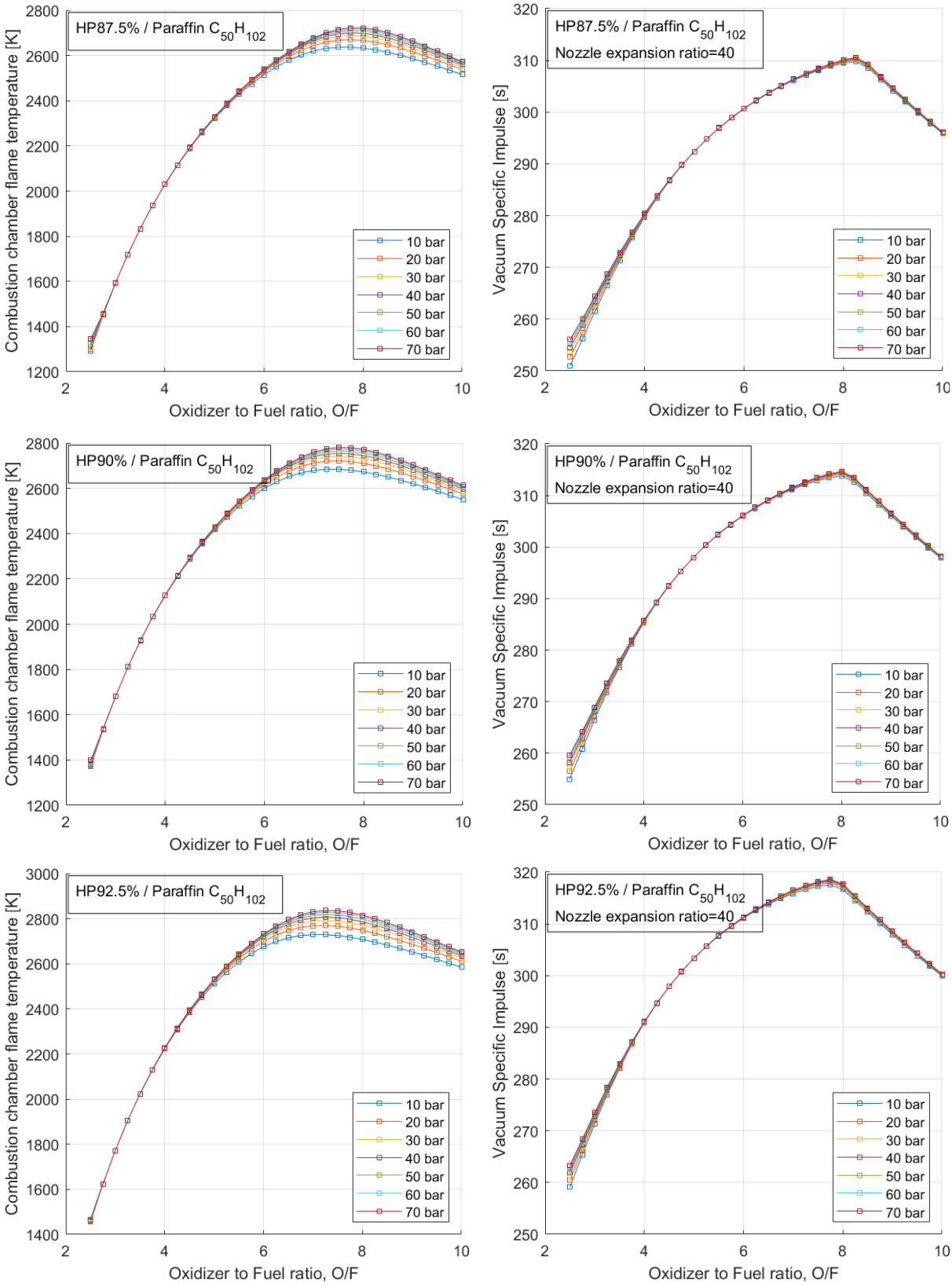

Figure 5.3: NASA CEA results of paraffin with HP at 87.5%, 90% and 92.5%.

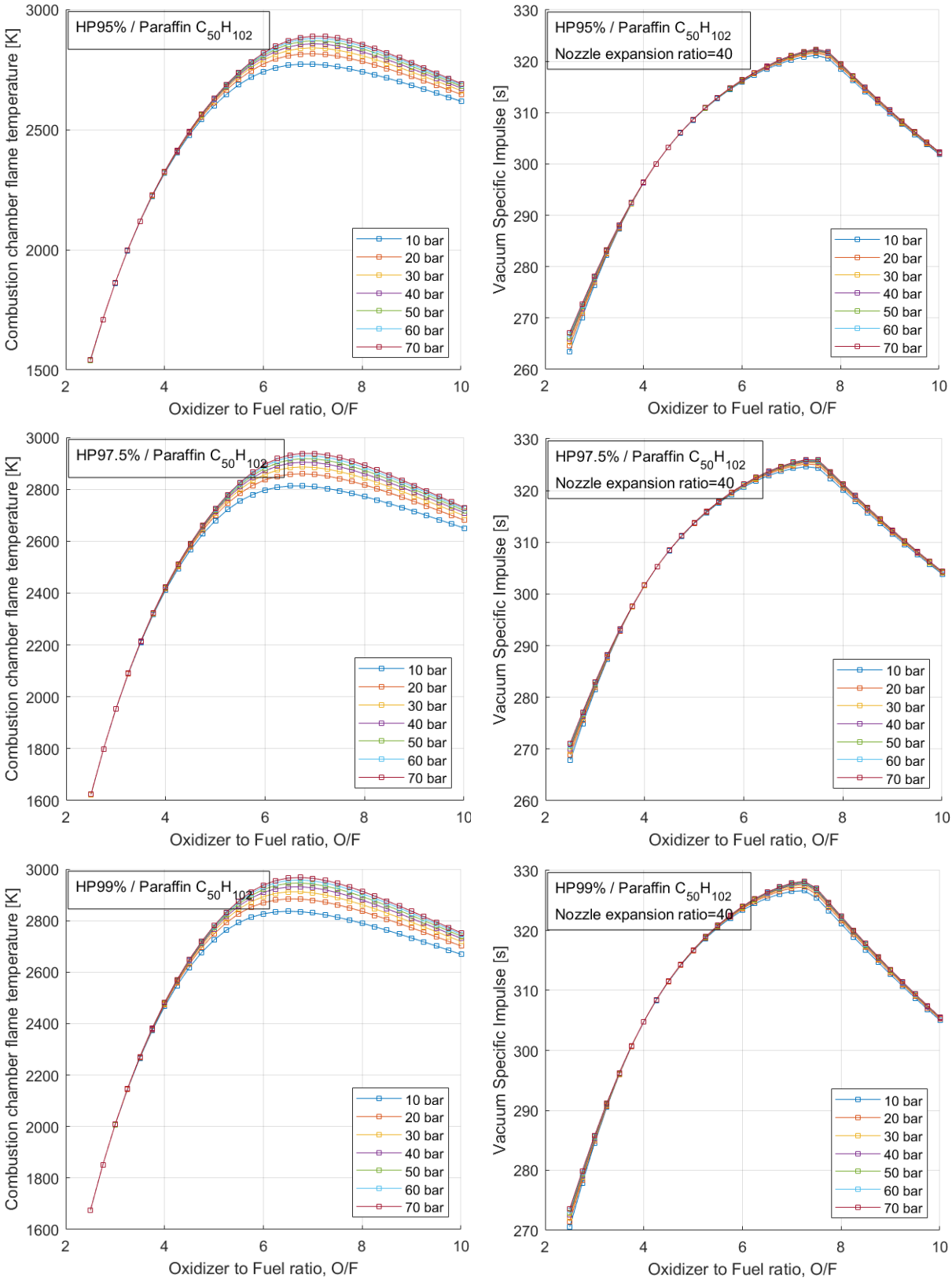

Figure 5.4: NASA CEA results of paraffin with HP at 95%, 97.5% and 99%.

5.1.3 HP 100% with HTPB and paraffin results

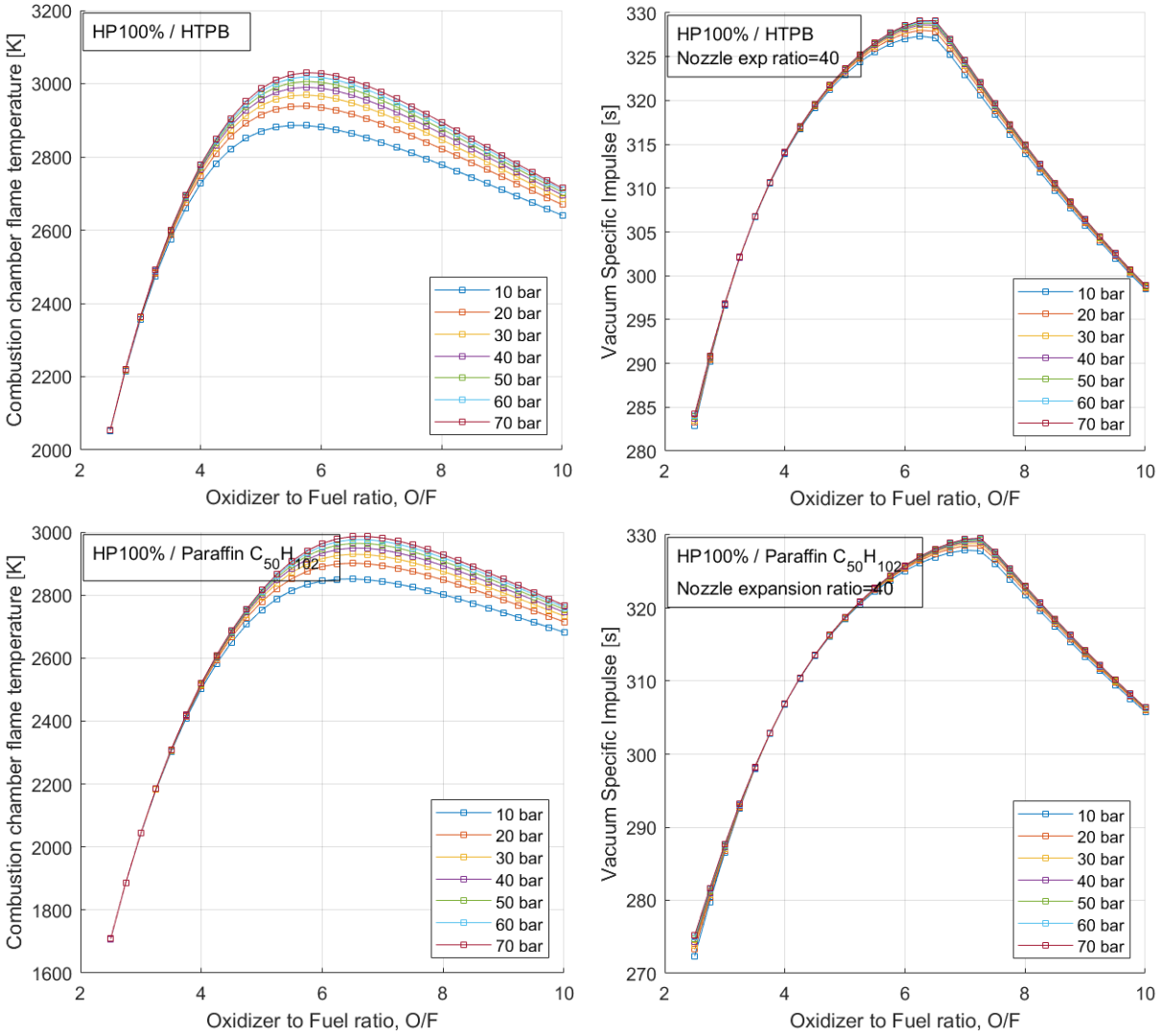

Figure 5.5: NASA CEA results of HP100% with HTPB and paraffin.

5.2 Hydrogen peroxide / paraffin performance analysis at different nozzle expansion ratio

This analysis focus on paraffin only with the highest grades of hydrogen peroxide: 97.5%, 99% and 100%. The aim is to observe the impact on the vacuum specific impulse of the nozzle expansion ratio and compare this influence to the one of pressure chamber and grade of HP. The results with nozzle expansion ratio of 20, 40 and 80 and with chamber pressure of 30 and 70 bar are presented in Fig. 5.6.

The chamber pressure from 30 bar to 70 bar has a minimal influence on the performance of HP/Paraffin systems. Going from 30 bar to 70 bar increases the maximum chamber temperature by 50 K and it increases the vacuum specific impulse by less than 1 s. However, the nozzle expansion ratio plays a significant role in the vacuum specific impulse performance. The maximum vacuum specific impulse for each cases is reported in Table 5.2.

Nozzle expansion ratio	20	40	80
HP 97.5% / paraffin max Isp [s]	314	326	336
HP 99% / paraffin max Isp [s]	316	328	338
HP 100% / paraffin max Isp [s]	317	329	340

Table 5.2: Maximum vacuum specific impulse performance of HP/paraffin systems with a chamber pressure of 70 bar at different nozzle expansion ratio.

Starting from a baseline nozzle with an expansion ratio of 40, it is possible to save mass by reducing the nozzle to an expansion ratio of 20 and loss 12 s of vacuum specific impulse. It is also possible to increase the vacuum specific impulse performance by 10 s by extending the nozzle to an expansion ratio of 80.

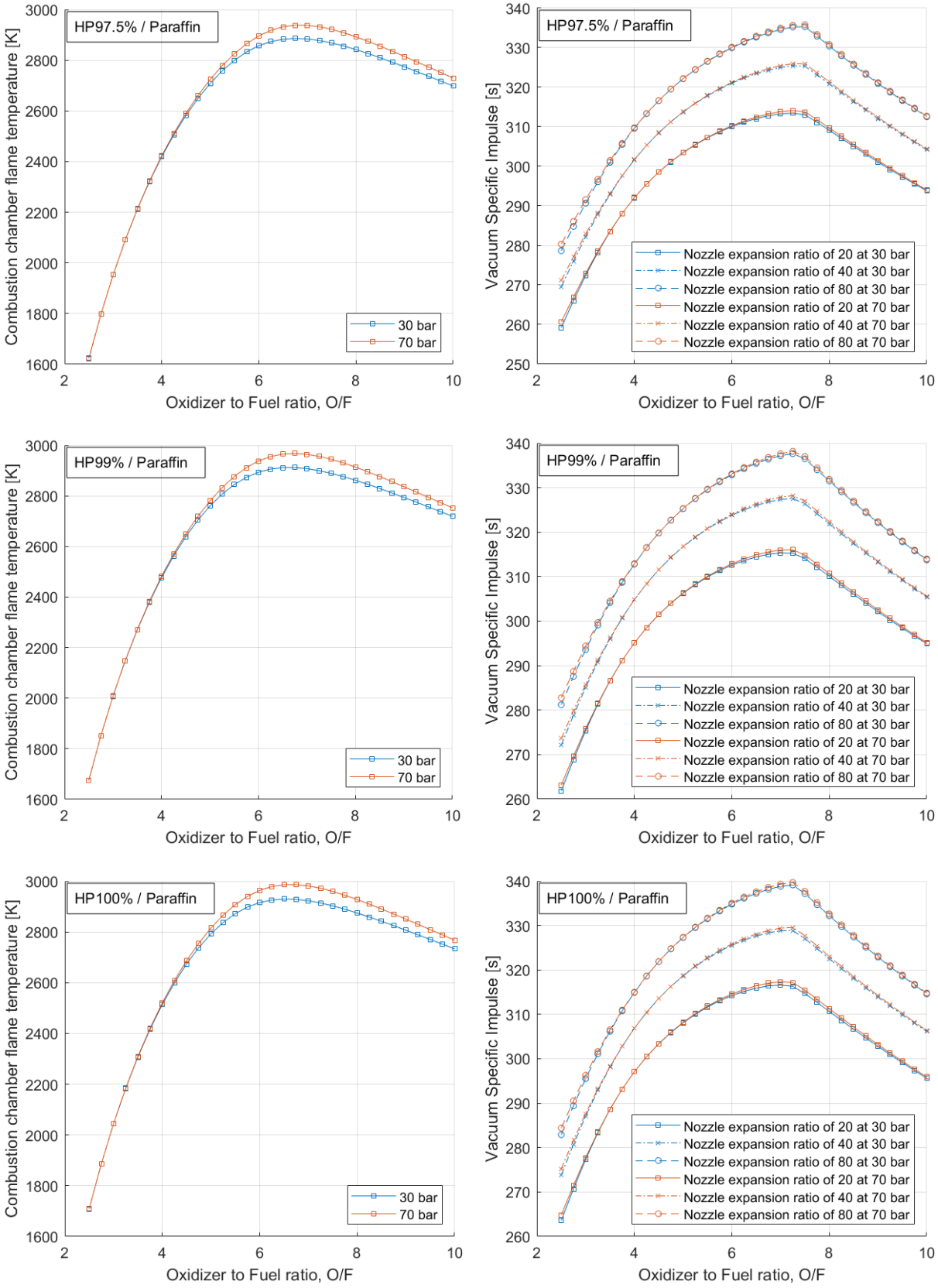

Figure 5.6: NASA CEA results of paraffin with HP at 97.5%, 99% and 100% with different nozzle expansion ratio.

5.3 Nitrous oxide / paraffin performance analysis

The results of N_2O/paraffin system are plotted in Fig. 5.7.

Like with the hydrogen peroxide, the chamber pressure has a minor impact on the performances of the hybrid rocket engine from the point of view of NASA CEA calculations. However in real tests, the chamber pressure plays an important role because it has a great influence of the combustion characteristics and on the fuel regression rate. In those calculations, increasing the chamber pressure from 30 bar to 70 bar increases the maximum combustion temperature by 100 K, from 3300 K to 3400 K, and it increases the vacuum specific impulse by 1 s.

Nitrous oxide and paraffin $C_{50}H_{102}$ system, with a nozzle expansion ratio of 40, offers a vacuum specific impulse of 315 s which corresponds to the performance of HP 90%. However compared to HP 90%, nitrous oxide produces an higher maximum flame for the same Isp performance (3400 K against 2800 K) and the optimal O/F ratio is also higher to produce this Isp of 315 s. The optimum O/F ratio for nitrous oxide and paraffin is of about 9.25. However, the O/F shift from this optimal value has a smaller impact on performances than with HP. Indeed, the slope of Isp reduction after the optimal O/F ratio is of about -6 s per O/F point with N_2O while it is of about -8 s per O/F point with HP.

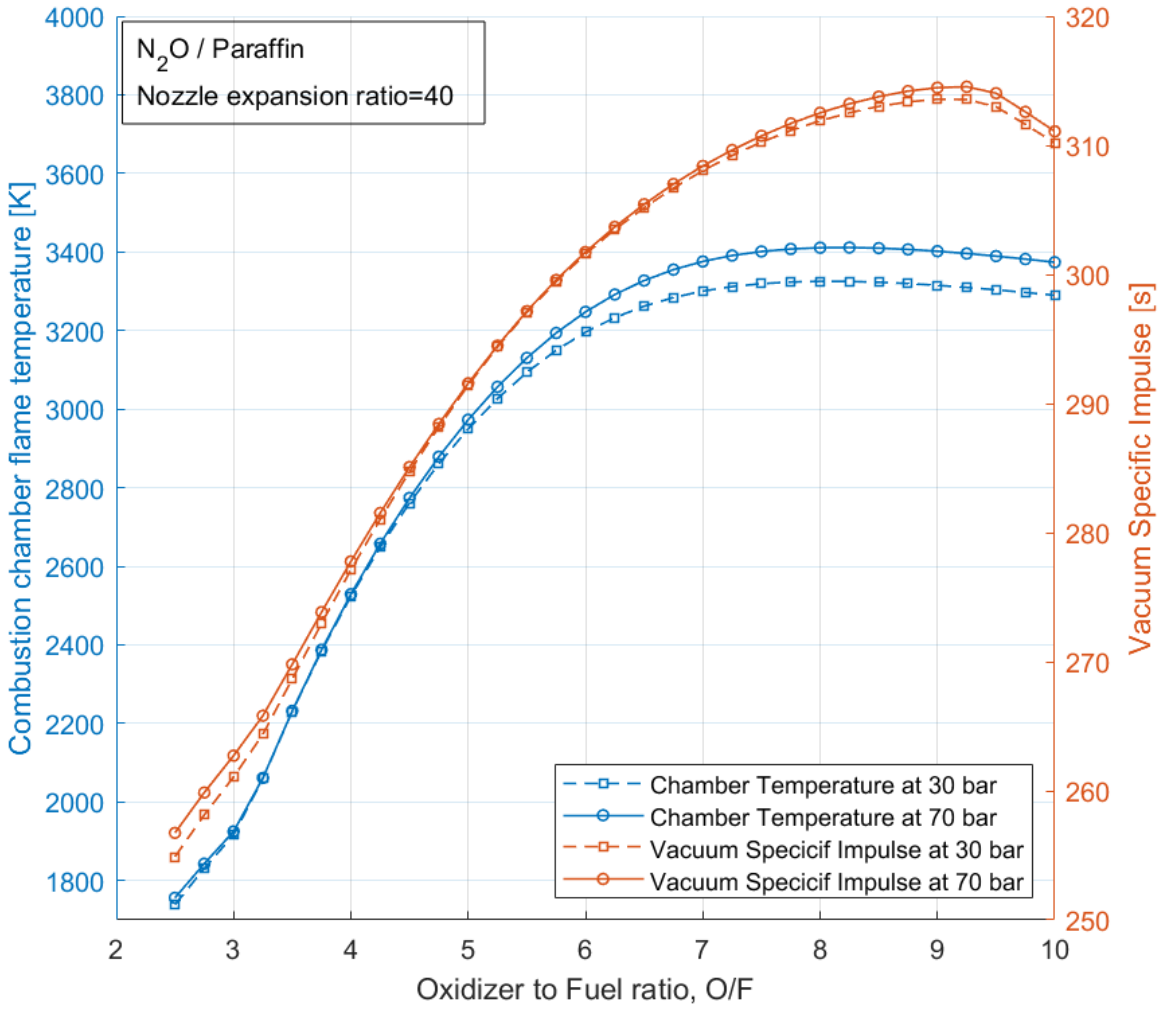

Figure 5.7: NASA CEA results of paraffin with liquid N_2O.

5.4 HAN / paraffin performance analysis

The results of HAN / paraffin system are plotted in Fig. 5.8.

The effect of pressure on HAN / paraffin system performances is similar than with the other oxidizers. The performances obtained with HAN / paraffin system are slightly lower than with the other oxidizers with a maximum vacuum specific impulse of 302 s. The main drawback of HAN observable with those results is the high optimum O/F ratio of 10.25. The reduction of Isp performance due to the O/F shift in HRE is similar than with N_2O with a slope of -6 s per O/F point.

As already discussed in section 4.4 on HAN application to hybrid rocket engines, those results do not reflect the full potential of HAN. More studies on the application HAN in hybrid rocket engines are needed to obtain a relevant conclusion on his performances.

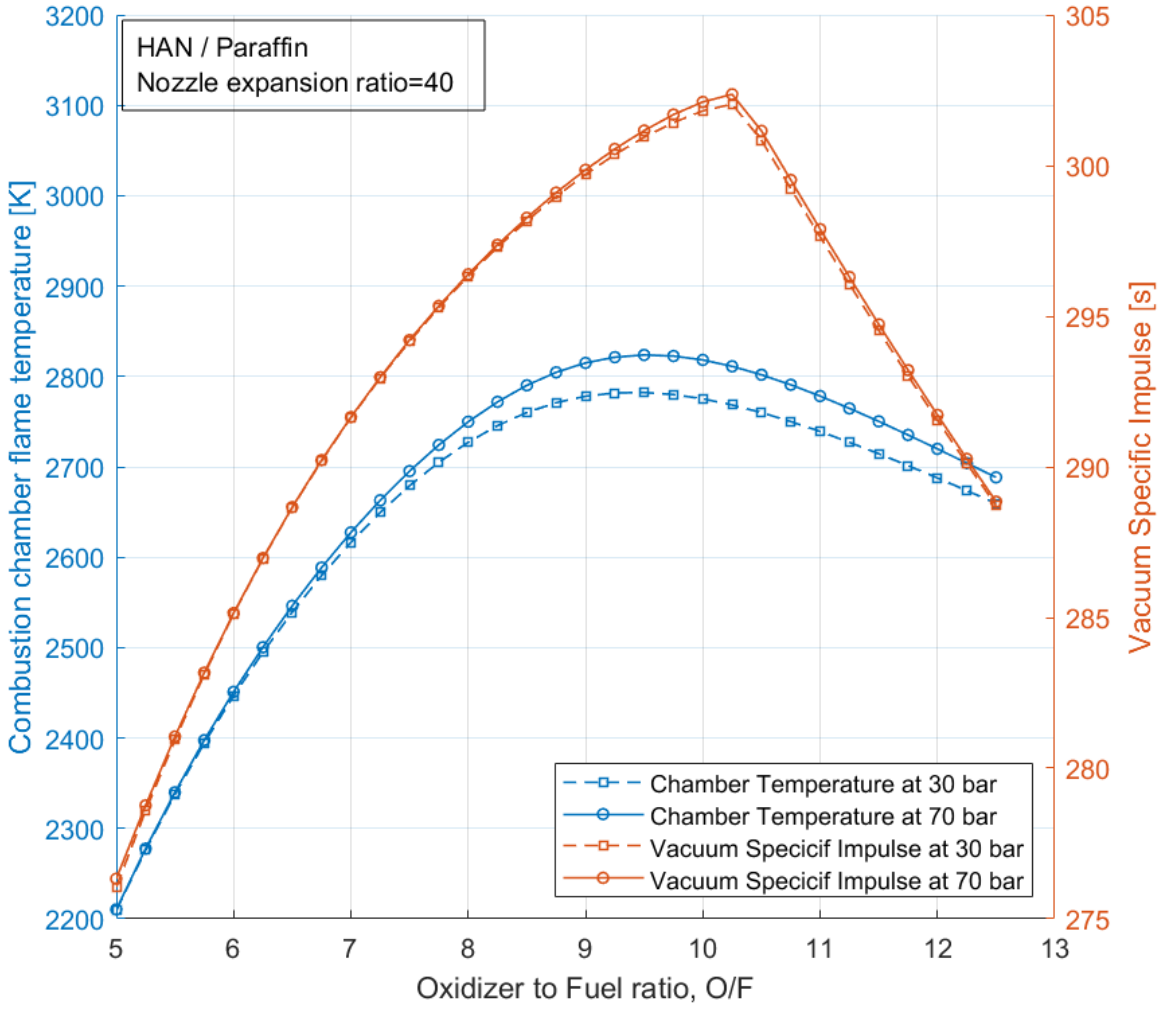

Figure 5.8: NASA CEA results of paraffin with HAN.

Chapter 6

Conclusion

A literature survey of the three most promising storable green oxidizers in hybrid rocket engines, hydrogen peroxide, nitrous oxide and hydroxyl-ammonium nitrate, have been performed in this thesis.

The development of technologies related to those oxidizers have long been limited because they provide a slightly lower performance than hybrid rocket engines using cryogenic liquid oxygen or monopropellant thrusters using polluting and toxic hydrazine. However, the increasing concerns about the environmental impact of space industry, the necessity to provide storable propellants, and the theoretical high performances and advantages of hybrid rocket engines have raised the interest in the storable green oxidizers and especially in hydrogen peroxide, nitrous oxide and hydroxyl-ammonium nitrate because their exothermic decomposition simplify the ignition system and make them also suitable for monopropellant applications.

Hydrogen peroxide provides the best performances and has the lowest environmental impact among the three oxidizers studied. The catalytic decomposition of hydrogen peroxide is necessary and very challenging due to the thermal conditions inside a catalyst bed; and as it is identified as the common topic connecting all types of chemical rocket propulsion, the catalytic decomposition of hydrogen peroxide is widely studied. This literature survey concludes that manganese oxide and platinum supported on alumina pellets or monolith exhibit the highest performance.

Nitrous oxide provides numerous system advantages. Its self-pressurization capability eliminates the additional weight, complexity and cost of the pressurization system. Added to its low cost, nitrous oxide is the ideal choice for small engines for which the systems and operational simplicity are the dominant driving forces.

Hydroxyl-ammonium nitrate is a powerful and very promising oxidizer but its representation in the open literature is poor, especially when applied to hybrid rocket engines. Blended with methanol, HAN-based monopropellants have been formulated and are the most promising candidates to substitute hydrazine in monopropellant thrusters by providing an higher specific impulse.

Finally, performance analysis of those oxidizers in a paraffin-fueled hybrid rocket engine have been conducted using the NASA CEA code. Results are consistent with the data found in the open literature and suggest that hydrogen peroxide can provide a 330 s vacuum specific impulse with paraffin and with a nozzle expansion ratio of 40. Performance is lowered with nitrous oxide at about 315 s, and with HAN at about 302 s.

To conclude, hybrid and monopropellant systems using those storable green oxidizers are potentially market disruptive in space propulsion field and could revolutionize the commercial space industry by offering high-performing, safe, storable and green space propulsion options.

Potential following studies of this thesis are:

- the study of arc ignition system with 3D-printed ABS fuel which have been mentioned several times in the literature survey;
- the conduct of tests using those storable green oxidizers to better characterize their performances in hybrid and monopropellant rocket engines.

Bibliography

[1] Jerome Anthoine et al. "Performances of a Multi-Pulsed Hybrid Rocket Engine Operating with Highly Concentrated Hydrogen Peroxide". In: *53rd AIAA/SAE/ASEE Joint Propulsion Conference*. American Institute of Aeronautics and Astronautics, 2017. DOI: 10.2514/6.2017-4906.

[2] Robert K. Masse and Robert L. Sackheim. "Green Propulsion Advancement - Challenging the Maturity of Monopropellant Hydrazine". In: *49th AIAA/ ASME/ SAE/ ASEE Joint Propulsion Conference*. American Institute of Aeronautics and Astronautics, 2013. DOI: 10.2514/6.2013-3988.

[3] Stephen Heister and Eric Wernimont. "Hydrogen peroxide, hydroxyl ammonium nitrate, and other storable oxidizers". In: *Progress in Astronautics and Aeronautics* 218 (2007), p. 457.

[4] Grzegorz Rarata, Karolina Rokicka, and Paweł Surmacz. "Hydrogen Peroxide as a High Energy Compound Optimal for Propulsive Applications". In: *Central European Journal of Energetic Materials* 13.3 (2016), pp. 778–790. DOI: 10.22211/cejem/65005.

[5] Pawel Surmacz. "Green rocket propulsion research and development at the institute of aviation: problems and perspectives". In: *Journal of KONES Powertrain and Transport* 23.1 (2016). DOI: 10.5604/12314005.1213534.

[6] Grzegorz rarata Pawel Surmacz. "Investigation of spontaneous ignition in a 100 N HTP/HTPB hybrid rocket engine". In: *Transactions of the Institute of Aviation* 240.3 (2015), pp. 69–79. DOI: 10.5604/05096669.1194990.

[7] Eric Wernimont. "System Trade Parameter Comparison of Monopropellants: Hydrogen Peroxide vs Hydrazine and Others". In: *42nd AIAA/ASME/SAE/ASEE Joint Propulsion Conference & Exhibit*. American Institute of Aeronautics and Astronautics, 2006. DOI: 10.2514/6.2006-5236.

[8] E Wernimont and S Heister. "Characterization of fuel regression in hybrid rockets utilizing hydrogen peroxide oxidizer". In: *31st Joint Propulsion Conference and Exhibit*. American Institute of Aeronautics and Astronautics, 1995. DOI: 10.2514/6.1995-3084.

[9] Nobuo Tsujikado and Atsushi Ishihara. "Improved Ignition Devices for 90% Hydrogen Peroxide/Polyethylene Hybrid Rocket Engine". In: *43rd AIAA/ASME/SAE/ASEE Joint Propulsion Conference & Exhibit*. American Institute of Aeronautics and Astronautics, 2007. DOI: 10.2514/6.2007-5365.

[10] Rocketdyne. *HYDROGEN PEROXIDE HANDBOOK*. Rockedyne, Chamical and Material Science Department, Canoga Park, California, 1967.

[11] Nobuo Tsujikado et al. “90% Hydrogen Peroxide/Polyethylene Solid Fuel Hybrid Rocket Engine”. In: *41st AIAA/ASME/SAE/ASEE Joint Propulsion Conference & Exhibit*. American Institute of Aeronautics and Astronautics, 2005. DOI: 10.2514/6.2005-4091.

[12] Salvatore Bonifacio, Giandomenico Festa, and Annamaria Russo Sorge. “Catalytic Ignition in Hydrogen Peroxide-based Space Propulsion Systems”. In: *48th AIAA/ ASME/ SAE/ ASEE Joint Propulsion Conference & Exhibit*. American Institute of Aeronautics and Astronautics, 2012. DOI: 10.2514/6.2012-3966.

[13] Stephen A. Whitmore et al. “High-Performing Hydrogen Peroxide Hybrid Rocket with 3-D Printed and Extruded ABS Fuel”. In: *2018 Joint Propulsion Conference*. American Institute of Aeronautics and Astronautics, 2018. DOI: 10.2514/6.2018-4443.

[14] C. K. McLane. “Hydrogen Peroxide in the Thermal Hydrogen Oxygen Reaction I. Thermal Decomposition of Hydrogen Peroxide”. In: *The Journal of Chemical Physics* 17.4 (1949), pp. 379–385. DOI: 10.1063/1.1747263.

[15] Eric Wernimont. “Monopropellant Hydrogen Peroxide Rocket Systems: Optimum for Small Scale”. In: *42nd AIAA/ASME/SAE/ASEE Joint Propulsion Conference & Exhibit*. American Institute of Aeronautics and Astronautics, 2006. DOI: 10.2514/6.2006-5235.

[16] Eric Wernimont. “System Trade Parameter Comparison of Monopropellants: Hydrogen Peroxide vs Hydrazine and Others”. In: *42nd AIAA/ASME/SAE/ASEE Joint Propulsion Conference & Exhibit*. American Institute of Aeronautics and Astronautics, 2006. DOI: 10.2514/6.2006-5236.

[17] Safija Islamovic, Borivoj Galic, and Mladen Milos. “A study of the inhibition of catalase by dipotassium trioxohydroxytetrafluorotriborate K2[B3O3F4OH]”. In: *Journal of Enzyme Inhibition and Medicinal Chemistry* 29.5 (2014), pp. 744–748. DOI: 10.3109/14756366.2013.848203.

[18] A. Hiroki and Jay A. LaVerne. “Decomposition of Hydrogen Peroxide at Water-Ceramic Oxide Interfaces”. In: *The Journal of Physical Chemistry B* 109.8 (2005), pp. 3364–3370. DOI: 10.1021/jp046405d.

[19] Paul M. Mader. “Kinetics of the Hydrogen Peroxide-Sulfite Reaction in Alkaline Solution”. In: *Journal of the American Chemical Society* 80.11 (1958), pp. 2634–2639. DOI: 10.1021/ja01544a009.

[20] Cláudio M. Lousada and Mats Jonsson. “Kinetics, Mechanism, and Activation Energy of H2O2 Decomposition on the Surface of ZrO2”. In: *The Journal of Physical Chemistry C* 114.25 (2010), pp. 11202–11208. DOI: 10.1021/jp1028933.

[21] Irwin W. Sizer. “TEMPERATURE ACTIVATION AND INACTIVATION OF THE CRYSTALLINE CATALASE-HYDROGEN PEROXIDE SYSTEM”. In: *Journal of Biological Chemistry* 154.2 (1944), pp. 461–473. DOI: 10.1016/s0021-9258(18)71929-7.

[22] J. Miłek. “ESTIMATION OF THE KINETIC PARAMETERS FOR H2O2 ENZYMATIC DECOMPOSITION AND FOR CATALASE DEACTIVATION”. In: *Brazilian Journal of Chemical Engineering* 35.3 (2018), pp. 995–1004. DOI: 10.1590/0104-6632.20180353s20160617.

[23] Robert E. Altomare, Paul F. Greenfield, and James R. Kittrell. "Inactivation of immobilized fungal catalase by hydrogen peroxide". In: *Biotechnology and Bioengineering* 16.12 (1974), pp. 1675–1680. DOI: 10.1002/bit.260161209.

[24] Preety and Vinita Hooda. "Immobilization and Kinetics of Catalase on Calcium Carbonate Nanoparticles Attached Epoxy Support". In: *Applied Biochemistry and Biotechnology* 172.1 (2013), pp. 115–130. DOI: 10.1007/s12010-013-0498-2.

[25] Katerina Voitko et al. "Catalytic performance of carbon nanotubes in H2O2 decomposition: Experimental and quantum chemical study". In: *Journal of Colloid and Interface Science* 437 (2015), pp. 283–290. DOI: 10.1016/j.jcis.2014.09.045.

[26] Jeremy Corpening et al. "A Model for Thermal Decomposition of Hydrogen Peroxide". In: *40th AIAA/ASME/SAE/ASEE Joint Propulsion Conference and Exhibit*. American Institute of Aeronautics and Astronautics, 2004. DOI: 10.2514/6.2004-3373.

[27] Pawel Surmacz. "Influence of various types of Al2O3/MnxOy catalysts on performance of a 100mm chamber for decomposition of 98%+ hydrogen peroxide". In: *Transactions of the Institute of Aviation* 240.3 (2015), pp. 58–68. DOI: 10.5604/05096669.1194986.

[28] José Hinckel et al. "Low Cost Catalysts for Hydrazine Monopropellant Thrusters". In: *45th AIAA/ASME/SAE/ASEE Joint Propulsion Conference & Exhibit*. American Institute of Aeronautics and Astronautics, 2009. DOI: 10.2514/6.2009-5232.

[29] Lucio Torre Angelo Cervone A. Pasini. "High Mass Flux Tests on Catalytic Beds for H2O2 Monopropellant Thruster". In: *ESA Space Propulsion Conference 2010* (2010).

[30] Eric Wernimont and Dick Durant. "State of the Art High Performance Hydrogen Peroxide Catalyst Beds". In: *40th AIAA/ASME/SAE/ASEE Joint Propulsion Conference and Exhibit*. American Institute of Aeronautics and Astronautics, 2004. DOI: 10.2514/6.2004-4147.

[31] IndiaMART. *Ceramic Honeycombs, Industrial Use*. URL: https://www.indiamart.com/proddetail/ceramic-honeycombs-1215163312.html.

[32] Carsten Scharlemann et al. "Development and Test of a Miniature Hydrogen Peroxide Monopropellant Thruster". In: *42nd AIAA/ASME/SAE/ASEE Joint Propulsion Conference & Exhibit*. American Institute of Aeronautics and Astronautics, 2006. DOI: 10.2514/6.2006-4550.

[33] Benjamin Greene Dennis D. Davis Louis A. Dee. *Fire, Explosion, Compatibility and Safety Hazards of Hydrogen Peroxide*. NTRS - NASA Technical Reports Server, 2005.

[34] Angelo Pasini et al. "Performance Modeling and Analysis of H2O2 Catalytic Pellet Reactors". In: *44th AIAA/ASME/SAE/ASEE Joint Propulsion Conference & Exhibit*. American Institute of Aeronautics and Astronautics, 2008. DOI: 10.2514/6.2008-5025.

[35] A. Pasini et al. "Reduced-Order Model for H2O2 Catalytic Reactor Performance Analysis". In: *Journal of Propulsion and Power* 26.3 (2010), pp. 446–453. DOI: 10.2514/1.44355.

[36] *Krishnan, S., Ahn, Sang-Hee, and Lee, Choong-Won, J. Mekanikal, 2010, vol. 30, pp. 24–36.*

[37] Chih-Kuang Kuan, Guan-Bang Chen, and Yei-Chin Chao. "The Effects of Preheating and pH Value on the Performance of Hydrogen Peroxide Monopropellant Micro-thrusters". In: *42nd AIAA/ASME/SAE/ASEE Joint Propulsion Conference & Exhibit*. American Institute of Aeronautics and Astronautics, 2006. DOI: 10.2514/6.2006-5240.

[38] Yung-An Chan, Hung-Wei Hsu, and Yei-Chin Chao. "Development of a HTP Mono-propellant Thruster by Using Composite Silver Catalyst". In: *47th AIAA/ ASME/ SAE/ ASEE Joint Propulsion Conference & Exhibit*. American Institute of Aeronautics and Astronautics, 2011. DOI: 10.2514/6.2011-5693.

[39] Seungkwan Baek et al. "Development of High-Performance Green-Monopropellant Thruster with Hydrogen Peroxide and Ethanol". In: *Journal of Propulsion and Power* 34.5 (2018), pp. 1256–1261. DOI: 10.2514/1.b37081.

[40] Sh. L. Guseinov et al. "Hydrogen Peroxide Decomposition Catalysts Used in Rocket Engines". In: *Russian Journal of Applied Chemistry* 93.4 (2020), pp. 467–487. DOI: 10.1134/s1070427220040011.

[41] Cristina Bramanti et al. "Experimental Characterization of Advanced Materials for the Catalytic Decomposition of Hydrogen Peroxide". In: *42nd AIAA/ ASME/ SAE/ ASEE Joint Propulsion Conference & Exhibit*. American Institute of Aeronautics and Astronautics, 2006. DOI: 10.2514/6.2006-5238.

[42] S. Bonifacio, G. Festa, and A. Russo Sorge. "Novel Structured Catalysts for Hydrogen Peroxide Decomposition in Monopropellant and Hybrid Rockets". In: *Journal of Propulsion and Power* 29.5 (2013), pp. 1130–1137. DOI: 10.2514/1.b34864.

[43] A. Pasini et al. "Performance Characterization of Pellet Catalytic Beds for Hydrogen Peroxide Monopropellant Rockets". In: *Journal of Propulsion and Power* 27.2 (2011), pp. 428–436. DOI: 10.2514/1.b34000.

[44] Laurence Pirault-Roy et al. "Hydrogen Peroxide Decomposition on Various Supported Catalysts Effect of Stabilizers". In: *Journal of Propulsion and Power* 18.6 (2002), pp. 1235–1241. DOI: 10.2514/2.6058.

[45] Rachid Amrousse et al. "CATALYTIC DECOMPOSITION OF H2O2 USING FeCrAl METALLIC FOAM-BASED CATALYSTS". In: *International Journal of Energetic Materials and Chemical Propulsion* 10.4 (2011), pp. 337–349. DOI: 10.1615/intjenergeticmaterialschemprop.2012005202.

[46] Lucio Torre et al. "Performance of Different Catalysts Supported on Alumina Spheres for Hydrogen Peroxide Decomposition". In: *43rd AIAA/ASME/SAE/ASEE Joint Propulsion Conference & Exhibit*. American Institute of Aeronautics and Astronautics, 2007. DOI: 10.2514/6.2007-5466.

[47] Pereira L.G. Maia F.F. Gouvea L.H. In: *Aerospace Technol. Manag* 6.1 (2014), pp. 61–67. DOI: 10.5028/jatm.vGi1.286.

[48] Woosuk Jung et al. "Demonstration of Ethanol-Blended Hydrogen Peroxide Gas Generator for Ramjet Combustor Flow Simulation". In: *Journal of Propulsion and Power* 34.3 (2018), pp. 591–599. DOI: 10.2514/1.b36633.

[49] Jean-Yves Lestrade et al. “Development of a catalyst for highly concentrated hydrogen peroxide”. In: *Space Propulsion 2016*. Rome, Italy, May 2016. URL: https://hal.archives-ouvertes.fr/hal-01353568.

[50] Lucio Torre et al. “Firing Performance of Advanced Hydrogen Peroxide Catalytic Beds in a Monopropellant Thruster Prototype”. In: *44th AIAA/ASME/SAE/ASEE Joint Propulsion Conference & Exhibit*. American Institute of Aeronautics and Astronautics, 2008. DOI: 10.2514/6.2008-4937.

[51] Angelo Pasini et al. “Endurance Tests on Different Catalytic Beds for H2O2 Monopropellant Thrusters”. In: *45th AIAA/ASME/SAE/ASEE Joint Propulsion Conference & Exhibit*. American Institute of Aeronautics and Astronautics, 2009. DOI: 10.2514/6.2009-5472.

[52] Guobiao Cai et al. “Optimal design of hybrid rocket motor powered vehicle for suborbital flight”. In: *Aerospace Science and Technology* 25.1 (2013), pp. 114–124. DOI: 10.1016/j.ast.2011.12.014.

[53] Shinjae Kang et al. “Design and performance evaluation of hybrid rocket using 95 wt.% H2O2”. In: *52nd AIAA/SAE/ASEE Joint Propulsion Conference*. American Institute of Aeronautics and Astronautics, 2016. DOI: 10.2514/6.2016-4864.

[54] Yash Pal, K. Harish Kumar, and Yueh-Heng Li. “Ballistic and mechanical characteristics of paraffin-based solid fuels”. In: *CEAS Space Journal* 11.3 (2019), pp. 317–327. DOI: 10.1007/s12567-019-00250-2.

[55] Arif Karabeyoglu et al. “Scale-Up Tests of High Regression Rate Paraffin-Based Hybrid Rocket Fuels”. In: *Journal of Propulsion and Power* 20.6 (2004), pp. 1037–1045. DOI: 10.2514/1.3340.

[56] Michael C. Lydon Timothy R. Brown. “Testing of Paraffin-Based Hybrid Rocket Fuel Using Hydrogen Peroxide Oxidizer”. In: *Colorado Space Grant Consortium* (2005).

[57] L.T. DeLuca et al. “Characterization of HTPB-based solid fuel formulations: Performance, mechanical properties, and pollution”. In: *Acta Astronautica* 92.2 (2013), pp. 150–162. DOI: 10.1016/j.actaastro.2012.05.002.

[58] T4i. *Chemical Propulsion*. URL: https://www.t4innovation.com/chemical-propulsion-3/.

[59] Fernando de Souza Costa and Ricardo Vieira. “Preliminary analysis of hybrid rockets for launching nanosats into LEO”. In: *Journal of the Brazilian Society of Mechanical Sciences and Engineering* 32.4 (2010), pp. 502–509. DOI: 10.1590/s1678-58782010000400012.

[60] Constans J. Verberne, Adrien J. Boiron, and Jan E. Rønningen. “Development and Testing of Hydrogen Peroxide Hybrid Rocket Motors at Nammo Raufoss”. In: *50th AIAA/ASME/SAE/ASEE Joint Propulsion Conference*. American Institute of Aeronautics and Astronautics, 2014. DOI: 10.2514/6.2014-3867.

[61] Arif Karabeyoglu et al. “Modeling of N2O Decomposition Events”. In: *44th AIAA/ASME/ SAE/ ASEE Joint Propulsion Conference & Exhibit*. American Institute of Aeronautics and Astronautics, 2008. DOI: 10.2514/6.2008-4933.

[62] PubChem. *Nitrous oxide (Compound)*. URL: https://pubchem.ncbi.nlm.nih.gov/compound/Nitrous-oxide.

[63] Arif Karabeyoglu. “Mixtures of Nitrous Oxide and Oxygen (Nytrox) as Oxidizers for Rocket Propulsion Applications”. In: *45th AIAA/ASME/SAE/ASEE Joint Propulsion Conference & Exhibit*. American Institute of Aeronautics and Astronautics, 2009. DOI: 10.2514/6.2009-4966.

[64] Nick Proctor. *Proctor and Hughes' Chemical hazards of the workplace*. Hoboken, N.J: Wiley-Interscience, 2004. ISBN: 0471268836.

[65] Grzegorz Giecko et al. “Fe2O3/Al2O3 catalysts for the N2O decomposition in the nitric acid industry”. In: *Catalysis Today* 137.2-4 (2008), pp. 403–409. DOI: 10.1016/j.cattod.2008.02.008.

[66] Stephen A. Whitmore. “Nytrox as “Drop-in” Replacement for Gaseous Oxygen in SmallSat Hybrid Propulsion Systems”. In: *Aerospace* 7.4 (2020), p. 43. DOI: 10.3390/aerospace7040043.

[67] L. Pauling. “The Electronic Structure of the Normal Nitrous Oxide Molecule”. In: *Proceedings of the National Academy of Sciences* 18.7 (1932), pp. 498–499. DOI: 10.1073/pnas.18.7.498.

[68] Allen E. Stearn and Henry Eyring. “Nonadiabatic Reactions. The Decomposition of N2O”. In: *The Journal of Chemical Physics* 3.12 (1935), pp. 778–785. DOI: 10.1063/1.1749592.

[69] Hisao Nakamura and Shigeki Kato. “Theoretical study on the spin-forbidden predissociation reaction of N2O: Ab initio potential energy surfaces and quantum dynamics calculations”. In: *The Journal of Chemical Physics* 110.20 (1999), pp. 9937–9947. DOI: 10.1063/1.478954.

[70] Agnes H. H. Chang and David R. Yarkony. “On the electronic structure aspects of spin-forbidden processes in N2O”. In: *The Journal of Chemical Physics* 99.9 (1993), pp. 6824–6831. DOI: 10.1063/1.465826.

[71] G. W. Rhodes. “Investigation of Decomposition Characteristics of Gaseous and Liquid Nitrous Oxide”. In: . (1974).

[72] John Ribovich, John Murphy, and Richard Watson. “Detonation studies with nitric oxide, nitrous oxide, nitrogen tetroxide, carbon monoxide, and ethylene”. In: *Journal of Hazardous Materials* 1.4 (1975), pp. 275–287. DOI: 10.1016/0304-3894(75)80001-x.

[73] “The thermal decomposition of nitrous oxide at pressures up to forty atmospheres”. In: *Proceedings of the Royal Society of London. Series A, Containing Papers of a Mathematical and Physical Character* 144.852 (1934), pp. 386–412. DOI: 10.1098/rspa.1934.0057.

[74] J. P. MONAT, R. K. HANSON, and C. H. KRUGER. “Kinetics of Nitrous Oxide Decomposition”. In: *Combustion Science and Technology* 16.1-2 (1977), pp. 21–28. DOI: 10.1080/00102207708946790.

[75] Peter Glarborg, Jan E. Johnsson, and Kim Dam-Johansen. “Kinetics of homogeneous nitrous oxide decomposition”. In: *Combustion and Flame* 99.3-4 (1994), pp. 523–532. DOI: 10.1016/0010-2180(94)90045-0.

[76] D. L. Baulch. *Evaluated kinetic data for high temperature reactions*. London: Butterworths, 1972. ISBN: 0408704802.

[77] Irvin Glassman. *Combustion*. Amsterdam Boston: Academic Press, 2008. ISBN: 9780080568812.

[78] Freek Kapteijn, José Rodriguez-Mirasol, and Jacob A. Moulijn. "Heterogeneous catalytic decomposition of nitrous oxide". In: *Applied Catalysis B: Environmental* 9.1-4 (1996), pp. 25–64. DOI: 10.1016/0926-3373(96)90072-7.

[79] Zhiming Liu et al. "Recent Advances in Catalytic Decomposition of N2O on Noble Metal and Metal Oxide Catalysts". In: *Catalysis Surveys from Asia* 20.3 (2016), pp. 121–132. DOI: 10.1007/s10563-016-9213-y.

[80] Michalis Konsolakis. "Recent Advances on Nitrous Oxide (N2O) Decomposition over Non-Noble-Metal Oxide Catalysts: Catalytic Performance, Mechanistic Considerations, and Surface Chemistry Aspects". In: *ACS Catalysis* 5.11 (2015), pp. 6397–6421. DOI: 10.1021/acscatal.5b01605.

[81] T. P. Gaidei et al. "The catalytic activity of metallic and deposited oxide catalysts in the decomposition of nitrous oxide". In: *Russian Journal of Physical Chemistry A* 81.6 (2007), pp. 895–900. DOI: 10.1134/s0036024407060106.

[82] Gabriele Centi, Siglinda Perathoner, and Zbigniew S Rak. "Reduction of greenhouse gas emissions by catalytic processes". In: *Applied Catalysis B: Environmental* 41.1-2 (2003), pp. 143–155. DOI: 10.1016/s0926-3373(02)00207-2.

[83] Nunzio Russo et al. "N2O catalytic decomposition over various spinel-type oxides". In: *Catalysis Today* 119.1-4 (2007), pp. 228–232. DOI: 10.1016/j.cattod.2006.08.012.

[84] Qun Shen et al. "A study on N2O catalytic decomposition over Co/MgO catalysts". In: *Journal of Hazardous Materials* 163.2-3 (2009), pp. 1332–1337. DOI: 10.1016/j.jhazmat.2008.07.104.

[85] Vadim Zakirov and Hai-yun Zhang. "A model for the operation of nitrous oxide monopropellant". In: *Aerospace Science and Technology* 12.4 (2008), pp. 318–323. DOI: 10.1016/j.ast.2007.08.003.

[86] Coit T. Hendley et al. "Catalytic Decomposition of Nitrous Oxide for Use in Hybrid Rocket Motors". In: *Journal of Propulsion and Power* 37.3 (2021), pp. 474–478. DOI: 10.2514/1.b38204.

[87] J Haber et al. "Catalytic decomposition of N2O". In: *Catalysis Today* 90.1-2 (2004), pp. 15–19. DOI: 10.1016/j.cattod.2004.04.002.

[88] T. P. Gaidei et al. "The influence of the nature and features of carrier on activity and efficiency of catalyst in reaction of nitrous oxide decomposition". In: *Russian Journal of Applied Chemistry* 83.6 (2010), pp. 1130–1138. DOI: 10.1134/s1070427210060431.

[89] Jian Lin et al. "Catalytic decomposition of propellant N2O Over Ir/Al2O3 catalyst". In: *AIChE Journal* 62.11 (2016), pp. 3973–3981. DOI: 10.1002/aic.15324.

[90] Shaomin Zhu et al. "A novel Ir-hexaaluminate catalyst for N2O as a propellant". In: *Chemical Communications* 17 (2007), p. 1695. DOI: 10.1039/b702502e.

[91] K. A. Lohner, B. J. Cantwell Y. D. Scherson B. W. Lariviere, and T. W. Kenny. *NITROUS OXIDE MONOPROPELLANT GAS GENERATOR DEVELOPMENT*.

[92] G. Gallo et al. “Experimental Investigation of N2O Decomposition with Pd/Al2O3 Cylindrical Pellets Catalyst”. In: *Journal of Spacecraft and Rockets* 57.4 (2020), pp. 720–727. DOI: 10.2514/1.a34700.

[93] G.D. Di Martino et al. “Design and testing of a monopropellant thruster based on N2O decomposition in Pd/Al2O3 pellets catalytic bed”. In: *Acta Astronautica* 180 (2021), pp. 460–469. DOI: 10.1016/j.actaastro.2020.12.016.

[94] Luciano Hennemann, José Carlos de Andrade, and Fernando De Souza Costa. “Experimental Investigation of a Monopropellant Thruster Using Nitrous Oxide”. In: *Journal of Aerospace Technology and Management* 6.4 (2014), pp. 363–372. DOI: 10.5028/jatm.v6i4.382.

[95] Guobiao Cai et al. “Design and performance characterization of a sub-Newton N2O monopropellant thruster”. In: *Aerospace Science and Technology* 23.1 (2012), pp. 439–451. DOI: 10.1016/j.ast.2011.10.003.

[96] Kevin Lohner et al. “Fuel Regression Rate Characterization Using a Laboratory Scale Nitrous Oxide Hybrid Propulsion System”. In: *42nd AIAA/ASME/SAE/ASEE Joint Propulsion Conference & Exhibit*. American Institute of Aeronautics and Astronautics, 2006. DOI: 10.2514/6.2006-4671.

[97] Eric Doran et al. “Nitrous Oxide Hybrid Rocket Motor Fuel Regression Rate Characterization”. In: *43rd AIAA/ASME/SAE/ASEE Joint Propulsion Conference & Exhibit*. American Institute of Aeronautics and Astronautics, 2007. DOI: 10.2514/6.2007-5352.

[98] Tsong-Sheng Lee and Hsin-Luen Tsai. “Fuel Regression Rate in a Paraffin-HTPB Nitrous Oxide Hybrid Rocket”. In: *7th Asia-Pacific Conference on Combustion, National Taiwan University, Taipei, Taiwan*. 2009.

[99] Lin-lin Liu et al. “Regression rate of paraffin-based fuels in hybrid rocket motor”. In: *Aerospace Science and Technology* 107 (2020), p. 106269. DOI: 10.1016/j.ast.2020.106269.

[100] Fiona K. Leverone et al. “Performance sensitivity study on a blowdown nitrous oxide paraffin wax hybrid sounding rocket”. In: *Acta Astronautica* 160 (2019), pp. 230–239. DOI: 10.1016/j.actaastro.2019.04.043.

[101] Laura Simurda et al. “Design and Development of a Thrust Vector Controlled Paraffin/Nytrox Hybrid Rocket”. In: *48th AIAA/ASME/SAE/ASEE Joint Propulsion Conference & Exhibit*. American Institute of Aeronautics and Astronautics, 2012. DOI: 10.2514/6.2012-4310.

[102] Paige K. Nardozzo et al. “DIFFUSION FLAME STUDIES OF SOLID FUELS WITH NITROUS OXIDE”. In: *International Journal of Energetic Materials and Chemical Propulsion* 19.1 (2020), pp. 73–93. DOI: 10.1615/intjenergetic\\materialschemprop.2020028356.

[103] C. Carmicino, F. Scaramuzzino, and A. Russo Sorge. “Trade-off between paraffin-based and aluminium-loaded HTPB fuels to improve performance of hybrid rocket fed with N2O”. In: *Aerospace Science and Technology* 37 (2014), pp. 81–92. DOI: 10.1016/j.ast.2014.05.010.

[104] M. Bouziane et al. “Performance comparison of oxidizer injectors in a 1-kN paraffin-fueled hybrid rocket motor”. In: *Aerospace Science and Technology* 89 (2019), pp. 392–406. DOI: 10.1016/j.ast.2019.04.009.

[105] Matthias Grosse. "Effect of a Diaphragm on Performance and Fuel Regression of a Laboratory Scale Hybrid Rocket Motor Using Nitrous Oxide and Paraffin". In: *45th AIAA/ASME/SAE/ASEE Joint Propulsion Conference & Exhibit*. American Institute of Aeronautics and Astronautics, 2009. DOI: 10.2514/6.2009-5113.

[106] Stephen A Whitmore and Robb L Stoddard. "N2O/O2 blends safe and volumetrically efficient oxidizers for small spacecraft hybrid propulsion". In: *Aeronautics and Aerospace Open Access Journal* 3.4 (2019), pp. 171–196. DOI: 10.15406/aaoaj.2019.03.00097.

[107] Vadim Zakirov and Timothy Lawrence Prof. Martin Sweeting. "An Update on Surrey Nitrous Oxide Catalytic Decomposition Research". In: *15th AIAA/USU Conference on Small Satellites* (2002).

[108] Alabama Marshall Space Flight Center. *Nitrous Oxide/Paraffin Hybrid Rocket Engines*. URL: https://www.techbriefs.com/component/content/article/tb/supplements/gdm/briefs/7631.

[109] Rachid Amrousse et al. "Hydroxylammonium nitrate (HAN)-based green propellant as alternative energy resource for potential hydrazine substitution: From lab scale to pilot plant scale-up". In: *Combustion and Flame* 176 (2017), pp. 334–348. DOI: 10.1016/j.combustflame.2016.11.011.

[110] Shweta Hoyani et al. "Thermal stability of hydroxylammonium nitrate (HAN)". In: *Journal of Thermal Analysis and Calorimetry* 129.2 (2017), pp. 1083–1093. DOI: 10.1007/s10973-017-6287-3.

[111] Ruchika Agnihotri and Charlie Oommen. "Impact of HAN Ternary Propellant System Decomposition on Catalytic Sustainability". In: *Propellants, Explosives, Pyrotechnics* 46.3 (2021), pp. 440–449. DOI: 10.1002/prep.202000110.

[112] Mueller et al. *Monopropellant Aqueous Hydroxyl Ammonium Nitrate/Fuel*. 1993.

[113] Rachid Amrousse et al. "New HAN-based mixtures for reaction control system and low toxic spacecraft propulsion subsystem: Thermal decomposition and possible thruster applications". In: *Combustion and Flame* 162.6 (2015), pp. 2686–2692. DOI: 10.1016/j.combustflame.2015.03.026.

[114] T. Katsumi et al. "Combustion characteristics of a hydroxylammonium nitrate based liquid propellant. Combustion mechanism and application to thrusters". In: *Combustion, Explosion, and Shock Waves* 45.4 (2009), pp. 442–453. DOI: 10.1007/s10573-009-0055-z.

[115] E. Wucherer, Stacy Christofferson, and Brian Reed. "Assessment of high performance HAN-monopropellants". In: *36th AIAA/ASME/SAE/ASEE Joint Propulsion Conference and Exhibit*. American Institute of Aeronautics and Astronautics, 2000. DOI: 10.2514/6.2000-3872.

[116] Yi-Ping Chang et al. "Combustion Characteristics of Energetic HAN/Methanol-Based Monopropellants". In: *38th AIAA/ASME/SAE/ASEE Joint Propulsion Conference & Exhibit*. American Institute of Aeronautics and Astronautics, 2002. DOI: 10.2514/6.2002-4032.

[117] Travis Belcher. "Improving The Regression Rate Of An HTPB Hybrid Rocket Fuel Grain". MSc dissertation. University of Texas, 2017.

[118] Dr. Steve Agnew Donald G. Harlow Dr. Rowland E. Felt. *Technical Report On Hydroxylamine Nitrate*. Tech. rep. U. S. Department Of Energy, 1998.

[119] Robert Jankovsky. "HAN-based monopropellant assessment for spacecraft". In: *32nd Joint Propulsion Conference and Exhibit*. American Institute of Aeronautics and Astronautics, 1996. DOI: 10.2514/6.1996-2863.

[120] Steven R. Vosen. "Hydroxylammonium nitrate-based liquid propellant combustion-interpretation of strand burner data and the laminar burning velocity". In: *Combustion and Flame* 82.3-4 (1990), pp. 376–388. DOI: 10.1016/0010-2180(90)90009-g.

[121] Shinjae Kang and Sejin Kwon. "Difficulties of Catalytic Reactor for Hydroxylammonium Nitrate Hybrid Rocket". In: *Journal of Spacecraft and Rockets* 52.5 (2015), pp. 1508–1510. DOI: 10.2514/1.a33255.

[122] Chang Hwan Hwang, Seung Wook Baek, and Sung June Cho. "Experimental investigation of decomposition and evaporation characteristics of HAN-based monopropellants". In: *Combustion and Flame* 161.4 (2014), pp. 1109–1116. DOI: 10.1016/j.combustflame.2013.09.026.

[123] Laurence Courthéoux et al. "Thermal and catalytic decomposition of HNF and HAN liquid ionic as propellants". In: *Applied Catalysis B: Environmental* 62.3-4 (2006), pp. 217–225. DOI: 10.1016/j.apcatb.2005.07.016.

[124] Sho Onodaka et al. "Ignition Characteristics of HAN Liquid for Gas-Hybrid Rockets". In: *49th AIAA/ASME/SAE/ASEE Joint Propulsion Conference*. American Institute of Aeronautics and Astronautics, 2013. DOI: 10.2514/6.2013-4051.

[125] Rachid Amrousse et al. "Chemical engineering study for hydroxylammonium nitrate monopropellant decomposition over monolith and grain metal-based catalysts". In: *Reaction Kinetics, Mechanisms and Catalysis* 111.1 (2013), pp. 71–88. DOI: 10.1007/s11144-013-0626-6.

[126] Rachid Amrousse et al. "HAN and ADN as liquid ionic monopropellants: Thermal and catalytic decomposition processes". In: *Applied Catalysis B: Environmental* 127 (2012), pp. 121–128. DOI: 10.1016/j.apcatb.2012.08.009.

[127] Rachid Amrousse et al. "Performance and deactivation of Ir-based catalyst during hydroxylammonium nitrate catalytic decomposition". In: *Applied Catalysis A: General* 452 (2013), pp. 64–68. DOI: 10.1016/j.apcata.2012.11.038.

[128] Xiaoguang REN et al. "Catalytic Decomposition of Hydroxyl Ammonium Nitrate at Room Temperature". In: *Chinese Journal of Catalysis* 28.1 (2007), pp. 1–2. DOI: 10.1016/s1872-2067(07)60006-0.

[129] Shinjae Kang and Sejin Kwon. "Preparation and Performance Evaluation of Platinum Barium Hexaaluminate Catalyst for Green Propellant Hydroxylamine Nitrate Thrusters". In: *Materials* 14.11 (2021), p. 2828. DOI: 10.3390/ma14112828.

[130] Dan Amariei et al. "Catalytic and thermal decomposition of ionic liquid monopropellants using a dynamic reactor". In: *Chemical Engineering and Processing: Process Intensification* 46.2 (2007), pp. 165–174. DOI: 10.1016/j.cep.2006.05.010.

[131] Ruchika Agnihotri and Charlie Oommen. "Cerium oxide based active catalyst for hydroxylammonium nitrate (HAN) fueled monopropellant thrusters". In: *RSC Advances* 8.40 (2018), pp. 22293–22302. DOI: 10.1039/c8ra02368a.

[132] Ruchika Agnihotri and Charlie Oommen. “Kinetics and Mechanism of Thermal and Catalytic Decomposition of Hydroxylammonium Nitrate (HAN) Monopropellant”. In: *Propellants, Explosives, Pyrotechnics* 46.2 (2021), pp. 286–298. DOI: 10.1002/prep.202000142.

[133] Toshiyuki Katsumi et al. “Combustion Wave Structure of Hydroxylammonium Nitrate Aqueous Solutions”. In: *46th AIAA/ASME/SAE/ASEE Joint Propulsion Conference & Exhibit*. American Institute of Aeronautics and Astronautics, 2010. DOI: 10.2514/6.2010-6900.

[134] J. Shinjo et al. “Physics of puffing and microexplosion of emulsion fuel droplets”. In: *Physics of Fluids* 26.10 (2014), p. 103302. DOI: 10.1063/1.4897918.

[135] Rachid Amrousse et al. “HYDROXYLAMMONIUM NITRATE AS GREEN PROPELLANT: DECOMPOSITION AND STABILITY”. In: *International Journal of Energetic Materials and Chemical Propulsion* 11.3 (2012), pp. 241–257. DOI: 10.1615/intjenergeticmaterialschemprop.2012004978.

[136] Keiichi Hori et al. “HAN-Based Green Propellant, SHP163 – Its R&D and Test in Space”. In: *Propellants, Explosives, Pyrotechnics* 44.9 (2019), pp. 1080–1083. DOI: 10.1002/prep.201900237.

[137] Asato Wada, Hiroki Watanabe, and Haruki Takegahara. “Combustion Characteristics of a Hydroxylammonium-Nitrate-Based Monopropellant Thruster with Discharge Plasma System”. In: *Journal of Propulsion and Power* 34.4 (2018), pp. 1052–1060. DOI: 10.2514/1.b36762.

[138] Biddle et al. *Highly Soluble, Non-Hazardous Hydroxyl Ammonium Salt Solutions For Use In Hybrid Rocket Motors*. 1985.

[139] Loehr. *Hydroxyl Amine Based Staged Combustion Hybrid Rocket Motor*. 2011.

[140] Purdue AAE Propulsion. *Heats of formation and chemical compositions*. URL: https://engineering.purdue.edu/~propulsi/propulsion/comb/propellants.html.